

POLYLACTIC ACID RECYCLING WITH ENVIRONMENTALLY BENIGN  
FLUIDS

A THESIS SUBMITTED TO  
THE GRADUATE SCHOOL OF NATURAL AND APPLIED SCIENCES  
OF  
MIDDLE EAST TECHNICAL UNIVERSITY

BY

ÇAĞLA BOZCUOĞLU

IN PARTIAL FULFILLMENT OF THE REQUIREMENTS  
FOR  
THE DEGREE OF MASTER OF SCIENCE  
IN  
CHEMICAL ENGINEERING

FEBRUARY 2022



Approval of the thesis:

**POLYLACTIC ACID RECYCLING WITH ENVIRONMENTALLY  
BENIGN FLUIDS**

submitted by **ÇAĞLA BOZCUOĞLU** in partial fulfillment of the requirements for  
the degree of **Master of Science in Chemical Engineering, Middle East Technical  
University** by,

Prof. Dr. Halil Kalıpçılar  
Dean, Graduate School of **Natural and Applied Sciences**

Prof. Dr. Pınar Çalık  
Head of the Department, **Chemical Engineering**

Assoc. Prof. Dr. Çerağ Dilek Hacıhabiboğlu  
Supervisor, **Chemical Engineering, METU**

Prof. Dr. Naime Aslı Sezgi  
Co-Supervisor, **Chemical Engineering, METU**

**Examining Committee Members:**

Prof. Dr. Fatma Suna Balcı  
Chemical Engineering, Gazi University

Assoc. Prof. Dr. Çerağ Dilek Hacıhabiboğlu  
Chemical Engineering, METU

Prof. Dr. Naime Aslı Sezgi  
Chemical Engineering, METU

Assist. Prof. Dr. Harun Koku  
Chemical Engineering, METU

Assoc. Prof. Dr. Erhan Bat  
Chemical Engineering, METU

Date: 07.02.2022

**I hereby declare that all information in this document has been obtained and presented in accordance with academic rules and ethical conduct. I also declare that, as required by these rules and conduct, I have fully cited and referenced all material and results that are not original to this work.**

Name Last name : Çaęla Bozcuoęlu

Signature :

## **ABSTRACT**

### **POLYLACTIC ACID RECYCLING WITH ENVIRONMENTALLY BENIGN FLUIDS**

Bozcuođlu, ađla  
Master of Science, Chemical Engineering  
Supervisor : Assoc. Prof. Dr. erađ Dilek Hacıhabibođlu  
Co-Supervisor: Prof. Dr. Naime Aslı Sezgi

February 2022, 130 pages

In the past few decades, petroleum-based polymers have been replaced by biodegradable polymers since they bring about environmental problems. Polylactic acid (PLA) is a good candidate for this replacement due to its biocompatible and biodegradable nature and favorable mechanical and thermal properties. Due to the increase in usage and demand, there will be a PLA waste problem in the near future. Although PLA is classified as a biodegradable polymer, only a few microorganisms, which are not present in all soil types, can degrade PLA. In addition, relatively high temperature and humidity conditions should be provided for PLA biodegradation. The existing techniques for PLA degradation have not been fully developed yet, and degradation techniques are still being researched and developed. Hence, the aim of this study is to present an effective and environmentally benign solution for the PLA waste problem.

In this study, the PLA degradation reaction was carried out in a deep eutectic solvent (DES) medium in two different systems with batch and semi-batch reactors. All degradation experiments were performed at 180°C for 8 hours. Zinc chloride-ethylene glycol DES was synthesized, characterized, and used as a reaction medium in the degradation reaction of PLA. The complexation between zinc chloride and

ethylene glycol was verified by shifting of the peak at  $3390\text{ cm}^{-1}$  in the ethylene glycol FTIR spectrum.

As a catalyst, aluminum-loaded silica aerogel was synthesized, characterized, and used in PLA degradation reaction. The support material was synthesized using the sol-gel method, and aluminum was loaded via the wet impregnation technique. Aluminum was loaded into silica aerogel supports in 15 and 25 weight percentages (SAUA115 and SAUA125, respectively). Both of them decreased the activation energy of the thermal degradation reaction of PLA, but SAUA115 performed better in decreasing activation energy and degradation temperature. SAUA115 decreased the activation energy from 262 kJ/mol to 193 kJ/mol, whereas SAUA125 decreased the activation energy from 262 kJ/mol to 238 kJ/mol.

The product distribution of the PLA degradation reaction in zinc chloride-ethylene glycol DES in the batch reactor was investigated with GC-MS analyses. Degradation of DES in the same reaction conditions as that of PLA degradation reaction was also investigated, and its degradation products were distinguished from PLA degradation products. Dioxane, decane and undecane were the main products formed by the degradation of DES. The main products formed in the PLA degradation reaction were diethylene glycol, triethylene glycol, and acetic acid hydrazino ethyl ester. In addition to these products, ethyl lactate and 3-methyl-2-hexanone were formed. The effect of SAUA115 on product distribution and its interaction with zinc chloride-ethylene glycol DES was investigated. Ethyl lactate amount increased by two-fold with the usage of catalyst.

The product distribution of PLA degradation reaction in zinc chloride-ethylene glycol DES carried out in the semi-batch reactor was also investigated with GC-MS analyses. 2-pentanol acetate, 3(2H)-furanone dihydro-2-methyl, and ethyl lactate were the main products formed by PLA degradation, while 1,3-dioxolane, 2,2-dimethyl, and dioxane were the main products formed by DES degradation. The effect of SAUA115 on product distribution was investigated. With the usage of

catalyst, 1,3-dioxolane, 2,2,4,5-tetramethyl was newly formed, and amounts of dioxane and 3(2H)-furanone dihydro-2-methyl increased. Analyses of gas products were carried out with GC analyses. In all experiments, hydrogen and carbon dioxide were mainly detected as gas products.

In the semi-batch system, for DES degradation reaction, conversion of DES was 35.4%. In PLA degradation reaction, conversion of PLA was calculated as 97.3%. Yields of gas and liquid products and solid part in the reactor resulting from PLA were found to be 56.8%, 40.6%, and 2.6%, respectively. In PLA catalytic degradation reaction, conversion of PLA was 97%. Yields of gas and liquid products and solid part resulting from PLA catalytic degradation were calculated as 59.50 %, 37.4%, and 3.1%, respectively.

Using zinc chloride-ethylene glycol DES as reaction medium, PLA was degraded, and value-added products were obtained. Aluminum loaded silica aerogel catalysts showed promising activity in the PLA degradation reaction.

Keywords: Polylactic Acid, Deep Eutectic Solvents, Silica Aerogel, Aluminum, Polymer Degradation





## ÖZ

### **POLİLAKTİK ASİTİN ÇEVREYE ZARARI OLMAYAN ÇÖZÜCÜLERLE GERİ DÖNÜŞÜMÜ**

Bozcuoğlu, Çağla  
Yüksek Lisans, Kimya Mühendisliği  
Tez Yöneticisi: Doç. Dr. Çerağ Dilek Hacıhabiboğlu  
Ortak Tez Yöneticisi: Prof. Dr. Naime Aslı Sezgi

Şubat 2022, 130 sayfa

Geçtiğimiz son 10 yılda, petrol bazlı polimerler çevresel problemlere neden olduğu için petrol bazlı polimerlerin yerini biyobozunur polimerler almaktadır. Polilaktik asit (PLA) biyobozunur ve biyouyumlu yapısı ve uygun mekanik ve ısıl özellikleri nedeniyle bu yer değiştirme için güçlü bir aday olarak görülmektedir. PLA'nın kullanımının ve PLA'ya olan ihtiyacın artmasıyla yakın gelecekte PLA atık problemi olacaktır. PLA biyobozunur polimerler sınıfında yer almasına rağmen, bu bozunumu sağlayabilen sadece birkaç tip mikroorganizma bulunmakta olup bu mikroorganizmalar da her toprakta bulunmamaktadır. Ayrıca, PLA'nın biyobozunumu için nispeten yüksek sıcaklık ve nem gibi koşulların sağlanması gerekmektedir. PLA'nın bozunumu için var olan mevcut teknikler henüz tam olarak geliştirilmemiştir ve bozunma teknikleri hala araştırılmakta ve geliştirilmektedir. Bu yüzden, bu çalışmanın amacı PLA atık sorununa etkili ve çevreye duyarlı bir çözüm sunmaktır.

Bu çalışmada, PLA'nın bozunum reaksiyonu derin ötektik çözücü (DÖÇ) ortamında kesikli ve yarı kesikli olarak iki farklı sistemde gerçekleştirilmiştir. Tüm bozunma deneyleri 180°C'de 8 saat boyunca gerçekleştirilmiştir. Çinko klorür-etilen glikol

DÖÇ sentezlenip karakterize edilerek, PLA bozunum reaksiyonunda ortam olarak kullanılmıştır. Çinko klorür ve etilen glikol arasındaki kompleksleşme, etilen glikolün FTIR spektrumundaki  $3390\text{ cm}^{-1}$ 'deki pikinin kayması ile doğrulanmıştır.

Katalizör olarak alüminyum yüklü silika aerojel sentezlenip karakterize edilerek PLA'nın bozunumu reaksiyonda kullanılmıştır. Destek malzeme sol-jel metodu ile üretilmiştir ve alüminyum yapıya ıslak emdirme yöntemi ile yüklenmiştir. Alüminyum, silika aerojel desteğine ağırlıkça %15 ve %25 yüklenmiştir (sırayla, SAUA115 ve SAUA125). Her ikisi de PLA'nın ısıl bozunma reaksiyonunun aktivasyon enerjisini düşürmüştür ancak SAUA115 aktivasyon enerjisini ve bozunma sıcaklığını düşürme açısından daha iyi performans göstermiştir. SAUA115 aktivasyon enerjisini  $262\text{ kJ/mol}$ 'den  $193\text{ kJ/mol}$ 'e düşürürken, SAUA125 aktivasyon enerjisini  $262\text{ kJ/mol}$ 'den  $238\text{ kJ/mol}$ 'e düşürmüştür.

Kesikli reaktörde çinko klorür-etilen glikol DÖÇ'te PLA bozunumu reaksiyonunun ürün dağılımı GC-MS analizi ile incelenmiştir. Ayrıca PLA bozunma reaksiyonu ile aynı koşullarda DÖÇ'ün bozunması da araştırılmıştır ve bozunma ürünleri PLA bozunma ürünlerinden ayırt edilmiştir. Dioksan, dekan ve undekan, DES'in bozunmasıyla oluşan ana ürünlerdir. PLA bozunma reaksiyonunda oluşan ana ürünler dietilen glikol, trietilen glikol ve asetik asit hidrazino etil esterdir. Bu ürünlere ek olarak etil laktat ve 3-metil-2-hekzanon oluşmuştur. SAUA115'in ürün dağılımına olan etkisi ve çinko klorür-etilen glikol DÖÇ ile olan etkileşimi incelenmiştir. Katalizör kullanımı ile etil laktat miktarı iki kat artmıştır.

Yarı kesikli reaktörde gerçekleştirilen çinko klorür-etilen glikol DÖÇ'te PLA bozunma reaksiyonunun ürün dağılımı da GC-MS analizleri ile incelenmiştir. PLA bozunması ile oluşan başlıca ürünler 2-pentanol asetat, 3(2H)-furanon dihidro-2-metil ve etil laktat iken, DES bozunması ile oluşan ana ürünler 1,3-dioksolan, 2,2-dimetil ve dioksandır. SAUA115'in ürün dağılımına olan etkisi incelenmiştir. Katalizör kullanımı ile 1,3-dioksolan, 2,2,4,5-tetrametil yeni oluşmuş, dioksan ve 3(2H)-furanon dihidro-2-metil miktarları artmıştır. Gaz ürün analizleri GC analizleri

ile gerekleřtirilmiřtir. Tm deneylerde, hidrojen ve karbon dioksit ana gaz rnler olarak tespit edilmiřtir.

Yarı kesikli sistemde D bozunma reaksiyonu iin D'n dnřm %35,4'tr. PLA bozunma reaksiyonunda PLA dnřm %97,3 olarak hesaplanmıřtır. PLA'dan elde edilen gaz ve sıvı rnlerin ve reaktrdeki katı kısım verimleri sırasıyla %56,8, %40,5 ve %2,6 olarak bulunmuřtur. PLA katalitik bozunma reaksiyonunda PLA'nın dnřm %97'dir. PLA katalitik bozunmasından kaynaklanan gaz ve sıvı rnler ve katı kısım verimleri sırasıyla %59,5, %37,4 ve %3,1 olarak hesaplanmıřtır.

Reaksiyon ortamı olarak inko klorr-etilen glikol D kullanılarak PLA bozundurulmuř ve katma deęeri yksek rnler elde edilmiřtir. Alminyum ykl silika aerojel katalizrleri, PLA bozunma reaksiyonunda umut verici bir aktivite gstermiřtir.

Anahtar Kelimeler: Polilaktik Asit, Derin tektik zcler, Silika Aerojel, Alminyum, Polimer Bozunumu

To my family...

## ACKNOWLEDGEMENTS

Firstly, I would like to thank my supervisor Assoc. Prof. Dr. Çerağ Dilek-Hacıhabiboğlu, and my co-supervisor Prof. Dr. Naime Aslı Sezgi for their precious contributions, guidance, endless supports, patience, and encouragement during my research. Owing to Çerağ Dilek-Hacıhabiboğlu, I have started to learn how to do scientific research and experiments in my undergraduate years and she encouraged me to start master's degree.

I would like to thank METU Chemical Engineering Department and the professors for their education and limitless information about chemical engineering discipline.

I am thankful for my laboratory mates Seda Sivri and Merve Sarıyer for their helps, advice and supports all the time. They are not only my lab-mates, but also my older sisters. They taught me a lot of valuable things in laboratory. Also, I would like to thank my other lab-mates Salih Ermiş and Sümeyye Koçak-Bütüner for their friendships and collaborations.

I would like to thank Mihrican Açıkgöz and Doğan Akkuş for their help in performing characterization analyzes. Also, thanks to Petroleum Research Center, GC-MS analyses can be carried out. I would like to thank Middle East Technical University Scientific Research Projects Coordination Unit for supporting this research financially under grant number 10186.

I would like to thank my lovely friends Elif Kurt, İrem Öztürk, E.Ümran Aşçı, Merve Özkutlu, Selin Karahan, Candan Karaevvaz, Enes Akyıldız, Almira Çaldıklıoğlu, Soner Yaşar, Nurkan Sarohan and İklim Gökçe for their friendships and supports. Very special thanks to M. Emin Cinalioğlu for his infinite support, patience, understanding and unconditional love.

Also, I am so lucky to have a lovely neighbor, Banu Tokmaklar. Thanks to her and her cute twin daughters Deniz and Eylül, I have relieved whenever I feel anxious. They fill my life with joy and happiness.

Above all, I would like to express my gratitude to my family. Special thanks to my mother Tülay Bozcuođlu, and my father Mustafa Bozcuođlu for their endless love and supports throughout my whole life. They support me through every step of the way. I would like to thank my brother Asil Kaan Bozcuođlu, and my sister-in-law Duygu Yıldırım-Bozcuođlu for their endless support, encouragements, and guidance. I believe I haven't made this accomplishment without my family.

## TABLE OF CONTENTS

ABSTRACT.....	v
ÖZ .....	ix
ACKNOWLEDGEMENTS .....	xiii
TABLE OF CONTENTS.....	xv
LIST OF TABLES .....	xxi
LIST OF FIGURES .....	xxiii
NOMENCLATURE .....	xxvii
1 INTRODUCTION AND LITERATURE SURVEY .....	1
1.1 Global Plastic Waste Problem .....	1
1.2 Polylactic Acid (PLA) and Its Usage Areas.....	3
1.2.1 PLA Depolymerization Methods .....	5
1.2.1.1 Biological Depolymerization of PLA.....	6
1.2.1.2 Mechanical Recycling of PLA.....	9
1.2.1.3 Chemical Depolymerization of PLA .....	10
1.2.1.3.1 Hydrolysis Studies: .....	10
1.2.1.3.2 Alcoholysis Studies:.....	12
1.2.1.3.3 Pyrolysis Studies: .....	14
1.3 Deep Eutectic Solvents (DES).....	16
1.3.1 Deep Eutectic Solvents in Polymer Recycling .....	19
1.4 Catalysts in Polymer Degradation .....	21

1.4.1	Silica Aerogel .....	21
1.4.1.1	Gel preparation stage: .....	22
1.4.1.2	Aging stage: .....	22
1.4.1.3	Drying stage: .....	23
1.4.2	Silica Aerogel Applications in Literature .....	23
1.5	The Aim of This Study .....	25
2	EXPERIMENTAL .....	27
2.1	Experimental Set-ups and Procedures .....	27
2.1.1	Synthesis of Deep Eutectic Solvents (DES) .....	27
2.1.1.1	Zinc Chloride-Urea DES Synthesis .....	27
2.1.1.2	Zinc Chloride-Ethylene Glycol DES Synthesis .....	28
2.1.1.3	Characterization of DES's.....	28
2.1.1.3.1	FTIR Analysis.....	29
2.1.1.3.2	TGA Analysis .....	29
2.1.2	Synthesis of Catalyst .....	29
2.1.2.1	Synthesis of Silica Aerogel Support Material .....	29
2.1.2.2	Aluminum Loading to the Silica Aerogel by Wet Impregnation Method.....	30
2.1.2.3	Characterization of Catalyst.....	31
2.1.2.3.1	FTIR Analysis.....	31
2.1.2.3.2	TGA Analysis .....	32
2.1.2.3.3	Nitrogen Sorption Analysis .....	32
2.1.2.3.4	Scanning Electron Microscope and Energy Dispersed X-ray Analysis....	32



2.1.2.3.5	Diffuse Reflectance Infrared Fourier Transform Spectroscopy Analysis.....	32
2.1.3	PLA Degradation Reaction Systems.....	33
2.1.3.1	Degradation of PLA with/without Catalyst Using Thermogravimetric Analyzer.....	33
2.1.3.2	Experimental Setup for PLA Degradation in Batch System .....	34
2.1.3.3	Experimental Setup for PLA Degradation in Semi-Batch System.....	36
2.1.3.4	Analysis of Liquid and Gas Products of the Degradation Reactions.....	37
2.1.3.4.1	GC-MS Analysis .....	38
2.1.3.4.2	GC Analysis .....	38
3	RESULTS AND DISCUSSION .....	39
3.1	Synthesis and Characterization of DES .....	39
3.1.1	Zinc Chloride-Urea DES.....	39
3.1.1.1	FTIR Analysis.....	40
3.1.1.2	Stability of DES.....	41
3.1.1.3	TGA Analysis .....	42
3.1.2	Zinc Chloride-Ethylene Glycol DES .....	45
3.1.2.1	FTIR Analysis.....	45
3.1.2.2	Stability of DES.....	46
3.1.2.3	TGA Analysis .....	47
3.1.2.4	Thermal Degradation of Zinc Chloride-Ethylene Glycol DES in Batch System .....	48

3.1.2.5	Thermal Degradation of Zinc Chloride-Ethylene Glycol DES in Semi-Batch System .....	50
3.2	Characterization Results of Catalysts .....	55
3.2.1	Characterizations of Silica Aerogel Support Material.....	55
3.2.1.1	FTIR Analysis .....	56
3.2.1.2	Nitrogen Sorption Analysis.....	56
3.2.1.2.1	Pore Size Distribution Analysis.....	57
3.2.1.2.2	Physical Properties of Synthesized Silica Aerogel .....	58
3.2.1.3	Scanning Electron Microscopy (SEM) Analysis .....	59
3.2.2	Characterization of Aluminum Loaded Silica Aerogel Catalyst.....	60
3.2.2.1	Nitrogen Sorption Analysis.....	60
3.2.2.1.1	Pore Size Distribution Analysis.....	61
3.2.2.1.2	Physical Properties of Synthesized Aluminum Loaded Silica Aerogels.....	62
3.2.2.2	TGA Analysis.....	62
3.2.2.3	Scanning Electron Microscopy (SEM) Analysis .....	63
3.2.2.4	Diffuse Reflectance Infrared Fourier Transform Spectroscopy (DRIFTS) Analysis.....	70
3.3	PLA Degradation Reaction Results.....	71
3.3.1	Performance of Aluminum Loaded Silica Aerogel Supports Using Thermogravimetric Analyzer .....	72
3.3.2	Zinc Chloride-Ethylene Glycol DES Medium in Batch System.....	74
3.3.3	Zinc Chloride-Ethylene Glycol DES Medium in Semi-Batch System... ..	79
3.4	Catalytic Degradation of PLA in DES Medium.....	85

3.4.1	Catalytic Degradation in Batch System .....	85
3.4.2	Catalytic Reaction in Semi-Batch System .....	88
4	CONCLUSIONS.....	95
5	RECOMMENDATIONS .....	99
	REFERENCES .....	101
	APPENDICES .....	113
A.	GC-MS Reports .....	113
B.	Mass Balances for Degradation Reactions in Semi-Batch System.....	120
C.	EDX Spectra of Different Mapped Areas of Catalysts .....	124
D.	Calculation of Activation Energy of PLA Thermal Degradation Reaction with Presence of Catalysts Using Thermogravimetric Analyzer .....	128



## LIST OF TABLES

### TABLES

<b>Table 1.1.</b> Different types of DES and melting points of resulting DES's and their constituents.....	19
<b>Table 2.1.</b> Furnace heating program used in GC-MS analysis.....	38
<b>Table 2.2.</b> Temperature program of GC column .....	38
<b>Table 3.1.</b> DES Degradation Products formed at 180°C for 8 hours .....	49
<b>Table 3.2.</b> Physical properties of silica aerogels from different batches.....	58
<b>Table 3.3.</b> Physical properties of aluminum loaded silica aerogels .....	62
<b>Table 3.4.</b> Weight percentages of elements in SAUA115 detected by EDX .....	66
<b>Table 3.5.</b> Weight percentages of elements in different parts of SAUA115.....	67
<b>Table 3.6.</b> Weight percentages of elements in SAUA125 detected by EDX.....	68
<b>Table 3.7.</b> Weight percentage of elements in different parts of SAUA125 .....	69
<b>Table 3.8.</b> Temperature values corresponds to 10, 50, and 90% weight loss.....	73
<b>Table 3.9.</b> Apparent activation energy values of PLA degradation reaction and its values in the presence of catalyst.....	74
<b>Table 3.10.</b> Products obtained from the PLA degradation reaction in ethylene glycol-zinc chloride DES medium.....	77
<b>Table 3.11.</b> PLA degradation products in the semi-batch system.....	80
<b>Table 3.12.</b> Products obtained from the catalytic PLA degradation reaction in zinc chloride-ethylene glycol DES medium in the batch system .....	86
<b>Table 3.13.</b> Comparison of peak areas of products obtained from the catalytic and non-catalytic PLA degradation reaction in zinc chloride-ethylene glycol DES medium.....	87
<b>Table 3.14.</b> Products formed when DES and catalyst were reacted at 180°C for 8 hours.....	88
<b>Table 3.15.</b> PLA catalytic degradation products resulted in the semi-batch system .....	89



## LIST OF FIGURES

### FIGURES

<b>Figure 1.1.</b> Production volume of plastics worldwide from 1980 to 2050. ....	1
<b>Figure 1.2.</b> Amount of plastic waste produced in U.S. in between 1960 and 2018.....	2
<b>Figure 1.3.</b> Chemical structure of PLA .....	3
<b>Figure 1.4.</b> Summary of synthesis methods of PLA .....	4
<b>Figure 1.5.</b> Binary phase diagram and melting point depression behavior of DES's .....	17
<b>Figure 2.1.</b> Experimental setup for DES synthesis .....	28
<b>Figure 2.2.</b> Experimental setup for silica aerogel synthesis.....	30
<b>Figure 2.3.</b> Experimental setup of the PLA degradation reaction in batch reactor	35
<b>Figure 2.4.</b> Photograph of the batch experimental setup used for PLA degradation .....	35
<b>Figure 2.5.</b> The semi-batch experimental setup used for PLA degradation.....	37
<b>Figure 3.1.</b> FTIR spectra of urea and DES .....	40
<b>Figure 3.2.</b> a) Freshly synthesized DES and b) an unstable DES, 3 days after the synthesis .....	42
<b>Figure 3.3.</b> TGA curve of zinc chloride-urea DES .....	43
<b>Figure 3.4.</b> Photographs of a) DES heated at 180°C for 2 hours and b) freshly synthesized DES .....	44
<b>Figure 3.5.</b> FTIR spectra of ethylene glycol and zinc chloride-ethylene glycol DES .....	46
<b>Figure 3.6.</b> TGA analysis of zinc chloride-ethylene glycol DES.....	47
<b>Figure 3.7.</b> TGA behavior comparison of DES and ethylene glycol .....	48
<b>Figure 3.8.</b> Chemical structure of di(2-ethylhexyl) phthalate .....	50
<b>Figure 3.9.</b> Change of hydrogen production amounts with time in the reaction....	52
<b>Figure 3.10.</b> Change of carbon dioxide production amounts with time in the reaction.....	53

<b>Figure 3.11.</b> Peak area changes of carbon monoxide and nitrogen with time in the reaction .....	54
<b>Figure 3.12.</b> Peak area changes of unidentified substance at different reaction times .....	55
<b>Figure 3.13.</b> FTIR spectrum of silica aerogel .....	56
<b>Figure 3.14.</b> Nitrogen adsorption and desorption isotherms of silica aerogel (filled circles represent adsorption branch and empty circles represent desorption branch). .....	57
<b>Figure 3.15.</b> Pore size distribution of silica aerogel .....	58
<b>Figure 3.16.</b> SEM image of silica aerogel .....	59
<b>Figure 3.17.</b> Nitrogen adsorption and desorption isotherms of aluminum loaded silica aerogels compared with that of silica aerogel (filled circles represent adsorption branches, empty circles represent desorption branches) .....	60
<b>Figure 3.18.</b> Pore size distribution comparison of silica aerogel and aluminum loaded silica aerogels.....	61
<b>Figure 3.19.</b> TGA analysis of SAUA115 .....	63
<b>Figure 3.20.</b> SEM images of SAUA115 at a) 1170x, b) 1700x, and c) 25000x magnifications .....	64
<b>Figure 3.21.</b> SEM images of SAUA125 at a) 25000x, b) 50000x, and c) 100000x magnifications .....	65
<b>Figure 3.22.</b> EDX spectrum of SAUA115.....	66
<b>Figure 3.23.</b> Mapped area of SAUA115 a): distribution of b) silicon, c) oxygen and d) aluminum.....	67
<b>Figure 3.24.</b> EDX spectrum of SAUA125.....	68
<b>Figure 3.25.</b> Mapped area of SAUA125 a): distribution of b) silicon, c) oxygen, and d) aluminum.....	69
<b>Figure 3.26.</b> DRIFTS spectra of the synthesized catalysts .....	70
<b>Figure 3.27.</b> TGA behavior of PLA in presence of aluminum loaded silica aerogels compared with neat PLA .....	72



<b>Figure 3.28.</b> Comparison of FTIR spectra of DES and the bottom phase of DES+ethyl acetate mixture .....	75
<b>Figure 3.29.</b> Comparison of FTIR spectra of ethyl acetate and the top phase of DES+ethyl acetate mixture .....	76
<b>Figure 3.30.</b> Chemical structures of a) PLA, b) 2-pentanol acetate, c) 3(2H)-Furanone, dihydro-2-methyl .....	80
<b>Figure 3.31.</b> Change of hydrogen production amounts with time in DES and DES+PLA experiments performed in the semi-batch system .....	82
<b>Figure 3.32.</b> Change of carbon dioxide production amounts with time in DES and DES+PLA experiments performed in the semi-batch system .....	83
<b>Figure 3.33.</b> Peak area values of carbon monoxide and nitrogen in DES and DES+PLA experiments.....	84
<b>Figure 3.34.</b> Peak area values of the unidentified peak with time in DES and DES+PLA experiments.....	85
<b>Figure 3.35.</b> Change of hydrogen production amounts with time in experiments performed in semi-batch system .....	91
<b>Figure 3.36.</b> Change of carbon dioxide production amounts with time in experiments performed in semi-batch system.....	92
<b>Figure 3.37.</b> Peak area values of carbon monoxide and nitrogen with time in all experiments .....	93
<b>Figure 3.38.</b> Peak area values of the unidentified component .....	94



## NOMENCLATURE

***A*** : Pre-exponential factor

***E<sub>a</sub>*** : Activation energy, kJ/mol

***m<sub>Catalyst,0</sub>*** : Initial weight of catalyst, g

***m<sub>DES,0</sub>*** : Initial weight of DES, g

***m<sub>EG,prep</sub>*** : Weight of ethylene glycol used in preparation of DES, g

***m<sub>PLA,0</sub>*** : Initial weight of PLA, g

***m<sub>ZnCl2</sub>*** : Weight of zinc chloride, g

***m<sub>gas product from PLA</sub>*** : Weight of gas products formed from PLA, g

***m<sub>gas</sub>*** : Weight of gas products, g

***m<sub>left in reactor</sub>*** : Weight of materials left in reactor, g

***m<sub>liq product from PLA</sub>*** : Weight of liquid products formed from PLA, g

***m<sub>liq</sub>*** : Weight of liquid products, g

***m<sub>solid in reactor from PLA</sub>*** : Weight of solid products formed from PLA, g

***m<sub>ZnCl2,prep</sub>*** : Weight of zinc chloride used in preparation of DES, g

***n*** : Number of moles, mol

***R*** : Gas constant, J/mol\*K

***T*** : Temperature, °C

***wt%<sub>gas product from DES</sub>*** : Weight percent of gas products formed from DES, %

***wt%<sub>liq product from DES</sub>*** : Weight percent of liquid products formed from DES, %

**$wt\%_{solid\ product\ from\ DES}$**  : Weight percent of solid products formed from DES, %

**$wt\%_{ZnCl_2}$**  : Weight percent of zinc chloride, %

**$X_{DES}$**  : Conversion of DES

**$X_{PLA}$**  : Conversion of PLA

**$Y_{gas}$**  : Yield of gas products, %

**$Y_{liq}$**  : Yield of liquid products, %

**$Y_{solid\ in\ reactor}$**  : Yield of solid products, %

### **Abbreviations**

**BET**: Brunauer Emmett Teller

**BJH**: Barrett Joyner Halenda

**DES**: Deep Eutectic Solvent

**DRIFTS**: Diffuse Reflectance Infrared Fourier Transform Spectroscopy

**EDX**: Energy Dispersive X-ray

**FTIR**: Fourier-Transform Infrared Spectroscopy

**GC**: Gas Chromatograph

**GC-MS**: Gas Chromatography-Mass Spectrometry

**GPC**: Gel Permeation Chromatography

**HPLC**: High-Performance Liquid Chromatography

**PCL**: Polycaprolactone

**PET**: Polyethylene Terephthalate

**PLA**: Polylactic Acid

**SAU:** Silica Aerogel Uncalcined

**SEM:** Scanning Electron Microscopy

**TCD:** Thermal Conductivity Detector

**TEOS:** Tetraethyl Orthosilicate

**TGA:** Thermogravimetric Analysis

**THF:** Tetrahydrofuran

**TMCS:** Trimethyl Chlorosilane

**TÜİK:** Turkish Statistical Institute

**VOC:** Volatile Organic Compound



# CHAPTER 1

## INTRODUCTION AND LITERATURE SURVEY

### 1.1 Global Plastic Waste Problem

Plastic consumption continues to increase all around the world. Huge consumption of plastics brings about plastic pollution issue, and it harms not only environment but also human health. In order to meet the rising demand for plastics, plastic production rates are increasing year by year. According to International Energy Agency (IEA, 2020), by 2050, worldwide plastic production volume will reach up to 600 million metric tons (Figure 1.1).

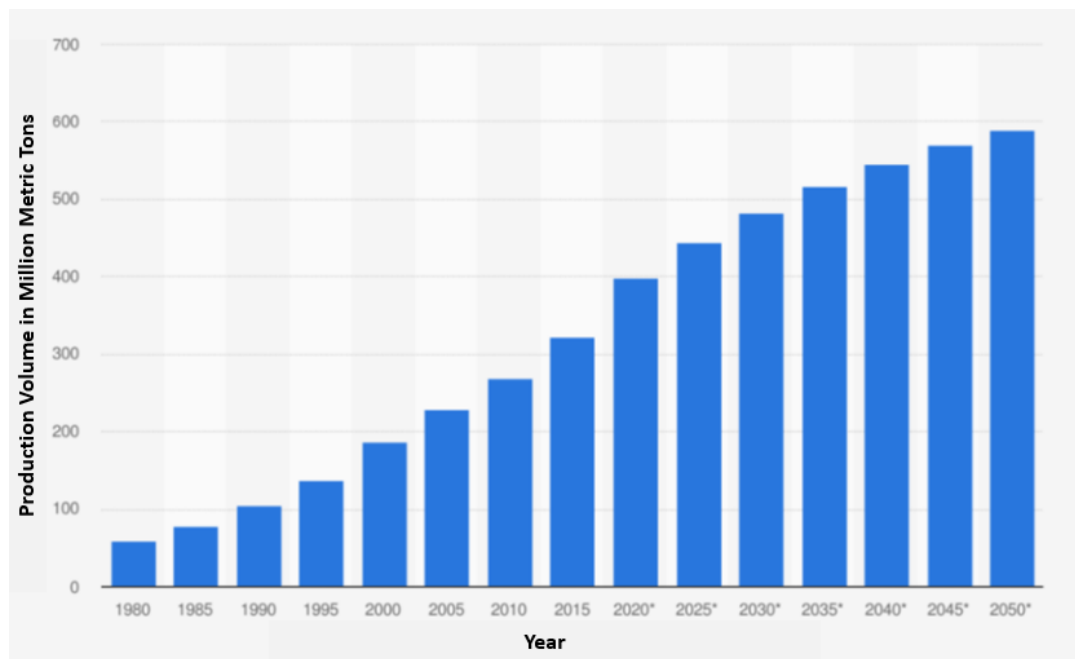


**Figure 1.1.** Production volume of plastics worldwide from 1980 to 2050 (IEA, 2020).

In parallel with increasing production and consumption, plastic waste generation is also increasing. In Figure 1.2, amount of plastic waste produced in United States between 1960 and 2018 is revealed (United States Environmental Protection Agency, 2020).

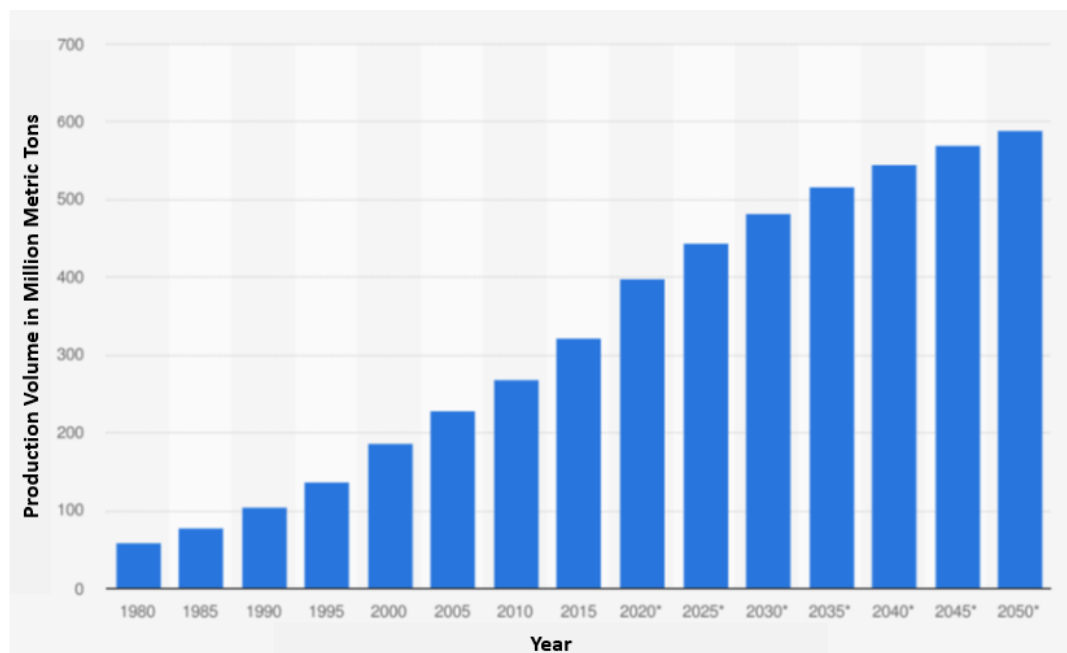


**Figure 1.2.** Amount of plastic waste produced in U.S. in between 1960 and 2018 (United States Environmental Protection Agency, 2020).

Bioplastics are a class of plastics that are made up of natural and renewable materials. Nowadays, bioplastics are gaining importance. For instance, worldwide known companies have started to use bioplastic materials for packaging. According to Grand View Research report (2014), in 2013 bioplastics constituted less than 1% of the total plastics market. In the same report, it is predicted that in 2030, it will rise to 40% of the total plastics market.

By a majority, it is thought that bioplastics can easily degrade in nature; however, nearly half of bioplastics are not able to degrade biologically (European Bioplastics, 2019). Temperature, humidity, soil type, and microorganisms in soil which can degrade specific bioplastics are the main factors that play role in biodegradation process. It takes long time to set the optimal conditions for biodegradation (Bahl et



al., 2020). Biodegradation itself is also a slow process. To illustrate, PLA was degraded after 60 days under compost conditions (temperature was set to 60°C and PLA-degrading microorganisms were present). In environmental conditions, even after 60 days, degradation was not observed for PLA (Tokiwa et al., 2006). As a result, an effective degradation pathway should be developed to prevent accumulation of plastic waste.

In this study, the main aim is providing an effective and environmentally benign solution for waste problem of polylactic acid (PLA), which is classified as biodegradable and aliphatic polyester (Garlotta, 2019).

## 1.2 Polyactic Acid (PLA) and Its Usage Areas

Polyactic acid (PLA) is a biopolymer that can be produced from natural resources such as, sugarcane and corn (Corbion Group Netherlands B.V, 2016). It is a member of aliphatic polyesters class. Also, it is a thermoplastic polymer (Garlotta, 2019). In Figure 1.3, the chemical structure of PLA is shown.

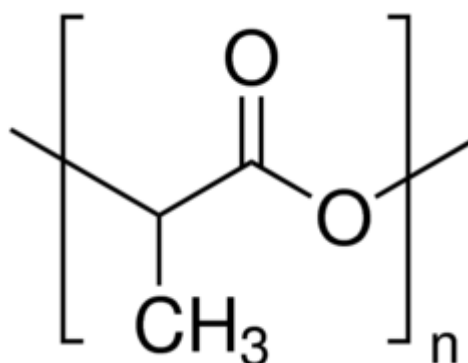


**Figure 1.3.** Chemical structure of PLA (Rong et.al., 2007)

It is claimed that PLA is synthesized for the first time via polycondensation of lactic acid by Theophile-Joules Pelouze in 1845 (Benninga, 1990). Carothers et al. (1932) came out with a method to produce PLA by polymerizing lactide in 1932. In 1954, Du Pont got patent for this procedure.

Lactic acid is the basic building block of PLA. Until Mitsui Totatsu Chemicals company got patent and commercialized the high molecular weight polyesters production from hydroxycarboxylic acid, it was thought that only way to produce high molecular weight and pure PLA was using lactide in ring opening polymerization reaction (Garlotta, 2019). However, they achieved to produce high molecular weight (weight average molecular weight greater than 10000) by azeotropic dehydration reaction of lactic acid and different metal compounds in a hydrocarbon solvent under reduced pressure (Enomoto et.al., 1992). In Figure 1.4, the synthesis procedures of PLA were summarized.

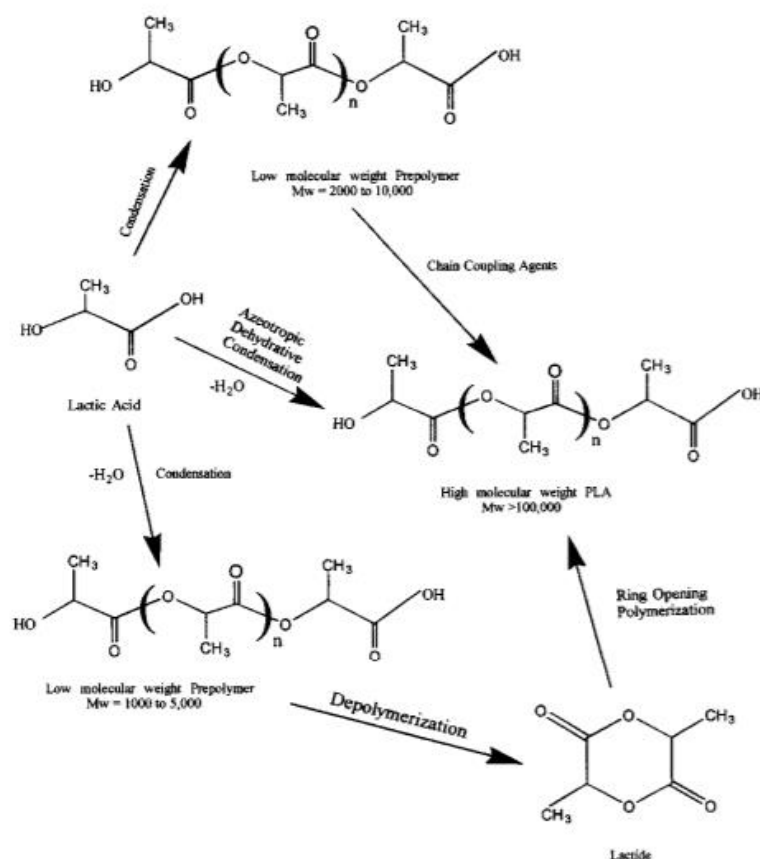


**Figure 1.4.** Summary of synthesis methods of PLA (Garlotta, 2019)

Nowadays, petroleum-based polymers have been tried to replace with biobased polymers because of environmental and human health concerns. Plastic wastes increase carbon footprint, and it triggers global warming (Bahl et al., 2020). As a

result, humans experience extreme weather conditions. Microplastics can accumulate in living organisms in case of being exposed to too many plastics (Thompson et al., 2009). Due to its relatively good mechanical properties, thermal characteristics and biocompatible nature, PLA is thought as an appropriate alternative for the replacement of conventional, petroleum-based polymers (Lopes et al., 2012; Farah et al., 2016). Due to its favorable features, it has various usage areas. It is used widely in packaging, textile, insulation, and many biomedical applications (Nampoothiri et al., 2010).

This replacement leads a dramatic increase in consumption and production amounts of PLA. Global market size value of PLA was approximately 526 million \$ in 2020 and, it is anticipated that the market size will grow at a compound annual growth rate of 18 % from 2021 to 2028 (Grand View Research, 2021). In Turkey, the foreign trade import value of PLA between 2015 and 2020 raised constantly. According to Turkish Statistical Institute (TÜİK), foreign trade import value was approximately 39.000\$ in 2015 whereas that of 2020 was around 4.600.000 \$ (TÜİK, 2020). In five years, import value of PLA has increased nearly one hundred twenty-fold.

Due to increasing usage area and consumption amount of PLA, there will be a PLA waste problem in near future. Although PLA is a biodegradable polymer, there are some certain conditions that should be satisfied for biodegradation in soil, such as high humidity, limited PLA-degrading microorganism types in soil, appropriate temperature and pH value etc. (Pranamuda et al., 1997). These constraints, which will be explained in detail under biological recycling methods title, reveal that there is a need for efficient degradation method for PLA wastes. In the next section, PLA recycling methods and present studies are introduced.

### **1.2.1 PLA Depolymerization Methods**

For polymer recycling there are three main techniques which are biological, mechanical, and chemical recycling.

Biodegradation is the transition of a bio-based chemical into smaller compounds by microorganisms (Bahl et al., 2020). Also, some biological enzymes are utilized for polymer degradation (Karamanlioglu, 2017). For an effective biological recycling of a polymer, there are a lot of parameters that depends on both properties of polymer and soil. Crystallinity, molecular weight, features of their functional groups, presence of additives are the important features of polymers that affect the biological recycling ability (Bahl et al., 2020). Humidity, pH value, presence of related microorganisms are the determinative features that depends on soil type (Bahl et al., 2020).

Mechanical recycling alludes to turning waste plastics into secondary raw materials by applying milling, washing, passing through a flotation separation, drying, re-granulating, and compounding processes, respectively (European Bioplastics, 2020). Only thermoplastic materials, which become flexible at a predetermined temperature and hardens when cooled, can be recycled mechanically.

Chemical recycling is a process in which a polymer can be reduced to its monomers or valuable substances so that it can be re-polymerized or re-processed (Garforth et al., 2004). In chemical recycling, there are hydrolysis, alcoholysis, and pyrolysis methods.

#### **1.2.1.1 Biological Depolymerization of PLA**

Due to its biodegradability and relatively good material properties, PLA is widely used not only for industrial purposes but also biomedical applications. Although PLA is classified as a biodegradable polymer, its degradation in nature is not an easy-going process. Temperature, pH, moisture, oxygen concentration are the factors that play role in biodegradation of PLA (Sangwan et al., 2008; Kale et al., 2007).

In general, PLA biodegradation takes place in two parts. It starts with hydrolysis process, by being exposed to moisture for months (Tokiwa et al., 2006). With hydrolysis, chain scission of ester linkages occurs, and this leads to decrease in

molecular weight. As the lower molecular weight PLA oligomers, dimmers etc. are produced, they can be degraded by microorganisms in soil (Sangwan et al., 2008; Auras et al., 2004). Under aerobic conditions, final products are carbon dioxide, water, and biomass. On the other hand, when conditions are anaerobic, products are hydrocarbons, methane, and biomass (Karamanlioglu et al., 2017). Rate of hydrolysis step mainly depends on temperature. In addition to crystallinity of polymer, temperature, water content and pH of soil and in the case of PLA blended polymers, presence of stabilizers, additives, end group concentration are important parameters that should be taken into account (Kolstad et al., 2012; Auras et al., 2004). Higher the temperature, higher the rate of hydrolysis reaction. More specifically, above the glass transition temperature due to increase in flexibility of polymer chains and water absorption capacity, PLA degradation rate is higher (Kale et al., 2007). However, the degradation rate is still not that much fast. To demonstrate the situation, Kolstad et al performed an anaerobic biodegradation experiment. In this study, two tests called Accelerated Landfill Condition test and High Solids Anaerobic Digestion test were applied to PLA. In these tests, humidity and temperature were the studied parameters. Biodegradation was controlled via release of methane gas. As a result of these tests, they concluded that PLA samples didn't release methane in noticeable level, so there was no direct anaerobic degradation and degradation of PLA in landfill conditions would need a chemical hydrolysis before biodegradation. In the same study, for aerobic degradation an approximation was made and it turns out that PLA with initial molecular weight of 100000 g/mol was kept at 20°C and 50% relative humidity for 100 years. As a result, molecular weight decreased to only 36000 g/mol, which is still beyond the level where microorganisms could degrade waste PLA (Kolstad et al., 2012). In another study conducted by Karamanlioglu et al., degradation of PLA coupons in soil and compost at a temperature range between 25 and 55°C was examined and loss of tensile strength and molecular weight data were measured and degradation rate was compared with that of obtained in aqueous environment. They conclude that at low temperatures below 40°C, almost no degradation occurred over 1 year, and this situation could

lead to accumulation of PLA in nature and pollution issues (Karamanlioglu et al., 2013). As mentioned before, microorganisms in soil play an important role in degradation of PLA having lower molecular weight. Pranamuda et al. was reported the PLA degrading actinomyces *Amycolatopsis*, sp. HT-32. They observed that PLA film having an initial weight of 100 mg was weighed nearly 40 mg after 14 days of liquid culture (Pranamuda et al., 1997). However, microorganisms that can degrade PLA, specifically *Amycolatopsis* and *Saccharotrix*, are found relatively rarely in the soil when compared to the availability of other polyester-degrading microorganisms in soil (Tokiwa et.al., 2004). Degradation of PLA in aqueous environment was also investigated by Tsuji et al. They stated that they didn't observe any evidence that proves microbial degradation when they kept PLA films in seawater at 25°C for 10 weeks (Tsuji et.al., 2002). In order for hydrolysis reaction to take place, temperature should be nearly at 50-60°C, and even at that temperature, it could be hydrolyzed into smaller molecules in 45-60 days (Tokiwa et.al., 2006). Then, microorganisms could degrade these smaller molecules into CO<sub>2</sub> and H<sub>2</sub>O in the compost. For example, PLA hydrolysis studies were done at 160-180°C when catalyst was not used (Piemonte et.al., 2013). Temperature of seas and oceans are much lower than the needed temperature value for an effective hydrolysis reaction. Low degradation rate in aquatic environments can bring about pollution in oceans and seas.

Degradation of PLA in soil and aquatic environments seems noneffective; hence, there is a need for productive solution to solve the PLA waste problem.

In addition to microbial degradation, there are a few studies utilizing microbial enzymes for degradation of PLA. Ebeling et al. (1974) and Williams (1981) reported serine protease, named proteinase K, for degradation of PLA. However, degradation of PLA with proteinase enzyme was succeeded in presence of gelatin which stimulates proteinase production (Jarerat et.al., 2001). In the absence of gelatin, degradation did not occur after 14 days. When gelatin was included, nearly 80 % of PLA was degraded by proteinase enzyme which was excreted by fungus (Jarerat et al., 2001). Hoshino et al. (2002), studied the effect of lipase enzymes from different microorganisms on degradation of several polyesters including PLA. As a result,

they concluded that none of the lipase enzymes could degrade PLA at 37°C; however, the rest of tested polyesters could be degraded by the lipase enzymes. Masaki et al., reported a promising cutinase-like enzyme which could degrade PLA. This enzyme was produced by yeast *Cryptococcus* which is used in wastewater treatment purposes. They found that this enzyme degraded PLA in 60 hours; however, other conditions such as, temperature were not mentioned (Masaki et al., 2005). Hence, feasibility of this degradation could be evaluated as doubtful.

In brief, in microbial degradation, PLA-degrading microorganisms secrete extracellular enzyme, depolymerase of PLA (Qi et al., 2017). To accelerate the production of depolymerase enzyme, some inducers, such as silk fibroin, elastin and gelatin should be present. Then, the depolymerase breaks the ester bonds in the structure of PLA. Breakage of bonds brings about formation of oligomers, dimers, and monomers. Subsequently, the lower molecular weight products enter from microbial membranes and degrade into carbon dioxide, water and biomass in aerobic condition. On the other hand, in addition to carbon dioxide, water and biomass, methane is produced in anaerobic condition (Qi et al., 2017). Hydrolysis of PLA plays an important role in biodegradation in terms of expediting the microbial degradation.

#### **1.2.1.2 Mechanical Recycling of PLA**

Mechanical recycling is the most predominantly used method for managing the post-consumer plastic waste problem (European Bioplastics, 2020). However, the resulting PLA from mechanical recycling has worse mechanical features such as, lower tensile strength at break and impact strength and higher melt flowrate, and water vapor and oxygen transmission (Zenkiewicz et al., 2009). Due to the worsening in mechanical properties, applicability of mechanical recycling to the waste polymer is limited. Piemonte et al., compared the chemical and mechanical recycling techniques and concluded that chemical recycling enables production of

valuable chemicals having same properties with the virgin material unlike mechanical recycling (Piemonte et al., 2013).

As the amount of PLA waste continues to increase, there should be a waste management solution that provides not only removal of waste but also economic advantages. Production of value-added raw materials from the waste plastics can make the process economically feasible.

### **1.2.1.3 Chemical Depolymerization of PLA**

Within the scope of chemical recycling title, there are hydrolysis, alcoholysis and pyrolysis studies. In some of alcoholysis and hydrolysis studies, polymer was dissolved in a solvent prior to degradation reaction. For this kind of studies, the used solution was indicated. As a result of chemical recycling, the chemical structure of polymer changes and different, preferably valuable compounds are produced. For PLA chemical recycling case, production of lactide and/or lactic acid from a chemical recycling reaction, can provide a closed loop system because lactide or lactic acid could be utilized to produce PLA.

#### **1.2.1.3.1 Hydrolysis Studies:**

Hydrolysis reaction of PLA dates back to 1998. Siparsky et al. (1998), performed hydrolysis in acetonitrile and water solution to exclude solid phase effects such as diffusion and crystallinity. In this study, hydrolysis of polycaprolactone (PCL) was also examined and two polymers were compared in terms of kinetics of the reaction. They concluded that PLA hydrolysis in acetonitrile-water solution is self-catalyzed whereas addition of acid catalyst is needed for PCL hydrolysis. As the product of PLA hydrolysis reaction, lactic acid was mentioned. Concentration of acid was determined by titration. Due to the fact that acetonitrile concentration in water influences the production of carboxylic end groups, kinetic study could be performed



solely in a narrow range of PLA solution concentrations because the production of carboxylic end groups was influenced by the solvent: water ratio.

Another hydrolysis study was conducted by Piemonte et al. (2013). They aimed to produce lactic acid from PLA, utilizing water as reaction medium at temperatures close to melting point of PLA. At 140-180°C, 1.5 MPa pressure was applied and PLA: water weight ratio of 5-10. Conversion of PLA was calculated from the initial weight and weight of solid PLA left after the reaction. Liquid product analysis was performed by using gas chromatography (GC) technique. In their conclusions, it was highlighted that for high PLA: water weight ratios, to be able to produce more concentrated lactic acid solutions, energy consumption demand for water evaporation could be lowered significantly; hence, higher PLA: water weight ratio levels should be investigated in detail for industrial applications.

Cristina et.al, performed another hydrolysis research (Cristina et al., 2018). In their work, hydrolysis reactions of post-consumer PLA at temperatures between 170-190°C with reaction times ranging from 45 to 90 minutes were carried out. PLA: water weight ratio was taken as 0.11. Low molecular weight oligomers and lactic acid was reported as the products. They suggest a model which accounts for two step processes. The first step is bulk degradation of PLA with solubilization of oligomers, and the second step is the hydrolysis of oligomers. For analysis, HPLC (High Performance Liquid Chromatography) method was used.

In another study, different types of ionic liquids, namely [bmim][OAc], [bmim][Cl], [emim][OAc], [emim][NTf<sub>2</sub>] and [HSO<sub>3</sub>-pmim][HSO<sub>4</sub>], were used as catalyst in hydrolysis reaction of PLA (Song et al., 2014). Catalyst:PLA weight ratio was changed from 0.1:1 to 0.5:1. Influence of reaction temperature, ratio of amount of catalyst to PLA and amount of water to PLA, and ionic liquid type were investigated. Reaction temperature was changed between 120-140°C. After the reaction, PLA residue was weighed and from the initial weight data, percent conversion of PLA was calculated and reported. In purification step, calcium carbonate was used; however, reason for this step was not explained. Due to usage of calcium carbonate,

end product of this study was stated as calcium lactate. They concluded that as catalysts: PLA weight ratio rises, conversion of PLA increases as well. Water:PLA weight ratio was changed from 2:1 to 8:1, and similar trend with catalyst:PLA weight ratio was observed in terms of conversion.

#### **1.2.1.3.2 Alcoholysis Studies:**

Hirao et al., conducted an alcoholysis study utilizing ethanol and butanol as reaction media (Hirao et al., 2010). Conventional and microwave heating techniques were also compared by keeping PLA:alcohol molar ratio as 1:10 constant. For ethanol, reaction temperature range was in between 140-180°C and that of butanol was 130-210°C. Reaction times were different for conventional and microwave heating cases. In conventional heating, reaction times were 20 to 60 minutes and that of microwave heating were 2 to 10 minutes. They highlighted that in both types of heating, activation energies were nearly the same; hence, reaction mechanism was the same as well. Activation energies were found from Arrhenius plots. It is reported that corresponding lactate product was produced as a result of alcoholysis reactions. However, which techniques were used to identify the products was not explained. Only explanation about product identification was determination of optical purity, and it was fulfilled via HPLC. Molecular weight of PLA was determined by Gel Permeation Chromatography (GPC) and it was stated that number average molecular weight of PLA was decreased from 96000 to 8200.

Another alcoholysis research using microwave heating was carried out by Nim et al. (2020). The used diols were ethylene glycol, propane-1,3-diol, and butane-1,4-diol. As catalyst, tetrabutyl orthotitanate was used. PLA: diol weight ratios were varied from 1:1 to 4:1. Reaction temperature and time were kept constant at 240°C and 10 minutes, respectively. The resulting product type depends on the structure of diol, main products were reported as lactate, lactyl lactate, and polylactate. Product characterization was done via Fourier transform infrared (FTIR) spectroscopy. Proton nuclear magnetic resonance (<sup>1</sup>H NMR) spectroscopy was used to investigate

chemical structure of products and their compositions. One different aspect of this study is that after alcoholysis reaction, the alcoholized products were further used to produce lactide-based polyurethanes by reacting with chain extenders. Mechanical tests were applied to the resulting polyurethanes, and they concluded that the produced polyurethanes have promising features to be used in different industries.

In another research linear alcohols, namely ethanol, propanol, and butanol, were employed as reaction media (Lamberti et al., 2020). In this work, corresponding alkyl lactates (ethyl lactate, propyl lactate and butyl lactate) were produced from the catalytic alcoholysis reactions of PLA. As catalyst, zinc ethylenediamine Schiff-based complex and propylenediamine Schiff-based complex were prepared and used. In experiments, firstly tetrahydrofuran (THF) and PLA were added to the reactor (12.5 g of PLA, and 250 ml of THF). After dissolution of pellets, alcohol (50 ml) and catalyst (1 g) were added. Reaction temperature range was between 50-130°C. For product analysis, gas chromatography (GC) and proton nuclear magnetic resonance (<sup>1</sup>H NMR) techniques were used. Activation energy and pre-exponential factor were calculated for lactate formation. They concluded that the reaction took place in ethanol is the fastest among other alcohol types. It was stated that nucleophilic ability diminishes as the chain length of used alcohol increases in THF solvent because of increase in steric hinderance.

Another alcoholysis study was performed by Song et al. (2013), and ionic liquids were employed as catalyst. Methanol was the only alcohol that is used as reaction medium and reaction product was methyl lactate. Effects of reaction temperature, amount of catalyst and amount of alcohol on PLA conversion and methyl lactate yield were explored. Temperature range was in between 90-120°C, the applied weight ratios of methanol to PLA were 4:1, 5:1, and 6:1, and the weight ratios of catalyst to PLA were 0.01:1, 0.02:1, 0.05:1, and 0.10:1. Reaction time was kept constant at 180 minutes. [bmim][Cl], [bmim][PF<sub>6</sub>], [bmim][Ac], [bmim][HSO<sub>4</sub>] ionic liquids were employed and [bmim][Ac] was chosen as the best catalyst. When the reaction ended up, reaction mixture was filtered, and the filtrate was distilled to

regain methanol and receive methyl lactate by vacuum distillation. It was stated that the molecular weights of PLA and primary degradation product were found by GPC.

### **1.2.1.3.3 Pyrolysis Studies:**

Thermal degradation of PLA dates back to 1999. Noda et al., worked on pyrolysis of PLA, which has number average molecular weight ( $M_N$ ) of 99800 g/mol, using titanium, aluminum, tin, zinc, and zirconia metals compounds i.e., metal alkoxides, organic acid salts, halide, and oxide forms as catalyst (Noda et al., 1994). The experimental part was summarized as heating of mixture to 190-245°C with stirring and distilling under reduced pressure (at 4-5 mm-Hg). Condenser temperature was stated as 80°C to avoid crystallization, and the distillate was analyzed via GC. As product, l-lactide, meso-lactide and d-lactide were reported. From the catalytic activity of view, tin has given the best results in terms of lactide production in high concentrations. After tin, zinc, zirconia, titanium, and aluminum have the best activity, respectively.

In another pyrolysis study, PLA was melt blended with tin in different compositions, from 20 to 607 ppm, and exposed to pyrolysis (Nishida et al., 2003). Molecular weight distribution of the synthesized PLA/tin samples was obtained by GPC analysis. It was mentioned that the dynamic pyrolysis reactions were conducted using thermal gravimetric analyzer, and isothermal pyrolysis reactions were carried on in a glass tube oven. Product analysis was done via pyrolysis-gas chromatography mass spectrometry and GC. Pyrolysis reactions were taken place at 40-400°C at a heating rate of 9°C/min. It was reported that when the high tin containing sample was subjected to pyrolysis, the product was lactide, whereas the low tin containing sample yielded cyclic oligomer of PLA. Also, they highlighted that as the tin content increases, degradation temperature of PLA and activation energy of degradation reaction decrease.

Along similar lines, PLA polymer blended with either zinc oxide and titanium dioxide by melt blending technique, and samples were analyzed with thermal

gravimetric analyzer (Wang et al., 2019). According to TGA results, they concluded that both metal oxides decreased the PLA decomposition temperature, but zinc oxide decreased the decomposition temperature by more than 85 K, whereas titanium dioxide decreased nearly between 2 and 10 K; hence, the catalytic activity of zinc oxide was decided to be better than that of titanium dioxide. Similarly, the activation energy of PLA was observed to decrease by 35 kJ/mol and 59 kJ/mol for zinc oxide blend and for titanium dioxide, the amount of decrease was in between 11 kJ/mol and 32 kJ/mol.

A similar study with that of Nishida et al. was conducted by Arrieta et al. In this study; however, PLA was not blended with any metals; virgin PLA was used instead (Arrieta et al., 2013). Pyrolyzer coupled with gas chromatography-mass spectrometry (GC-MS) was used for thermal degradation of PLA. PLA films were used rather than pellets. PLA films were exposed to fast pyrolysis, they were held at 600°C for 0.5 second, and this procedure was repeated for 36 times. As product, meso-lactide, lactide, dimer, trimer and tetramer were mentioned.

Badia et al. (2012), investigated energetic valorization procedure of biobased polymers and selected PLA as a model. Pyrolysis of virgin PLA and mechanically reprocessed PLA were carried out via TGA. Released gas analysis, thermal stability, and decomposition reaction kinetics were provided. Analysis of produced gas was done by using on-line FTIR with the help of 2D IR correlation characterization. From the evolved gas IR analysis, main products were listed as acetaldehyde, lactide, short chain acids and their dimers and trimers, carbon dioxide, carbon monoxide and water. They concluded that pyrolysis process for unprocessed i.e., virgin PLA could be applied for valorization of its processed versions.

The existing PLA depolymerization studies have some drawbacks in terms of sustainability and environmentally friendliness. In hydrolysis processes, water has been utilized. However, water resources have been running out. Because of global warming, there may be water-scarce regions. On the other hand, during alcoholysis reactions volatile organic compounds (VOC) can be released to the atmosphere.

Discharging VOC's to the atmosphere causes ecological and health threats (Mudliar et al., 2010). In pyrolysis processes, due to working at high temperatures (generally  $>200^{\circ}\text{C}$ ), energy consumption can be high. These drawbacks bring about a need for an effective and environmentally benign solution for PLA waste problem. For this purpose, deep eutectic solvents (DES) are considered to be a good choice as the reaction medium for degradation reaction of PLA due to their environmentally friendly, non-toxic, and tunability properties (Abbott et al., 2003).

### **1.3 Deep Eutectic Solvents (DES)**

DES's are a class of mixtures characterized by noteworthy decreases in melting temperatures compared to those of individual components of the mixture. Deep eutectic solvents are prepared by mixing hydrogen bond donor (HBD) and hydrogen bond acceptor (HBA) components in a predetermined molar ratio until a homogenous liquid is formed. DES's have gained attention after Abbott et.al. observed an unusual melting point depression at eutectic composition of predetermined HBD's and HBA's (Abbott et al., 2003). This situation was observed firstly in 1:2 mole ratio combination of choline chloride and urea. Individually, melting temperature of choline chloride is  $302^{\circ}\text{C}$ , that of urea is  $133^{\circ}\text{C}$ , and the resulting mixture maintained its liquid form at room temperature. The reported melting point of the mixture at eutectic composition is  $12^{\circ}\text{C}$ . Due to the low melting temperature of DES's, they are considered as economically feasible and accessible solvents for different applications. In Figure 1.5, melting temperature depression behavior of DES's was visualized.

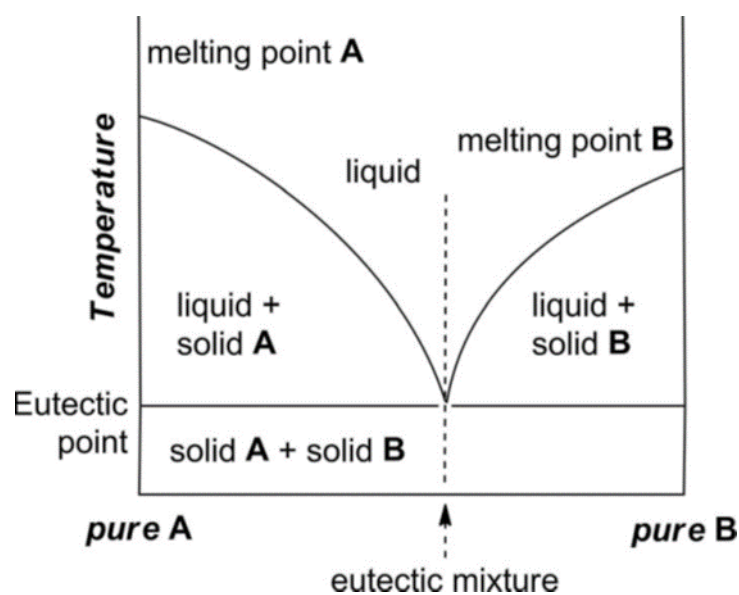


**Figure 1.5.** Binary phase diagram and melting point depression behavior of DES's (Abbott et al., 2003).

In the literature, DES's are seen as an alternative to ionic liquids due to their common features such as, ability to dissolve organic and inorganic compounds, having low volatility and being classified as green solvents (Płotka-Wasyłka et al., 2020). In terms of generally high thermal stability, low toxicity, low volatility, and non-flammability, DES's would not only replace ionic liquids, but also replace VOC in appropriate conditions (Pollet et al., 2014). Having low toxicity and low vapor pressure, DES's are classified as green and sustainable solvents. In addition, DES's are cheaper than ionic liquids and easier to prepare. Ionic liquids can be either purchased or prepared; however, there is no commercially available DES due to the easiness of preparing. Mostly used method of preparation includes mixing of components in desired molar ratio at a predetermined temperature value until homogenous liquid formation occurs. Optionally, inert atmosphere could be preferred during mixing.

Other preparation techniques incorporate vacuum evaporation, grinding, and freeze drying. In the vacuum evaporation method, components of DES are dissolved in water and then most of the water is vaporized at nearly 50°C under vacuum. After

evaporation, mixture is put into desiccator until it has a constant weight value. Grinding method is used when all components are in solid form. In grinding method, solid components are put into a mortar, and they were granulated until a homogenous liquid is produced. In this method inert atmosphere conditions are preferred (Hansen et al., 2021). In freeze drying method, two components of DES are mixed in 5 wt. % water, separately and then two aqueous mixtures are mixed, frozen, and later on freeze dried to obtain a homogenous liquid (Pollet et al., 2014; Hansen et al., 2021).

In general, DES's are viscous liquids, and their colors can vary from white to brownish yellow. Below eutectic point temperature, they appear in cloudy, opaque crystal solid form (Hansen et al., 2021). Different than many standard compounds, DES's display a variety of thermal transition characteristics, such as glass transition and crystallization (Hansen et al., 2021). Glass transition is an important and common characteristic, and it can be observed even under relatively low cooling rates. The commonness of vitrification among DES's points out the interactions which play an important role in DES formation and molecular dynamics. The main judgement states that DES's are produced via self-associated intermolecular interactions, van der Waals interactions, hydrogen, and/or ionic bonding (Hammond et al., 2016; Van Osch et al., 2019). The physical interactions induce a considerable decrease in melting point of mixture by stabilizing liquid configuration; however, individual effects of these interactions are still indefinite and there is a need for further investigation about basics of DES's (Hansen et al., 2021).

Customarily, DES's are composed of two constituents; however, there are some DES types which consist of three components. Nonetheless, tertiary DES's have been hardly studied and investigated until now (Mjalli et al., 2015). In Table 1.1, there are some examples of two-component DES's.



**Table 1.1.** Different types of DES and melting points of resulting DES's and their constituents

Hydrogen Bond Donor & Its Melting Temperature (°C)	Hydrogen Bond Acceptor & Its Melting Temperature (°C)	Melting Temperature of the Resulting DES (°C)
Glycerol, 290	Choline Chloride, 302	17 (2:1 molar ratio) (Mjalli, 2016)
Urea, 133	Choline Chloride, 302	12 (2:1 molar ratio) (Mjalli, 2016)
Ethylene Glycol, -12.9	Zinc Chloride, 290	-30 (4:1 molar ratio) (Abbott et al., 2007)
Choline Chloride, 302	Zinc Chloride, 290	52 (1:2 molar ratio) (Ghareh Bagh et al., 2015)
Acrylic Acid, 14	Choline Chloride, 302	-4 (1.6:1 molar ratio) (Mota-Morales et al., 2011)

Due to their promising features and flexibility of component choice, DES's are widely used in many fields. According to usage purpose, one could select the components of DES and decide its molar composition. This concept brings about easiness of creation of the optimal solvent for desired processes. Some of the application areas of DES's are pharmaceutical and medical research, nanomaterial synthesis, battery technologies, gas capturing and separation, and electrodeposition (Hansen et al., 2021).

### 1.3.1 Deep Eutectic Solvents in Polymer Recycling

Degradation reaction of cellulose that is produced from sunflower stalk was investigated using choline chloride-oxalic acid, choline chloride-citric acid and choline chloride-tartaric acid DES's as both catalyst and solvent (Sert et al., 2018). They used both conventional heating and microwave heating methods. In addition to

heating method, reaction time (30-150 minutes for conventional heating, 1-10 minutes for microwave heating) and temperature (130-180°C) effects were studied. As a result of degradation of sunflower stalk-based cellulose, levulinic acid, 5-HMF, furfural and formic acid were reported. After reaction, products were extracted with ethyl acetate and product analysis was done via HPLC. It was concluded that microwave heating provided energy efficiency by shortening the reaction time to obtain value-added chemicals and utilizing DES as solvent and catalyst was evaluated as efficient to get value-added products from biomass.

In another study, biomass degradation and lignin depolymerization were investigated in three types of DES's (Muley et al., 2019). Microwave heating was used, and choline chloride-formic acid, choline chloride-oxalic acid and choline chloride-lactic acid type DES's were utilized. Temperature range was in between 110-150°C, reaction time was in between 1-15 minutes. Rather than identifying which products were formed after the reaction, molecular weight and bond structure analysis of lignin were reported. It was concluded that oxalic acid and formic acid provided higher yield than lactic acid.

There are also some studies that use DES as auxiliary component in decomposition reactions. In Liu et al.,'s research, bacterial lignin depolymerization was investigated. Prior to bacterial process, lignin samples pretreated with DES (Liu et al., 2018). Wang et al., used DES as catalyst in glycolysis reaction of poly(ethylene terephthalate)(PET) (Wang et al., 2015). Choline chloride-urea and ethylene glycol-choline chloride based DES's were used in electrochemical depolymerization of kraft lignin (Di Marino et al., 2016).

In our work, zinc chloride-urea and zinc chloride-ethylene glycol DES's were used. Firstly, zinc chloride-urea DES was used because it has been widely used in the literature. More specifically, it has been used in depolymerization studies (Lian et al., 2015; Di Marino et al., 2016). Due to stability problems, which will be explained in upcoming sections, another DES containing zinc chloride and ethylene glycol was

investigated. Zinc chloride was kept as the component of DES due to its positive contribution on the thermal stability of DES.

#### **1.4 Catalysts in Polymer Degradation**

In polymer degradation reactions, generally acidic catalysts are used. Commonly used catalysts in these processes are zeolites, amorphous aluminosilicates and other mesoporous materials (Obali et al., 2012; Aydemir et al., 2013). Degradation of polymers which have high molecular weight and complex arrangements is a challenging process. Hence, utilizing an effective catalyst for these processes is crucial. Silica aerogels provide high pore diameter, high surface area, and thermal stability; hence, they can be evaluated as a strong candidate to be used in polymer degradation reactions as catalyst. Except the study which was conducted by our research group (Sivri et al., 2019), there isn't any study that uses aluminum loaded silica aerogel in PLA degradation reaction. In this work, aluminum loaded silica aerogel is used as catalyst due to its promising reported results by Sivri et.al. (2019).

##### **1.4.1 Silica Aerogel**

Kistler et al., synthesized silica aerogel firstly in 1932, and since then silica aerogels have been used in many different areas such as support for catalysts, drug delivery, thermal insulation, and gas sorption purposes (Malfait et al., 2015). In general, for the preparation of silica aerogels, sol-gel method is used. By utilizing different precursors, synthesis method could be altered. Also, changes in synthesis in terms of aging time, drying procedure and solvent type make difference in properties of produced silica aerogels. In a regular silica aerogel synthesis procedure, an alkoxy silane is aggregated with water in alcoholic solutions. Hydrolysis and polycondensation reactions take place at the same time and bring about creation of small silica particles. Reactive groups (hydroxyl or alkoxy) placed on the surface of the particles interact with similar groups on adjacent molecule, and form linkages.

Formation of linkages results in 3-D network of silica molecules. When the network becomes large enough, the liquid sol turns into semi-solid gel. Solid silica molecules adopt a locked position in the network and cannot close pack to have a dense solid mass of silica. Water and alcohol occupy the bulk volume of the structure (Dunn et al., 2005). When the water and alcohol molecules are taken away without disturbing the network, aerogel is produced.

There are three fundamental stages in sol-gel method, which are gel preparation, aging of the gel and drying.

#### **1.4.1.1 Gel preparation stage:**

In this step, hydrolysis and condensation reactions are taking place. Silicon alkoxides (TMOS or TEOS) reacts with water and silanol groups are produced in the presence of solvents (alcohols). For complete hydrolysis, Si: H<sub>2</sub>O proportion is crucial. Hydrolysis reaction usually takes place with acid or base catalysts.

Resulting silanol groups constitute siloxane bridges. They can either react with each other or alkoxides, and water or alcohol is produced. Usually, condensation takes place when alcohols and basic catalyst are present (Gurav et al., 2010). The main silica particles are formed during hydrolysis and condensation stages. These particles connect with each other, and 3-D silica network has been formed.

#### **1.4.1.2 Aging stage:**

Aging process is a crucial stage to reinforce the silica network. Shrinking of pores can be prevented with aging. For aging process, alcohol is poured over the gel to cover the gel. The system is left overnight. During aging process, reactions are completed, and silica aerogels are produced. After aging stage, solvent exchange is applied several times to obviate capillary stress. In solvent exchange, water in the pores could be substituted with hexane (Thapliyal et al., 2014).

### 1.4.1.3 Drying stage:

Shrinkage of gels can be caused by capillary pressure which occurs during evaporation process. The main reason behind this phenomenon is weakness of siloxane bonds towards capillary pressure. To inhibit the formation of cracked aerogels, one solution is replacing some siloxane bonds (Si-O-Si) with the more flexible bond, which is Si-R. The organic group helps aerogel to maintain its wet size by excluding any shrinkage in the gel. Another solution is surface modification. Capillary forces on the silica network are changed with surface modification. Hydroxyl groups linked to silicon molecules are replaced with alkyl groups. As a result of this replacement, more hydrophobic surfaces are formed. Trimethylchlorosilane (TMCS) and methyltrichlorosilane (MTCS) are hydrophobic compounds which are mainly used for the surface modification. TMCS reacts with both silanol groups placed on surface and water inside the pores (Malfait et al., 2015). The last solution employs relation between capillary pressure and surface tension. A solvent can lower the capillary pressure while evaporating in contrast to alcohols and water. However, the utilized solvent should have low surface tension. For example, water in the pores is exchanged with hexane. Because water has surface tension value of 72.53 mN/m at 20°C (Gianino, 2006) whereas that of hexane is 18.43 mN/m at 20°C (Harkins et al., 1921).

Silica aerogels have highly mesoporous structures with high surface area (generally between 500-1200 m<sup>2</sup>/g), high porosity (about 80-90%), low thermal conductivity (0.005 W/mK) and low density (approximately 0.003 g/cm<sup>3</sup>). Their pore sizes change between 5-100 nm, with an average pore diameter between 10-40 nm (Soleimani et al., 2008).

### 1.4.2 Silica Aerogel Applications in Literature

In Yu et al.'s study, cobalt was loaded on silica aerogel support. Then, cobalt loaded silica aerogel catalyst was used to produce hydrogen from aqueous ammonium

borane (Yu et al., 2015). BET surface area, pore size and pore volume of the synthesized catalyst were reported as 449 m<sup>2</sup>/g, 1.4 cm<sup>3</sup>/g and 12.3 nm, respectively. Performance of silica aerogel supported cobalt catalyst was compared with that of mesoporous silica supported cobalt catalyst. It was concluded that silica aerogel supported cobalt catalyst showed nearly 40% higher hydrogen production. Also, silica aerogel supported cobalt catalyst decreased the activation energy of reaction more than mesoporous silica supported catalyst; however, percentages of these decreases were not given. As a result, silica aerogel supported cobalt is an efficient catalyst to generate hydrogen from aqueous ammonia borane.

In another study, silica aerogel supported cobalt containing catalysts were used for Fischer-Tropsch synthesis (Dunn et al., 2005). Cobalt was loaded at three different mass percent; 2, 6, and 10 weight percent. In drying stage, supercritical ethanol conditions were used. Synthesized catalysts have surface area between 570-770 m<sup>2</sup>/g, pore volume between 3.7 and 4.7 cm<sup>3</sup>/g, and pore diameter ranging from 21 to 37 nm. As conclusion, they stated that three different mass percent metal loaded catalysts were active in Fischer-Tropsch synthesis with good selectivity for hydrocarbons having more than 10 carbon. Amiri et al. (2015), also used the copper loaded silica aerogel catalysts, but they utilized the catalyst in methanol steam reforming reaction. In this work, chemical surface modification and ambient pressure drying processes were applied. Synthesized catalysts had surface area and pore size distribution in between 1-10 nm. Also, particle size was evaluated as uniform, it ranged between 5-20 nm.

Related with usage of metal loaded silica aerogels in depolymerization reactions, there is a work conducted by our research group (Sivri et al., 2019). In this work, aluminum loaded silica aerogels were synthesized and used in thermal degradation of PLA. Aerogels were synthesized via sol-gel method and metal loading was carried out via wet impregnation method. Aluminum was loaded at three different weight percent, 2.5, 10, and 15. Thermal degradation experiments were performed in TGA. It is concluded that the greatest decrease in the activation energy of thermal

degradation reaction of PLA was achieved with 15 % aluminum loaded silica aerogel catalysts, decreasing the activation energy by 27 %.

## **1.5 The Aim of This Study**

Due to its mechanical, thermal, and optical properties, usage areas of PLA is increasing day by day. The increased demand for PLA will lead to a rise in amount of PLA waste.

In literature, there were biological, chemical, and mechanical degradation studies regarding the emerging PLA waste problem. Although PLA is classified as a biodegradable plastic, only a few microorganism type can play a role in PLA biodegradation, and they are not present in all soil types. Some certain conditions such as, temperature, pH and moisture content of soil or compost should also be provided for biodegradation. Chemical recycling techniques are pyrolysis, hydrolysis and alcoholysis. These techniques can be regarded as unsustainable in terms of energy consumption in pyrolysis, usage of water which is limited renewable resource in hydrolysis, and emission of volatile organic compounds in alcoholysis studies. According to literature survey, PLA degradation has not been studied in DES medium. In addition, catalytic degradation of PLA has not been investigated in DES medium.

Hence, the aim of this study is to present an effective and environmentally benign solution for PLA waste problem. In this study, the following steps were aimed and carried out:

- To synthesize and characterize a deep eutectic solvent (DES) and metal loaded silica aerogel catalysts.
- To determine the apparent activation energy of the PLA degradation reaction.
- To investigate the degradation of PLA in DES medium in different reactor systems.

- To search for the activity of the metal loaded silica aerogel in PLA degradation in DES medium.
- To observe the effect of catalyst and system type on the obtained product distribution.



## CHAPTER 2

### EXPERIMENTAL

#### 2.1 Experimental Set-ups and Procedures

Experimental part of this study consists of three main parts, which are synthesis and characterization of DES, synthesis and characterization of catalysts and, degradation reaction of PLA at 180°C for 8 hours in two different reactors.

##### 2.1.1 Synthesis of Deep Eutectic Solvents (DES)

To be used as reaction medium in the degradation reaction of PLA, two kinds of DES were synthesized. These DES's were zinc chloride-urea DES and zinc chloride-ethylene glycol DES.

###### 2.1.1.1 Zinc Chloride-Urea DES Synthesis

Prior to synthesis, zinc chloride and urea were dried in an oven at 110°C for 24 hours. To synthesize urea-zinc chloride DES, zinc chloride (Sigma Aldrich) and urea (Merck) were mixed. This type of DES was synthesized in 4:10 molar ratio. For 4:10 molar ratio, 5.47 g zinc chloride and 6 g urea were weighed and put into a glass reagent bottle, respectively. After that, the reagent bottle was put into the water bath operating at 80°C. The water bath was placed on a heated magnetic stir plate with a thermocouple. They were mixed until a homogenous liquid was obtained and this process took nearly 3 hours.

### 2.1.1.2 Zinc Chloride-Ethylene Glycol DES Synthesis

Before synthesis, zinc chloride was dried in oven at 110°C for 24 hours. To synthesize zinc chloride-ethylene glycol DES, zinc chloride (Sigma Aldrich) and ethylene glycol (Sigma Aldrich) were mixed in 1:3 molar ratio (zinc chloride: ethylene glycol). For 1:3 molar ratio, approximately 6 g zinc chloride and 8.19 g ethylene glycol were weighed and put into a glass reagent bottle, respectively. Then, the reagent bottle was put into the water bath that operates at 80°C. Temperature of water bath was kept constant with heated magnetic stir plate with a thermocouple. Zinc chloride and ethylene glycol were mixed for nearly 2 hours until a homogenous solution was formed. In Figure 2.1, experimental setup for DES preparation was shown.

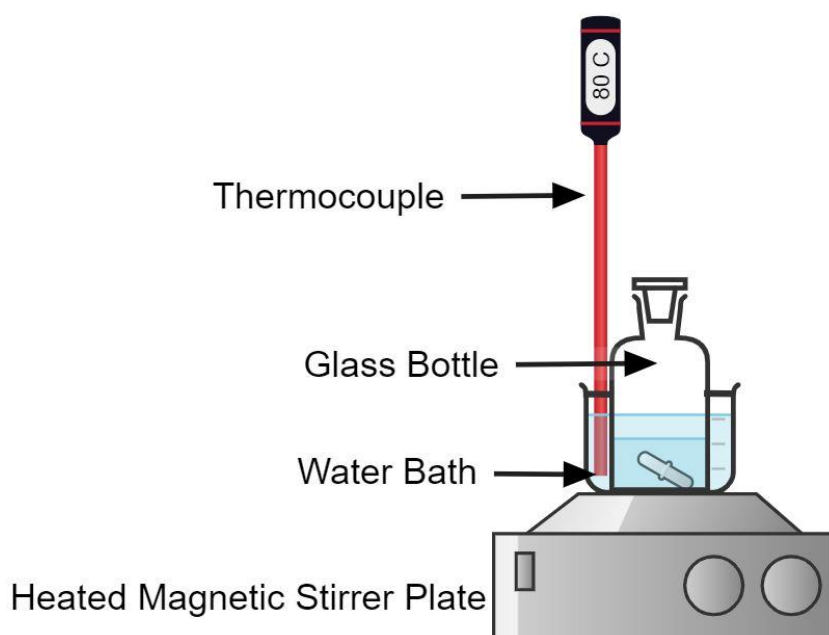


**Figure 2.1.** Experimental setup for DES synthesis

### 2.1.1.3 Characterization of DES's

Synthesized DES's were characterized with FTIR and TGA.

#### **2.1.1.3.1 FTIR Analysis**

FTIR analysis was performed to observe complexation between components of DES. Perkin Elmer Spectrum Two Model FTIR spectrophotometer with Attenuated Total Reflection (ATR) was used in the analyses. The spectra were obtained in the wavenumber range of 500  $\text{cm}^{-1}$  and 4000  $\text{cm}^{-1}$  accumulated of 256 scans with 4  $\text{cm}^{-1}$  resolution.

#### **2.1.1.3.2 TGA Analysis**

TGA analysis was carried out to determine the thermal stability of the synthesized DES. Shimadzu TA-60 WS device was used. Analyses were done under nitrogen atmosphere with a flowrate of 50 ml/min. Temperature was increased from room temperature to 500°C with a heating rate of 5°C/min.

### **2.1.2 Synthesis of Catalyst**

Aluminum loaded silica aerogel catalyst was used in the degradation reaction of PLA. Silica aerogel was synthesized according to sol-gel method. Then, aluminum was loaded on silica aerogel in two different weight percentages i.e., 15 and 25 %. Wet impregnation method was used for loading of aluminum.

#### **2.1.2.1 Synthesis of Silica Aerogel Support Material**

For the synthesis of silica aerogel firstly, 5.64 g absolute ethanol (Sigma Aldrich), 1.73 g pure water and 10.01 g tetraethyl orthosilicate (TEOS, Merck), which is the silica source, were mixed at room temperature. After that, to the mixed solution, 62  $\mu\text{L}$  of 1 M HCl was added drop by drop and they mixed for two hours. Then, to the mixed solution, 3.85 g pure water and 9.92 g ethanol were added at room temperature. For gel formation, 650  $\mu\text{L}$  of 1 M ammonia ( $\text{NH}_3$ , 25% v/v, Merck) and

800  $\mu\text{L}$  of ammonium fluoride ( $\text{NH}_4\text{F}$ , Merck) solutions were dropped to the solution. When the gel was formed, it was cut into smaller parts and ethanol was poured onto gel pieces and at room temperature, 8 hours of aging process was started. After aging, ethanol was drained over the gel and 30 ml hexane (Sigma Aldrich) was poured onto gel and gel was put into water bath which operates at  $45^\circ\text{C}$  for 2 hours. After completion of 2 hours, hexane was refreshed with 30 ml hexane and trimethyl chlorosilane (TMCS, Merck), which is the silylation agent, was dropped to the solution. When TMCS was added, water formation was occurred, and it was removed from the solution and fresh hexane was added to complete the hexane volume to 30 ml. Then, the gel was put into water bath operating at  $45^\circ\text{C}$ . In every 5 hours, hexane was refreshed for two times. As final step, gel was put into an oven at a temperature of  $125^\circ\text{C}$  for 2 hours (Değirmencioğlu, 2018; Habib, 2019). Experimental setup, and steps were summarized in Figure 2.2.

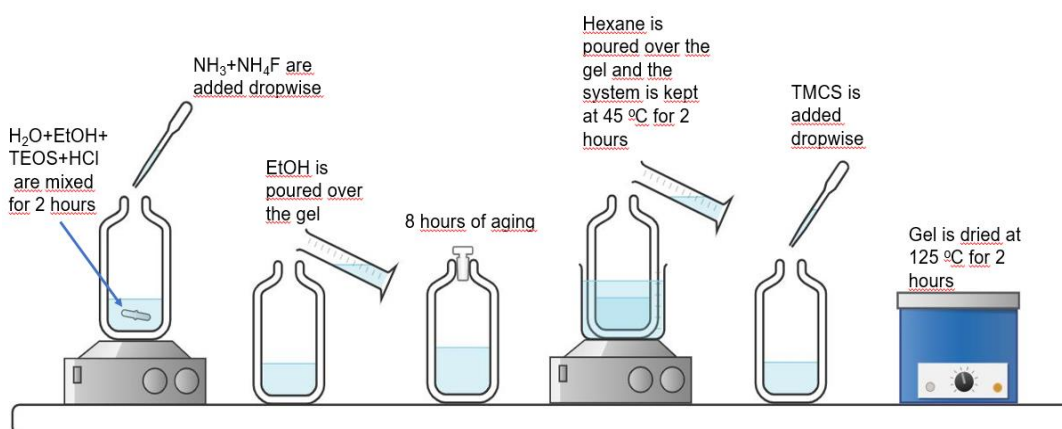


**Figure 2.2.** Experimental setup for silica aerogel synthesis

### 2.1.2.2 Aluminum Loading to the Silica Aerogel by Wet Impregnation Method

Aluminum (15 and 25 wt. %) was loaded to the synthesized silica aerogel support material using wet impregnation method. Aluminum nitrate nonahydrate ( $(\text{Al}(\text{NO}_3)_3 \cdot 9\text{H}_2\text{O})$ , Sigma Aldrich) was used as aluminum source. 1 g silica aerogel

was weighed and added to 20 ml of ethanol. In the meantime, aluminum precursor (2.1 g) was dissolved in 10 ml of ethanol. Silica aerogel-ethanol and aluminum precursor-ethanol pairs were mixed separately for two hours at room temperature. After completion of two hours, metal precursor solution was added to the silica aerogel solution dropwise and the solution was mixed for 24 hours at room temperature. Then, the mixture was dried in an oven at 60°C for 24 hours. As a final step, the dried sample was calcined in a tubular quartz reactor and heated from room temperature to 500°C with a heating rate of 1°C/min and the catalyst was kept at this temperature for 12 hours in nitrogen atmosphere with a flowrate of 50 ml/min. At the end of calcination step, the aluminum loaded silica aerogel catalyst was synthesized.

### **2.1.2.3 Characterization of Catalyst**

The synthesized silica aerogel and aluminum loaded silica aerogel catalysts were characterized with FTIR, TGA, Nitrogen sorption, Scanning Electron Microscopy with Energy Dispersive X-ray Spectroscopy (SEM-EDX), and Diffuse Reflectance Infrared Fourier Transform Spectroscopy (DRIFTS).

#### **2.1.2.3.1 FTIR Analysis**

FTIR analysis was carried out to observe the structure and chemical bonds of silica aerogel. Perkin Elmer Spectrum Two Model FTIR spectrophotometer with Attenuated Total Reflection (ATR) was used in the analysis. The spectra were obtained in the wavenumber range of 500  $\text{cm}^{-1}$  and 4000  $\text{cm}^{-1}$  accumulated of 128 scans with 4  $\text{cm}^{-1}$  resolution.

#### **2.1.2.3.2 TGA Analysis**

TGA analysis was used to get information about thermal stability of the synthesized catalyst. TGA analyses were performed with Shimadzu TA-60 WS device under nitrogen atmosphere with a flowrate of 50 ml/min. Temperature was increased from room temperature to 700°C with a heating rate of 5°C/min.

#### **2.1.2.3.3 Nitrogen Sorption Analysis**

With nitrogen sorption analysis, pore volume, pore size distribution, Braun Emmett Teller (BET) surface area of silica aerogel and catalysts were determined. Adsorption-desorption isotherm plots of the synthesized materials were obtained in the relative pressure ( $P/P_0$ ) range of 0.0001 and 0.99. Micromeritics Tristar II 3020 equipment was used. Before analysis, samples were degassed at 200°C for 4 hours.

#### **2.1.2.3.4 Scanning Electron Microscope and Energy Dispersed X-ray Analysis**

Morphological properties and elemental content of synthesized catalysts and silica aerogel were observed using QUANTA 400F field-emission scanning electron microscope in the Central Laboratory, METU. In addition, TESCAN VGA3 scanning electron microscope in METU Chemical Engineering Department was also used. Prior to analyses, samples were coated with Au/Pd.

#### **2.1.2.3.5 Diffuse Reflectance Infrared Fourier Transform Spectroscopy Analysis**

DRIFTS analysis was performed to determine the acid sites of the synthesized catalysts. Perkin-Elmer Spectrum One FTIR spectrophotometer was used and the

wavelength range was set to 400-4000  $\text{cm}^{-1}$ . 100 scans were recorded at 4  $\text{cm}^{-1}$  resolution.

Before the analysis, 0.1 g of each sample was weighed and put into an oven at 120°C for 12 hours to remove the moisture content. Then, all catalysts were put into desiccator together with nearly 10 ml pyridine, and they were kept in the desiccator for one week in order for catalysts to adsorb pyridine vapor. After one week, firstly the background spectrum of KBr and then, the spectra of fresh and pyridine-adsorbed catalysts were recorded. Final spectrum of the catalyst was obtained by subtracting the spectrum of pyridine-adsorbed catalyst from that of the fresh catalyst.

### **2.1.3 PLA Degradation Reaction Systems**

PLA degradation reactions were carried out in DES medium and in two different systems, which are batch and semi-batch systems, with/without metal loaded silica aerogel catalysts. In both systems, reaction temperature and duration were constant at 180°C and 8 hours, respectively. To test the activity of the catalysts, thermogravimetric analysis was performed.

#### **2.1.3.1 Degradation of PLA with/without Catalyst Using Thermogravimetric Analyzer**

Performance of the synthesized catalysts in PLA degradation reaction was also evaluated using thermogravimetric analyzer (Shimadzu TA-60 WS). PLA (NatureWorks 2003D, Specific Gravity: 1.24, Melting Point: 145-160°C, and Melt Flowrate: 6 g/10 min) and catalyst were put into TGA cell with the PLA: catalyst weight ratio of 2. Temperature was increased from room temperature to 500°C with a heating rate of 5°C/min. Analyses were performed under nitrogen atmosphere with a flowrate of 50 ml/min.

### **2.1.3.2 Experimental Setup for PLA Degradation in Batch System**

Degradation reaction of PLA in DES medium in batch system was carried out in a glass flask which has volume of 10 ml. Approximately 8.2 g of DES and 3 g of PLA were added to a glass flask. In catalytic experiment, approximately 1.5 g catalyst was added. The glass flask was put into an oil bath and thermo couple of the heater was immersed in oil. Oil temperature was adjusted to 180°C using the heated magnetic stirrer plate. A condenser was placed to the exit of flask to condense volatile components. Condenser temperature was set to 10°C. DES and PLA were mixed with the help of magnetic stirrer. At the end of 8 hours of reaction, it was waited until the glass flask cooled to room temperature. Then, glass flask with reaction mixture was weighed. To extract the reaction products from the reaction mixture, ethyl acetate solvent was used. Approximately 5 ml of ethyl acetate was added to glass flask. The mixture was stirred with magnetic stirrer for 2 hours. Two-phase mixture was formed. Then, the top phase of the heterogenous mixture was collected with a plastic dropper, and put into another glass container. This step was repeated for nearly 5 times. In Figure 2.3 and Figure 2.4, the diagram and photograph of the experimental setup were shown, respectively.



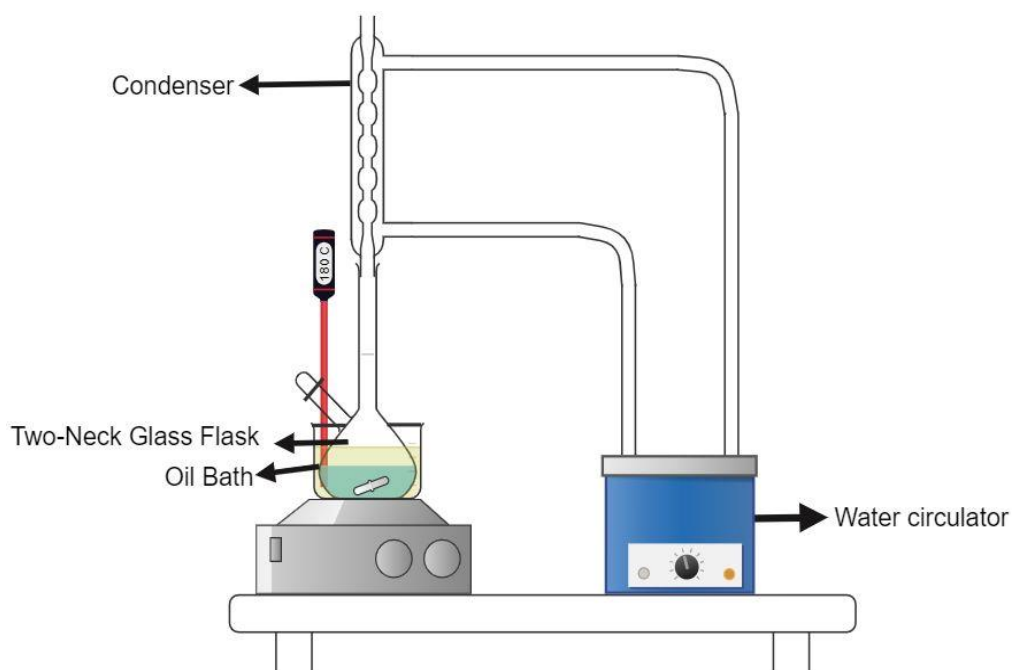


**Figure 2.3.** Experimental setup of the PLA degradation reaction in batch reactor



**Figure 2.4.** Photograph of the batch experimental setup used for PLA degradation

### **2.1.3.3 Experimental Setup for PLA Degradation in Semi-Batch System**

In the semi-batch system, nitrogen gas passed through the system during the reaction period. Nitrogen tank was connected to mass flow controller (Alicat Scientific) to set the gas flowrate to the desired value. 8.2 g DES, 3 g PLA, and in catalytic experiment 1.5 g catalyst were put into reactor and tightly sealed to avoid gas leakage. Before starting the experiment, gas leakage control was carried out. For this purpose, nitrogen gas passed through the system and flowrate was checked from the soap bubble meter. Heating program, and furnace temperature were set from the screen placed on the reactor panel. The degradation reactions were carried out at 180°C for 8 hours. Nitrogen stream leaving the gas tube entered to the reactor. The exit stream from the reactor was heated to the reaction temperature with a thermocouple connected to a heating tape in order to prevent condensation of products in the exit stream. At the exit of the reactor, there were three traps to collect non-volatile products. Traps were immersed into water bath at 20°C. The exit stream of the third trap was connected to condenser with a hose. Condenser temperature was set to -5°C. At the bottom of the condenser there was a small container to collect condensed samples. Gas samples leaving the condenser passed through gas collecting bottle, and gas samples were taken within certain time intervals and analyzed with Gas Chromatography (GC). In order to control the gas flowrate, and check whether there is any gas leakage, soap bubble meter was placed. From the exit of soap bubble tube, gas stream was gone to ventilation system. In Figure 2.5, schematic drawing of semi-batch system was shown.

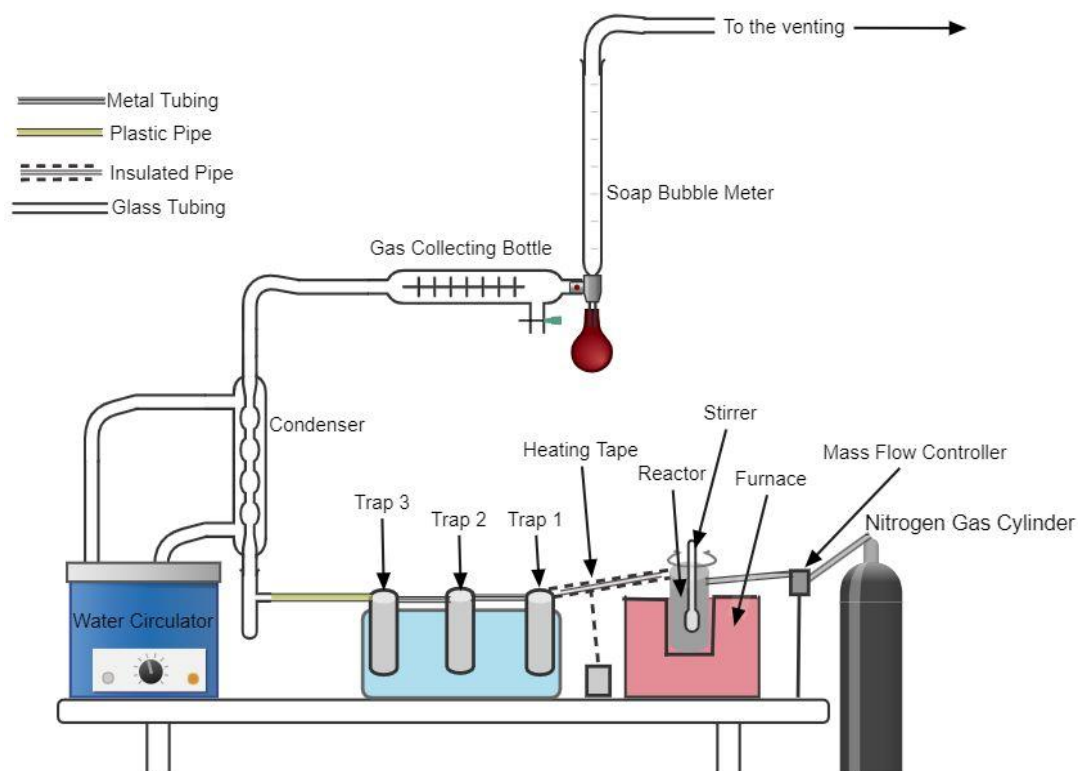


**Figure 2.5.** The semi-batch experimental setup used for PLA degradation

After the reaction, it was waited until the reactor temperature decreased to about 100°C. Then, gas flowrate was decreased gradually and then closed. Reactor and traps were weighed and subtracted from the empty weights of traps and reactor to determine the amount of liquid and solid formed. In all experiments, there was only liquid product in the first trap. The others were empty. For liquid product analysis, contents of the first trap were dissolved in acetone according to 20 mg/ml concentration. The obtained solution was analyzed with Gas Chromatography-Mass Spectrometry (GC-MS).

#### 2.1.3.4 Analysis of Liquid and Gas Products of the Degradation Reactions

Liquid products from degradation reaction of PLA in both batch and semi-batch systems were analyzed using GC-MS. Gas products resulted from degradation reaction in semi-batch system were analyzed with GC.

#### 2.1.3.4.1 GC-MS Analysis

GC-MS analysis was used to determine the distribution of the products obtained with extraction of the reaction mixture in batch degradation reactions and distribution of liquid products obtained from semi-batch degradation reactions. Shimadzu QP2020 –GCMS device with TRB-1 column was used. Injection and MS detector temperature was 200°C. The carrier gas was helium with flowrate of 1.5 ml/min. The library used for identification of peaks was WilyNist (W9N11). In Table 2.1, heating program of furnace was shown.

**Table 2.1.** Furnace heating program used in GC-MS analysis

Temperature (°C)	Hold Duration (min)	Heating Rate (°C/min)
35	2	8
300	25	-

#### 2.1.3.4.2 GC Analysis

Analyses of gas products from degradation reaction in the semi-batch system were carried out with GC equipped with Porapak Q column and thermal conductivity detector (TCD). Detector temperature was 200°C. Argon was the carrier gas with a flowrate of 30 ml/min. Column temperature program was shown in Table 2.2.

**Table 2.2.** Temperature program of GC column

Temperature (°C)	Hold Duration (min)	Heating Rate (°C/min)
38	6	-
120	1	4
130	0.1	1
170	0.4	20

## **CHAPTER 3**

### **RESULTS AND DISCUSSION**

In this thesis study, firstly DES and catalysts were synthesized. The following part is dedicated to the characterization results of the synthesized DES and catalysts. Following, the degradation of DES in batch and semi-batch systems was investigated; the product distribution obtained in each system is given. Finally, catalytic and non-catalytic degradation reactions of PLA in zinc chloride-ethylene glycol DES medium in batch and semi-batch systems were investigated, and the results are presented and discussed in the dedicated parts.

#### **3.1 Synthesis and Characterization of DES**

Deep eutectic solvents were prepared as described in the experimental part. After synthesis, some characterizations and observations related with their stability were carried out and compared with literature data.

##### **3.1.1 Zinc Chloride-Urea DES**

Zinc chloride-urea DES is one of the mostly used DES's in the literature. It is environmentally benign. Its components are also relatively cheap and easily accessible. Hence, the first selection for reaction medium was zinc chloride-urea DES.

### 3.1.1.1 FTIR Analysis

In order to verify DES formation between urea and zinc chloride, FTIR analysis technique was used. Comparison of FTIR spectra of urea and the synthesized DES provided important information about the complexation.

In Figure 3.1, FTIR spectra of urea and the synthesized DES are compared in the light of Lian et al.'s work.

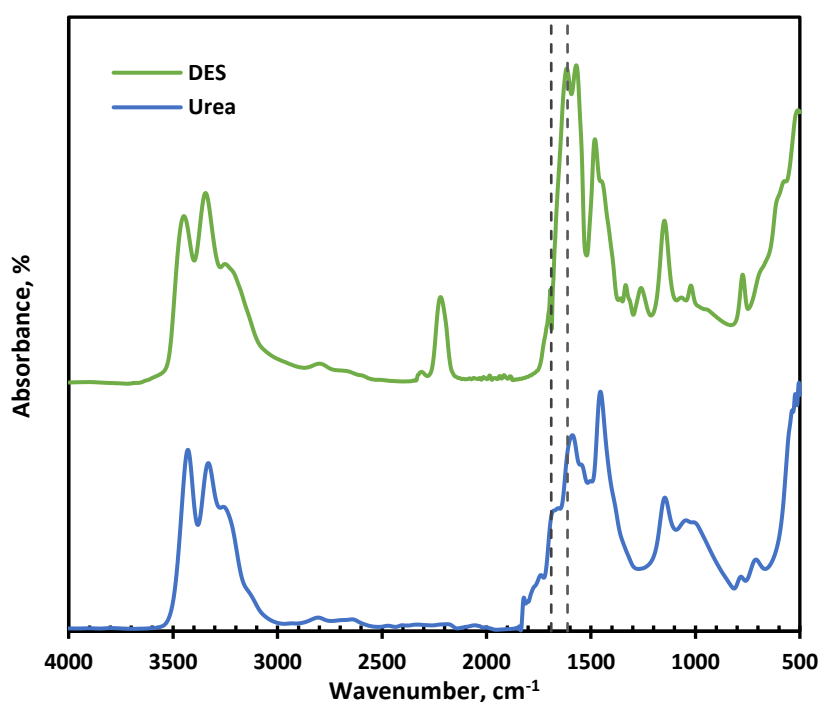


**Figure 3.1.** FTIR spectra of urea and DES

In FTIR spectrum of urea, the peak at  $1690\text{ cm}^{-1}$  was attributed to carbonyl (C=O) stretching vibrations (Gözde, 2019; Premanathan, 2010). The peaks located between  $3300\text{--}3500\text{ cm}^{-1}$  are ascribed to stretching of N-H bonds (Bacher, 2002). According to Figure 3.1, it was observed that new peaks were formed in DES. The peaks at  $2210$ ,  $1328$ , and  $1250\text{ cm}^{-1}$  were the newly formed peaks in DES. These peaks were considered as the indication of formation of new bonds in DES. In the literature, formation of these peaks were also observed at  $2210$ ,  $1320$  and around  $1240\text{ cm}^{-1}$  wavenumbers (Wang et al., 2015; Lian et al., 2015; Gözde, 2019).

Another difference between spectra of urea and DES was related to the shifting in the peak of carbonyl group of urea from  $1690\text{ cm}^{-1}$  to  $1608\text{ cm}^{-1}$  because of DES formation.

The function of urea as ligand was considered to be dependent on the type of transition metal ion that will bond to urea (Theophanides et al., 1987). Urea contains two functional groups, carbonyl and amino, which are able to form metal-urea complex groups. In case of oxygen atom in carbonyl group participates in complexation with metal ion, stretching vibration of carbonyl group moves to lower wavenumbers, which was observed in this study. On the other hand, if nitrogen atom in amino group participates in complexation, stretching vibration of carbonyl group moves to higher wavenumbers (Lian et al., 2015).

Zn-O bonding in transition metal salts with urea has been studied in literature (Custelcean et al., 2006). While bonding,  $\text{Zn-O-C=N}$  and  $\text{Zn-O=C-N}$  resonance structures could be observed. The newly formed peaks in DES spectrum may be attributed to the presence of resonant structures as a consequence of the complexation of urea and zinc chloride.

As a result of observing complexation peaks, it can be said that DES was synthesized successfully.

### **3.1.1.2 Stability of DES**

Stability of DES indicates the duration in which DES retains its liquid state. Zinc chloride-urea DES was synthesized in 4:10 molar ratio. According to literature, stability of 4:10 ratio was reported as 7 days (Lian et al., 2015). However, our synthesized DES in 4:10 molar ratio kept its liquid state for 3 days. The differences in stability observations may be caused by storage conditions or seasonally changing room temperature values.

In Figure 3.2, freshly synthesized DES and DES starting to lose its stability were shown. The freshly synthesized DES has a clear and homogenous appearance. On

the other hand, cloudy appearance in DES was firstly observed in an unstable DES and then as the time passes this cloudiness spread.

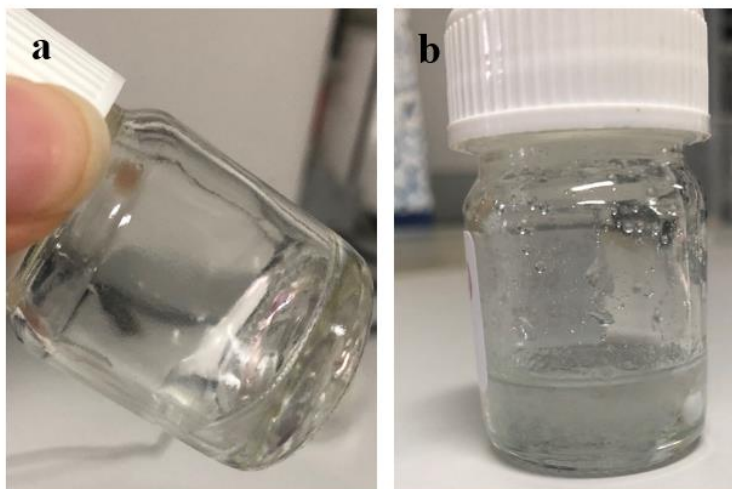


**Figure 3.2.** a) Freshly synthesized DES and b) an unstable DES, 3 days after the synthesis

The solidification in DES can be attributed to the breakage of hydrogen bonds that are responsible for complexation.

### 3.1.1.3 TGA Analysis

Thermal stability of zinc chloride-urea DES in 4:10 molar ratio was tested via thermogravimetric analyzer (TGA) and compared with literature data. In Figure 3.3, TGA curve is shown.



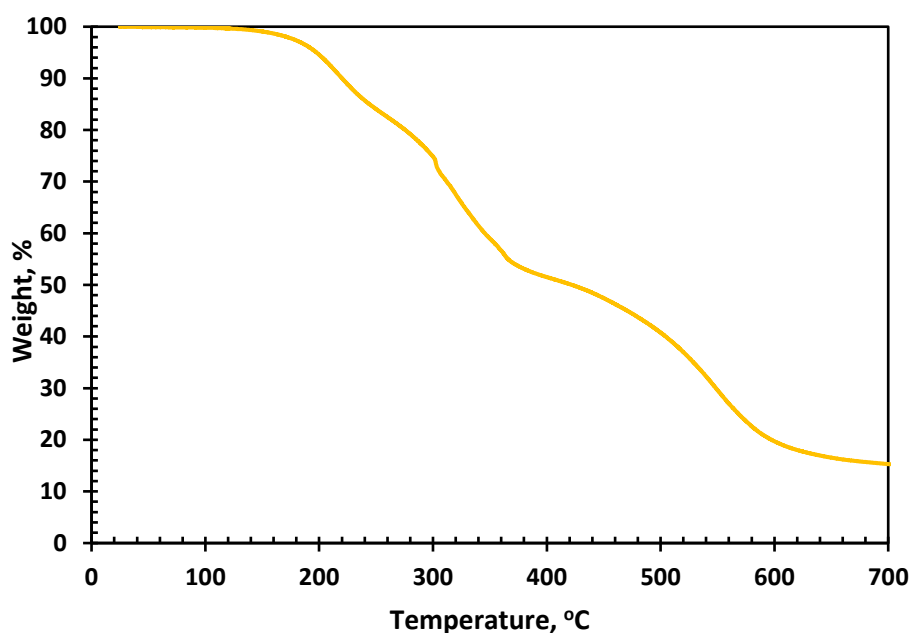


**Figure 3.3.** TGA curve of zinc chloride-urea DES

Weight loss at 180°C is recorded as 2.7 %. Moisture content in zinc chloride was seen as the reason of this weight loss. In the study of Lian et.al., for 3:10 molar ratio the first step was observed at 227°C, similarly our TGA curve gave the first step at 226.9°C. The second and third steps were reported at 325 and 528°C, respectively. In our TGA curve, there were peaks at 327.8 and 524.7°C, which are consistent with the reported literature data. The weight loss observed after 400°C can be due to the evaporation of zinc chloride (Jones et al., 2013).

In order to see the effect of long-term exposure to heat, only DES was heated at 180°C for 2 hours. When 2 hours of heating was completed, there was a solid and liquid phases in the mixture inside the reactor. The liquid part was separated into another glass container. In Figure 3.4, there are pictures which were taken from DES heated at 180°C and freshly synthesized DES, respectively.

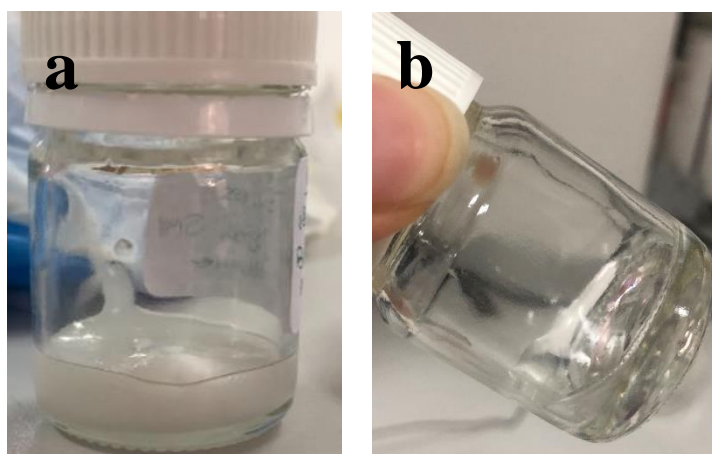


**Figure 3.4.** Photographs of a) DES heated at 180°C for 2 hours and b) freshly synthesized DES

As seen in Figure 3.4, even after keeping for 2 hours at 180°C, appearance of DES was changed. It has a clear, homogenous, and transparent appearance when synthesized freshly; however, after heating it become a white, solid-like state. Hence, it can be concluded that the hydrogen bonds which are formed during synthesis of DES are disrupted. Due to this solidification issue, another DES was searched to be used as reaction medium for degradation of PLA. One component of the new DES was kept as zinc chloride in order to enhance the thermal stability of DES due to its thermally stable nature. The other new component was preferred to be in liquid form at room temperature in order not to experience solidification problems. Literature survey was carried out for selection of other component and ethylene glycol was decided to use. Ethylene glycol is an affordable and accessible chemical substance. Zinc chloride-ethylene glycol DES was used in arylation reaction of benzoxazoles as catalyst (Tran et al., 2018), and in this study the important weight loss of DES was observed between 200-475°C, revealing a preferable thermal stability. Ethylene glycol was also used as reaction medium in an alcoholysis study of PLA (Nim et al., 2020). Hence, in this study, another DES was selected as zinc chloride-ethylene glycol.

### 3.1.2 Zinc Chloride-Ethylene Glycol DES

Due to its reported thermal stability zinc chloride-ethylene glycol DES was synthesized in 1:3 and 1:4 molar ratios (Tran et al., 2018), and some characterizations were carried out.

Since the decomposition temperature of zinc chloride is higher than the decomposition temperature of ethylene glycol, the higher concentration of zinc chloride in DES has been preferred in this study.

#### 3.1.2.1 FTIR Analysis

In order to verify DES formation between ethylene glycol and zinc chloride, FTIR analysis technique was used. Comparison of FTIR spectra of ethylene glycol and the synthesized DES provided important information about the complexation.

FTIR spectra of ethylene glycol was shown in Figure 3.5. At around  $3390\text{ cm}^{-1}$  characteristic wavelength of -OH group was observed (Bacher, 2002). The peaks located at  $2944, 2878\text{ cm}^{-1}$  wavenumbers are ascribed to -CH<sub>2</sub> stretching. At  $1034$  and  $1084\text{ cm}^{-1}$ , C-O stretching was observed. When the FTIR spectra of DES and ethylene glycol were observed, it can be said that they almost overlapped with each other. Exceptionally, the peak at  $3390\text{ cm}^{-1}$  in ethylene glycol, which represents the -OH stretching vibration, shifts to a lower wavenumber in DES. Tran et.al., reported the same observations and attributed this shifting to -OH groups in ethylene glycol playing role in the formation of hydrogen bond with the anion part of zinc chloride (Tran et al., 2018).

In Figure 3.5, FTIR spectra of ethylene glycol and DES are shown.

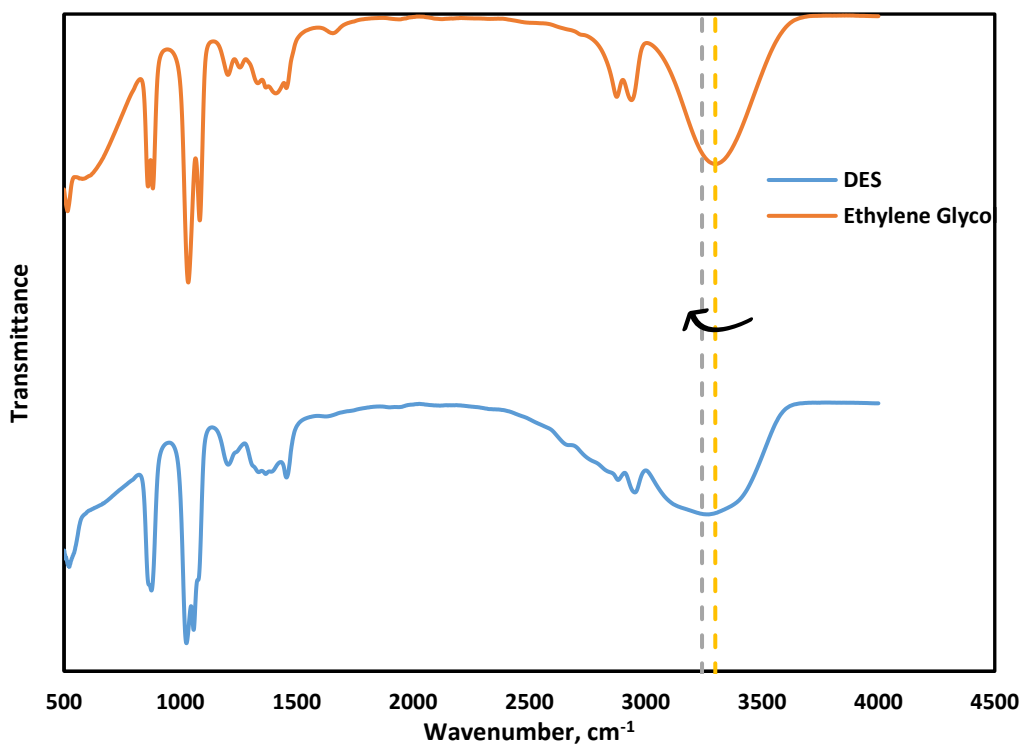


**Figure 3.5.** FTIR spectra of ethylene glycol and zinc chloride-ethylene glycol DES

As seen in Figure 3.5, the mentioned shifting around  $3390\text{ cm}^{-1}$  was observed in our synthesized DES. Hence, -OH group in ethylene glycol took part in formation of DES. According to analysis, zinc chloride-ethylene glycol DES was synthesized successfully.

### 3.1.2.2 Stability of DES

In regard to our observation, zinc chloride-ethylene glycol DES maintains its liquid state over 7 months. According to our literature review, zinc chloride-ethylene glycol DES was not studied in terms of stability.

### 3.1.2.3 TGA Analysis

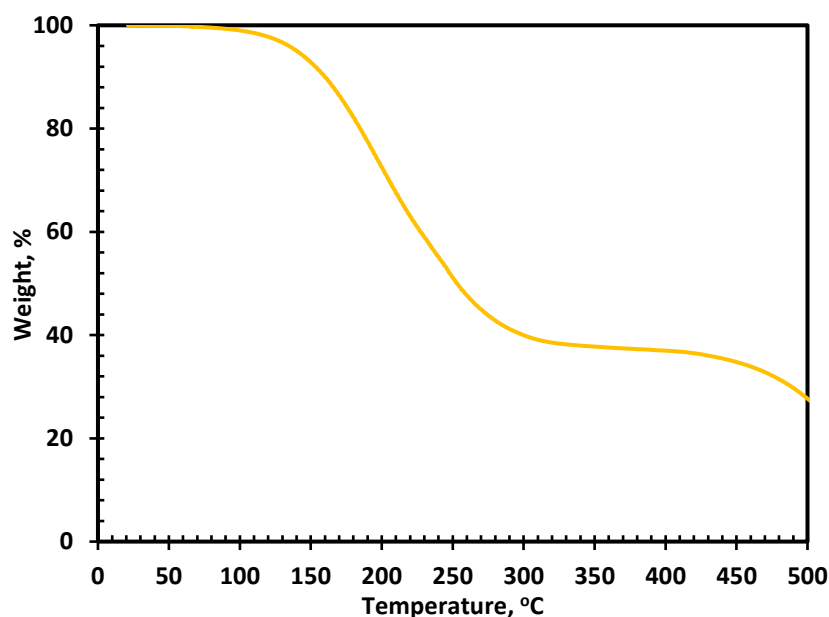


**Figure 3.6.** TGA analysis of zinc chloride-ethylene glycol DES

In Figure 3.6, TGA analysis for this DES is given. According to Figure 3.6, at 200°C, weight loss is nearly 28 % and that of 475°C is 68 %. It was thought that the weight loss observed after 400°C may be due to the evaporation of zinc chloride (Jones et al., 2013). Thermal stability analysis of zinc chloride-ethylene glycol DES was investigated by Tran et al. (2018). According to their TGA data, they stated that the noteworthy weight loss observed between 200-475°C. The obtained TGA data were consistent with the literature data.

For reaction temperature selection, thermal behavior of DES and melting temperature of PLA were taken under consideration. At 180°C, there is nearly 17 % weight loss in DES, which can be seen as a moderate weight loss value. Also, melting temperature of PLA is found as between 145-160°C (Sivri et al., 2019). Hence, 180°C is considered as optimum temperature for degradation reaction of PLA.

In order to see the effect of complexation between zinc chloride and ethylene glycol on thermal characteristics, TGA results of DES and ethylene glycol were compared

in Figure 3.7. The degradation of ethylene glycol started at a lower temperature when compared to DES. According to these results, it can be concluded that zinc chloride plays an important role to enhance thermal stability of DES. The obtained data were compared with data found from literature, and almost identical results were observed (Toxqui-Terán et al., 2018). For ethylene glycol, it was stated that the initial weight loss was observed at 58°C. At that temperature, we have nearly 0.1 % weight loss, which is consistent with the literature. They described the thermal behavior of ethylene glycol as a sharp single-step weight loss behavior, and this trend ended at 164°C. In parallel with this statement, a sharp weight loss was also observed at the temperature range of 98°C and 164°C.

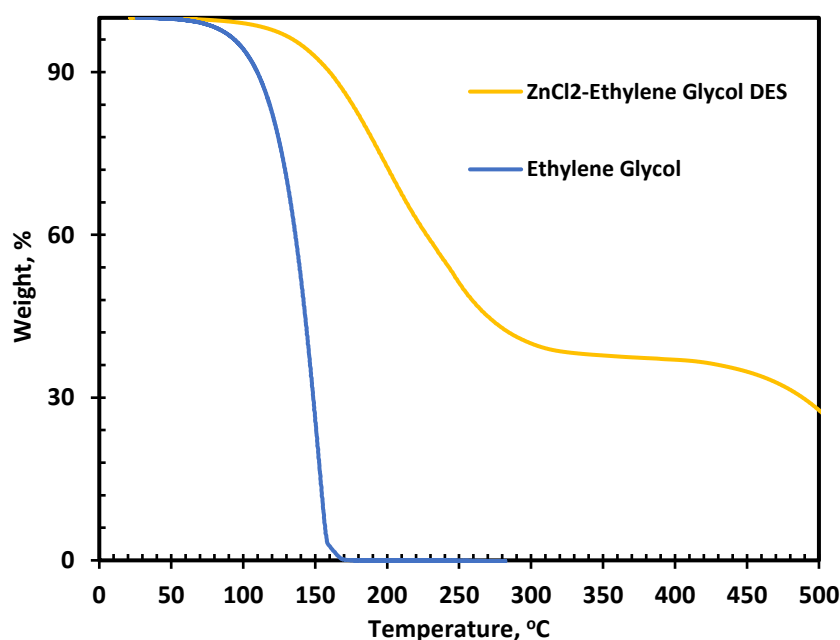


**Figure 3.7.** TGA behavior comparison of DES and ethylene glycol

#### 3.1.2.4 Thermal Degradation of Zinc Chloride-Ethylene Glycol DES in Batch System

In order to see whether DES is degraded at the reaction conditions, at 180°C for 8 hours, DES was kept under these conditions. Extraction with ethyl acetate was carried out and GC-MS analysis of mixture in the reactor was done to see degradation

products. The original GC-MS analysis report is given in Appendix A (see Figure A. 1). Dioxane, decane, undecane, 4-methyldecane, ethylene glycol, and di(2-ethylhexyl) phthalate are the main products. Products which have peak area higher than 2 % are listed in Table 3.1.

**Table 3.1.** DES Degradation Products formed at 180°C for 8 hours

<b>Product Name</b>	<b>Product Name in GC-MS Report</b>	<b>Peak Area (%)</b>
Dioxane	1,4 Dioxane	22.33
Decane	Decane	14.32
Undecane	Undecane	10.83
4-methyldecane	Decane,4-methyl	6.34
Ethylene glycol	1,2-Ethanediol	6.09
Di(2-ethylhexyl) phthalate	Bis(2-ethylhexyl) phthalate	5.67
Heptane, 3,3,5-trimethyl	Heptane, 3,3,5-trimethyl	2.76
1,2,4-Trimethylbenzene	Benzene, 1,2,4-trimethyl	2.71
Dodecane	Dodecane	2.67
2-methyldecane	Decane,2-methyl	2.54
3-methyldecane	Decane,3-methyl	2.47
Octane, 2,6-dimethyl	Octane, 2,6-dimethyl	2.22

Summation of tabulated peak areas equals to 81 %, the remaining part consists of products having peak areas lower than 2 %.

Ethylene glycol formation can be evidence for destruction of complexation between zinc chloride and ethylene glycol. Being exposed to 180°C for 8 hours caused some of the bonds forming DES to be broken while new chemical bonds formed leading to formation of different chemical species.

One of the newly formed chemicals was 1,4 Dioxane. In literature, Kobayashi et.al., proposed a mechanism for production of dioxane from ethylene glycol, and they

stated that ethylene glycol is a precursor to dioxane (Kobayasahi et al., 2013). Thus, the formation of dioxane in thermal degradation of DES is possibly due to the chemical transformation of ethylene glycol into dioxane.

Decane, undecane and 4-methyldecane have similar chemical structures. Undecane and 4-methyldecane have 11 carbons in chain, only difference is the location of a methyl group. Decane has 10 carbons in chain. In literature there is no study that relates decane, undecane or 4-methyldecane and ethylene glycol or dioxane. They may be formed through free ethylene glycol chains by the removal of their -OH groups.

Di(2-ethylhexyl) phthalate has a more complex chemical structure, as shown in Figure 3.8. It consists of a ring structure, carbonyl groups and branched carbon chains.

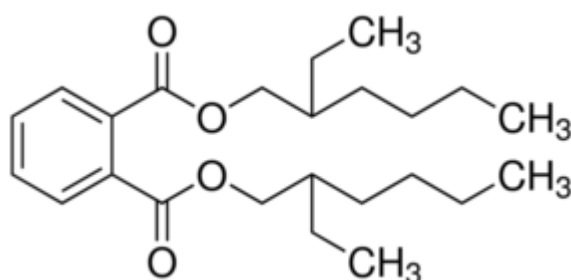


**Figure 3.8.** Chemical structure of di(2-ethylhexyl) phthalate (Lenga, 1988)

These results showed that DES also undergoes degradation, and some products are formed due to its degradation.

### 3.1.2.5 Thermal Degradation of Zinc Chloride-Ethylene Glycol DES in Semi-Batch System

Zinc chloride-ethylene glycol DES was kept at 180°C for 8 hours in the semi-batch system. At the end of the reaction, reactor and the first trap were weighed. In the second and third traps, there were no condensed material.



Gas product amount was calculated by subtracting contents of reactor and first trap from the initial amount of DES. Liquid products were obtained from the first trap. Conversion of DES was calculated as 35.36%. Detailed calculations are given Appendix B.

Liquid products formed from reactions taking place in the semi-batch reactor were weighed and then dissolved in acetone. GC-MS analysis was carried out to the liquid products dissolved in acetone. The full report of this analysis is shown in Appendix A (see Figure A. 2).

The result of GC-MS analysis showed that there were mainly 1,3-dioxolane, 2,2-dimethyl and dioxane as products. The peak area of 1,3-dioxolane, 2,2-dimethyl was 96.07 %, whereas that of dioxane was 2.15 %. Sum of the peak areas was made 98.22 %, the other 1.78 % part consisted of substances having peak area lower than 1%. Due to having high peak area, it was considered that there may be a relationship between ethylene glycol and formation of 1,3-dioxolane, 2,2-dimethyl. Sanderson et.al., came up with a mechanism relating with 1,3-dioxolane, 2,2-dimethyl formation from ethylene glycol (Sanderson et al., 1987). Reaction of ethylene glycol and hydromethyl derivative of 1,3-dioxolane, 2,2-dimethyl was resulted in 1,3-dioxolane, 2,2-dimethyl formation. In this DES study, hydromethyl derivative of 1,3-dioxolane, 2,2-dimethyl may be formed as an intermediate compound which then, may react with ethylene glycol to form 1,3-dioxolane, 2,2-dimethyl. Dioxane formation was also observed in DES reaction in batch system. However, the peak area of dioxane was 22.33%, whereas in semi-batch system that of dioxane decreased to 2.15%. When the GC-MS analysis results of batch and semi-batch systems were compared, it can be said that in the semi-batch system a different reaction mechanism took place and different products were formed. This situation can be ascribed to the operation differences in two systems. In batch system, evaporated substances condense back into the reaction mixture and possibly continued reacting with other substances. However, in the semi-batch system, evaporated materials moved away from the reactor and condensed in the trap, or were collected as gas product. As a result, different reaction mechanisms occurred in these systems.

Analyses of gas products were performed for DES degradation with GC. Hydrogen, carbon dioxide, carbon monoxide, and an unidentified component were detected. Calibration factors of hydrogen and carbon dioxide were 0.11 and 0.85, respectively (Şener, 2019). Number of moles of hydrogen and carbon dioxide were calculated by multiplying the calibration factors with peak areas.

Change of hydrogen production amounts in DES reaction with time was shown in Figure 3.9.

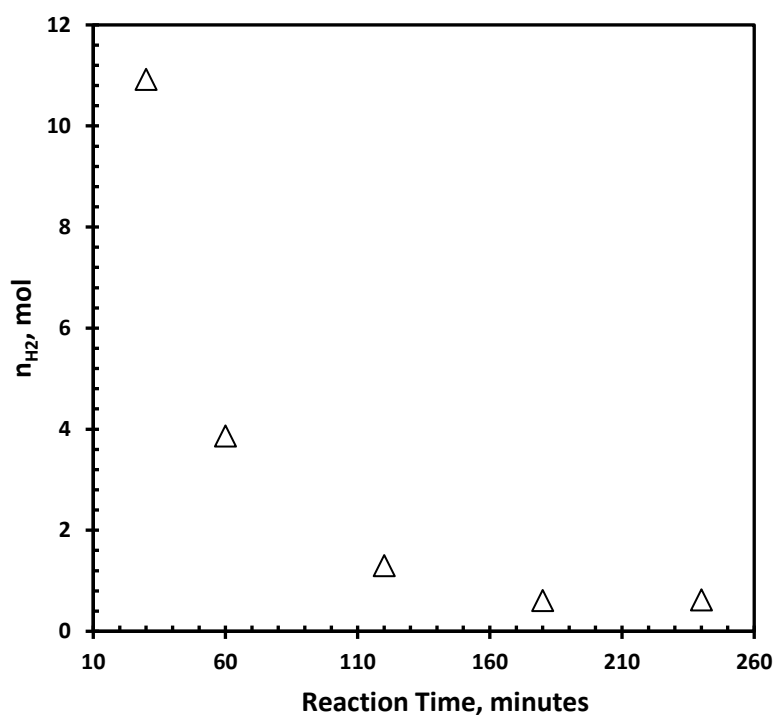


**Figure 3.9.** Change of hydrogen production amounts with time in the reaction

Decrease in hydrogen production was observed as the reaction proceeded. The decrease in hydrogen amount may be related to its reactions with other substances and forming new compounds. Hydrogen production in DES experiment shows that ethylene glycol degradation plays a role in hydrogen formation. In the literature, there are studies reporting hydrogen formation from decomposition of ethylene glycol (Kim et al., 2007; Saliccioli et al., 2011).

In Figure 3.10, carbondioxide production amounts were revealed.

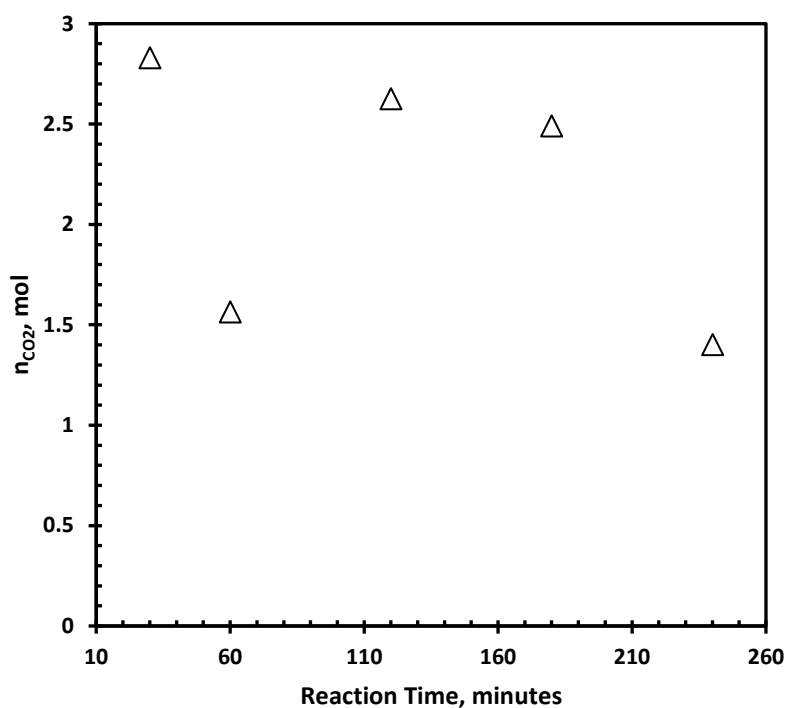


**Figure 3.10.** Change of carbon dioxide production amounts with time in the reaction. Nearly 3 moles of carbon dioxide were produced by ethylene glycol degradation, and the mole numbers more or less remained the same up to 160 minutes and then fell by half. In the literature, there were studies which reported the carbon dioxide formation due to degradation of ethylene glycol (Kim et al., 2007).

In the used column for GC analysis, retention times of carbon monoxide and nitrogen, which is the carrier gas, were overlapped with each other. As a result of this situation, peak areas at this retention time were given rather than number of moles (see Figure 3.11).

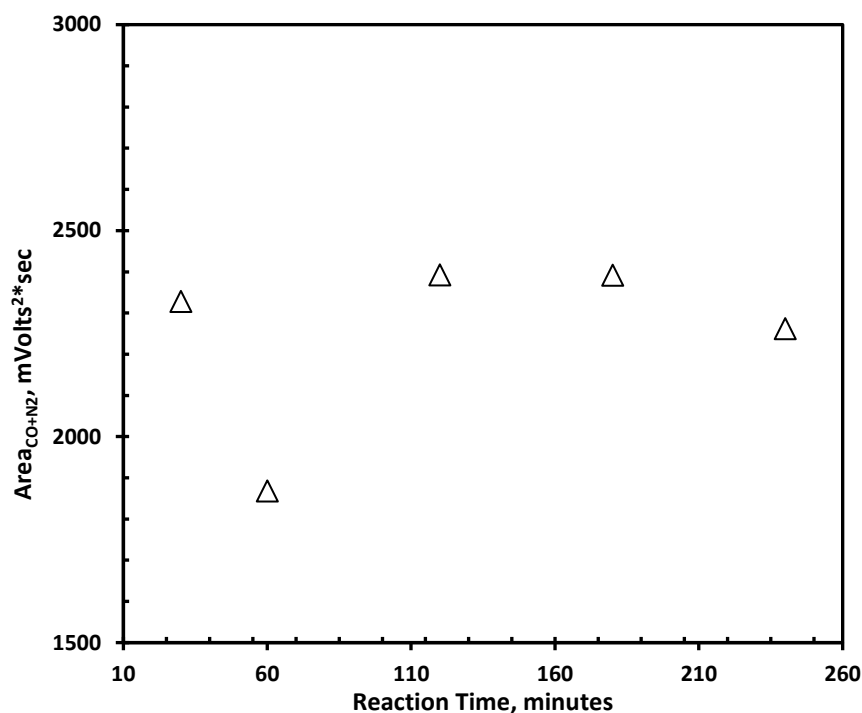


**Figure 3.11.** Peak area changes of carbon monoxide and nitrogen with time in the reaction

From the Figure 3.11, it can be seen that there was only a decrease at 60 minutes' data. Except this decrease, peak areas were nearly remained constant. There may be a measuring error in GC at 60 minutes. Hence, it may be concluded that mainly nitrogen was detected and the produced carbon monoxide possibly reacted with other components and new products were formed. Carbon monoxide formation was expected because in literature there were studies in which carbon monoxide production was observed in ethylene glycol decomposition (Kim et al., 2007; Saliccioli et al., 2011).

The final gas component was detected at retention time of 33 seconds; however, it was not identified. Hence, peak areas at this retention time were given rather than number of moles (see Figure 3.12)

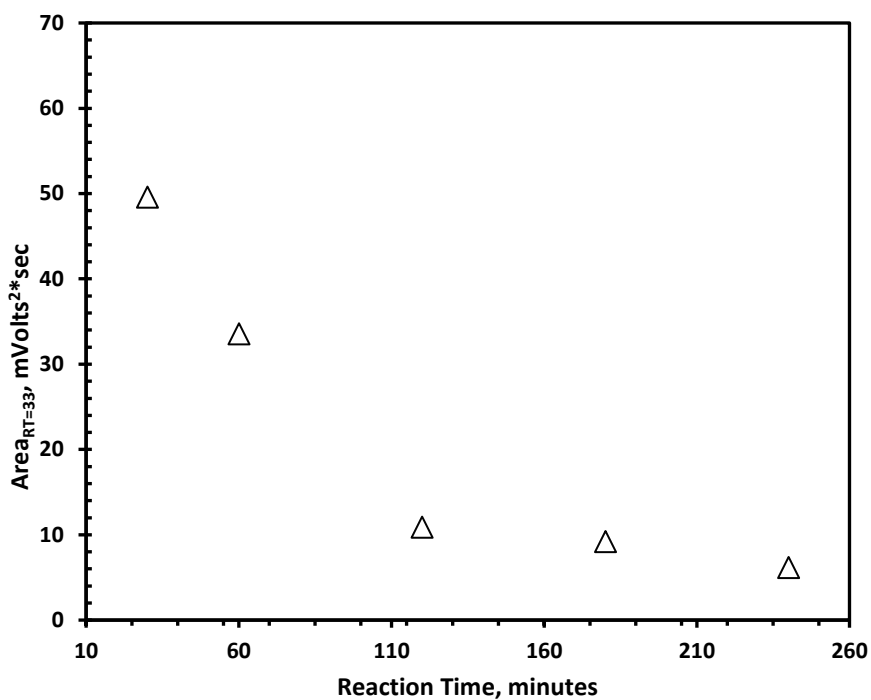


**Figure 3.12.** Peak area changes of unidentified substance at different reaction times. The peak area of this compound showed decreasing trend as the reaction proceeded. It can be said that the presence of ethylene glycol played a role in formation of this compound.

## 3.2 Characterization Results of Catalysts

### 3.2.1 Characterizations of Silica Aerogel Support Material

Silica aerogel is a support material preferred for synthesis of catalysts due to its high pore diameter, surface area and relatively good thermal stability. In this study, silica aerogel was synthesized as support material and then, aluminum metal was loaded into the silica aerogel.

### 3.2.1.1 FTIR Analysis

FTIR spectrum of the synthesized silica aerogel is shown in Figure 3.13. Peaks at 548, 800, and 955  $\text{cm}^{-1}$  represent Si-O stretching vibration. The peaks observed in 691, 757 and 810  $\text{cm}^{-1}$  belong to Si-O-Si stretching. Because of the surface modification with TMCS, at 2962  $\text{cm}^{-1}$  C-H stretching peak is detected. Peaks at 845 and 1256  $\text{cm}^{-1}$  are related to Si-C stretching. The sharp peak observed around 1065  $\text{cm}^{-1}$  and its shoulder around 1168  $\text{cm}^{-1}$  indicate Si-O-Si stretching. When the obtained spectrum and literature spectrum of silica aerogel were compared, they overlapped with each other (Sivri et al., 2019; Al-Oweini et al., 2009). This indicates that the synthesized material is silica aerogel.

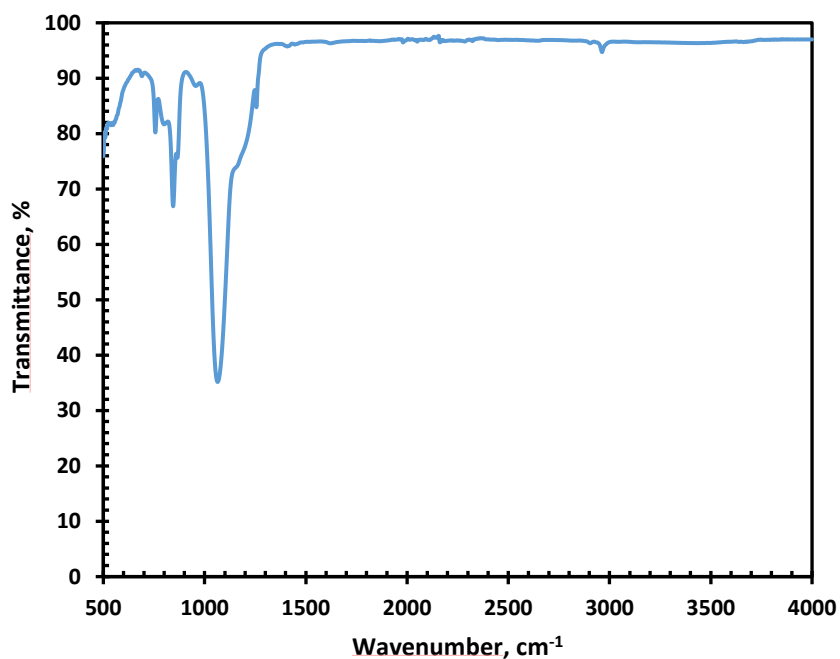


**Figure 3.13.** FTIR spectrum of silica aerogel

### 3.2.1.2 Nitrogen Sorption Analysis

In Figure 3.14, nitrogen adsorption and desorption isotherms of silica aerogels are shown. According to IUPAC classification, silica aerogel exhibited Type IV

isotherm which implies mesoporous structure. H3 type hysteresis loop was also inspected at relative pressure between 0.72 and 0.94. This type of hysteresis denotes aggregates of non-rigid and plate-like particles having slit shaped pores (Lowell, 2005).

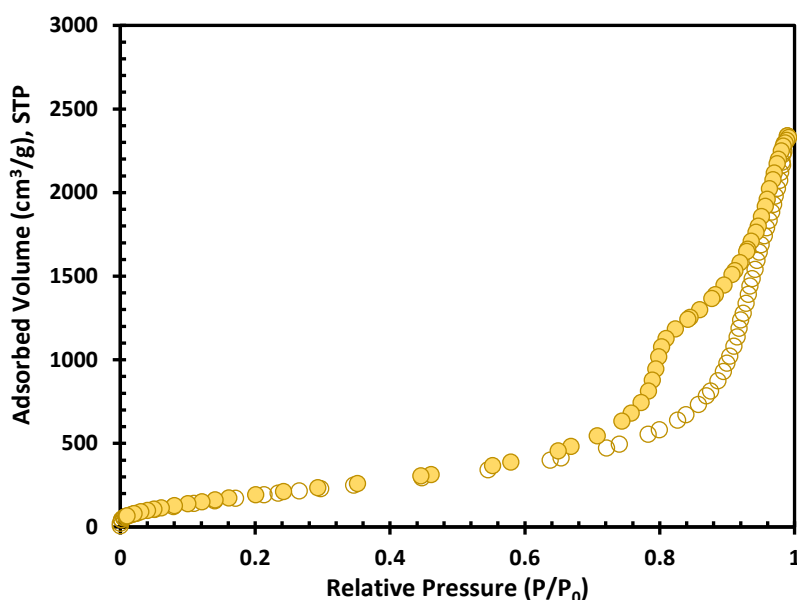


**Figure 3.14.** Nitrogen adsorption and desorption isotherms of silica aerogel (filled circles represent adsorption branch and empty circles represent desorption branch).

### 3.2.1.2.1 Pore Size Distribution Analysis

In Figure 3.15, there is the pore size distribution of the synthesized silica aerogel. On the figure, there are lines which indicate 2 and 50 nm. There were macropores (pore diameter greater than 50 nm) and mesopores (pore diameter between 2 and 50 nm). According to pore size distribution, silica aerogel has mesoporous structure dominantly. Micropores (pore diameter less than 2 nm) were less than macro and mesopores. Pore size distribution results are in good agreement with nitrogen adsorption-desorption isotherms.

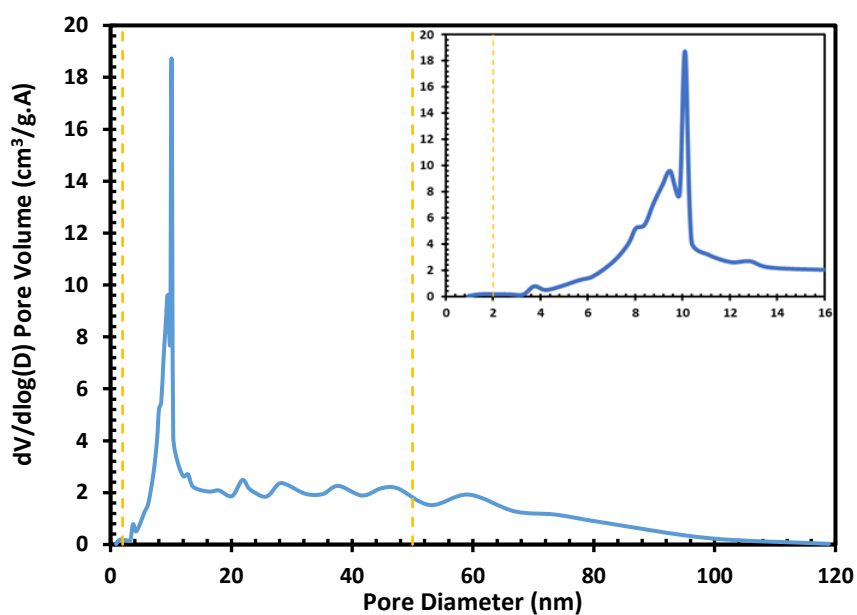


**Figure 3.15.** Pore size distribution of silica aerogel

### 3.2.1.2.2 Physical Properties of Synthesized Silica Aerogel

Physical properties of the silica aerogels from different batches are tabulated in Table 3.2, including their standard deviations.

**Table 3.2.** Physical properties of silica aerogels from different batches

Support Material in Different Batches	Multipoint BET Surface Area (m <sup>2</sup> /g)	BJH Desorption Pore Volume (cm <sup>3</sup> /g)	BJH Desorption Pore Diameter (nm)
SA 1	788	3.28	10.66
SA 2	795	3.44	10.62
SA 3	780	3.60	11.07
<b>Average</b>	788±6	3.44±0.13	10.80±0.20



Small values of standard deviations indicated that the support material with more or less the same physical properties was synthesized. This result revealed that the synthesis of these materials were repeatable.

### 3.2.1.3 Scanning Electron Microscopy (SEM) Analysis

SEM image of the synthesized silica aerogel material was taken by our research group and shown in Figure 3.16. In this figure, porous and sponge-like morphology of silica aerogels is observed. Red circles in this figure reveal pores in the structure with different sizes. These results are in good agreement with the pore size distribution results of silica aerogel. (Figure 3.15).

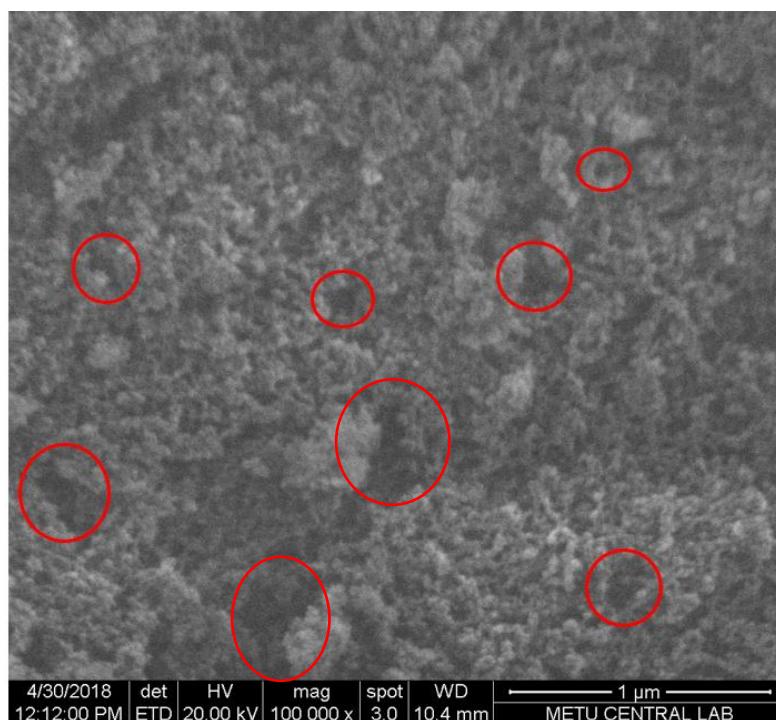


**Figure 3.16.** SEM image of silica aerogel

## 3.2.2 Characterization of Aluminum Loaded Silica Aerogel Catalyst

### 3.2.2.1 Nitrogen Sorption Analysis

Influence of aluminum loading on adsorption-desorption isotherms is given in Figure 3.17. Aluminum loaded silica aerogels showed Type IV isotherm as well, so the mesoporous structure is maintained in both of the metal loading amounts. Hysteresis loop of aluminum loaded catalysts was decided as H1. In general, H1 hysteresis loops are represented by porous materials. These pore structures were considered as rigid, almost uniformly clustered spheres (Yurdakal et al., 2019).

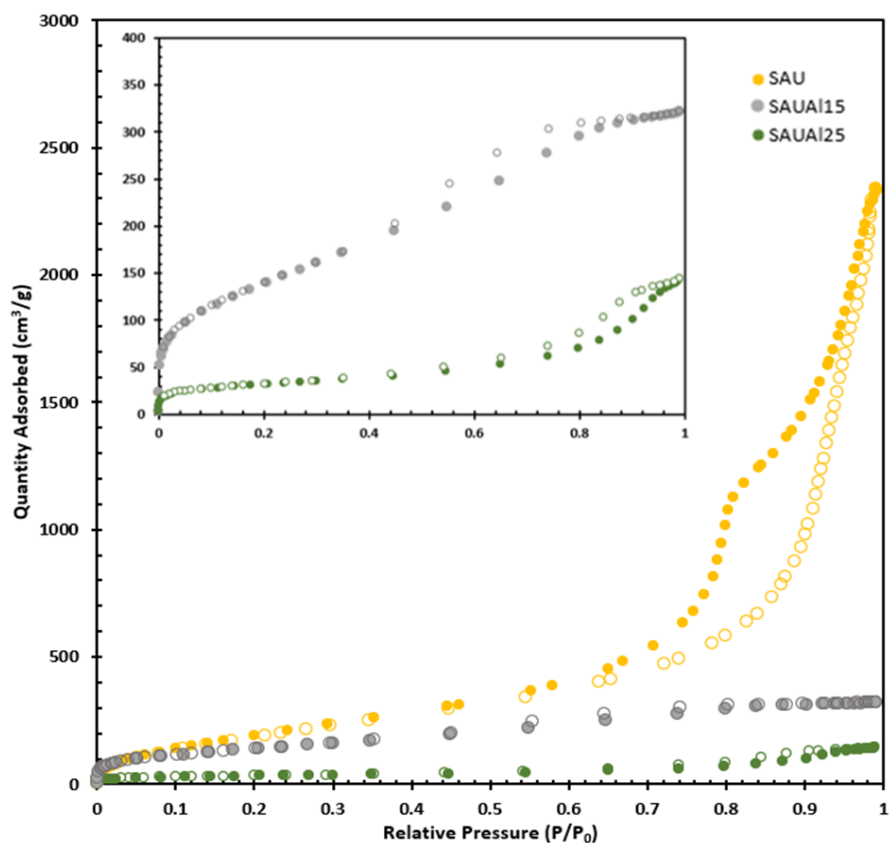


**Figure 3.17.** Nitrogen adsorption and desorption isotherms of aluminum loaded silica aerogels compared with that of silica aerogel (filled circles represent adsorption branches, empty circles represent desorption branches)

From Figure 3.17, it was seen that loading of metal and increasing the weight percentage of metal caused a decrease in adsorbed nitrogen volume. Blockage of the pores with metal particles possibly played a role in this situation.

Hysteresis of SAUA115 started at relative pressure of 0.44, and that of SAUA125 started at 0.64. Hysteresis of SAUA115 started at a lower relative pressure compared to that of SAUA125. This situation showed that SAUA115 had lower pore diameter than SAUA125.

### 3.2.2.1.1 Pore Size Distribution Analysis

In Figure 3.18, the pore size distribution of silica aerogel and metal loaded silica aerogels is provided.

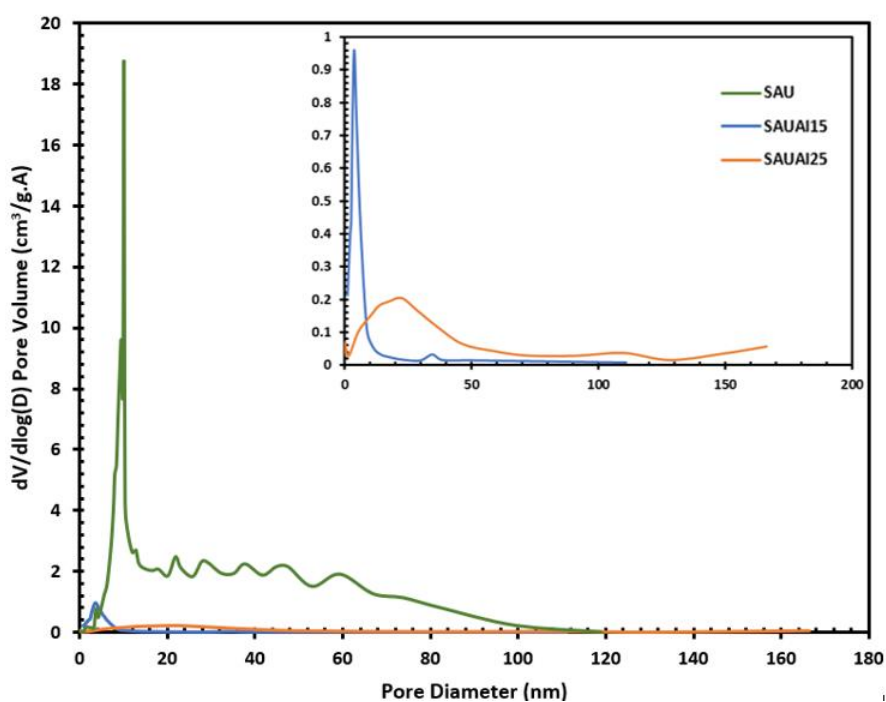


**Figure 3.18.** Pore size distribution comparison of silica aerogel and aluminum loaded silica aerogels

When compared to silica aerogel, pore size distribution of aluminum loaded silica aerogels shift to lower diameters. Metal particles possibly located mainly on meso and macropores, so pore size distribution shifted to lower diameters in metal loaded silica aerogels.

### 3.2.2.1.2 Physical Properties of Synthesized Aluminum Loaded Silica Aerogels

In Table 3.3, surface area, desorption volume and desorption pore diameter values of metal loaded silica aerogels are tabulated.

**Table 3.3.** Physical properties of aluminum loaded silica aerogels

	<b>Multipoint BET Surface Area (m<sup>2</sup>/g)</b>	<b>BJH Desorption Pore Volume (cm<sup>3</sup>/g)</b>	<b>BJH Desorption Pore Diameter (nm)</b>
<b>SAUAl15</b>	482	0.47	2.61
<b>SAUAl25</b>	110	0.23	5.58

As the aluminum content is increased, surface area and pore volume of the catalyst have decreased significantly. This behavior can be attributed to blockage of pores with aluminum. In SAUAl15, there were fewer macropores when compared to SAUAl25, so this situation led to lower average pore diameter in SAUAl15 (see Figure 3.18).

### 3.2.2.2 TGA Analysis

In Figure 3.19, TGA analysis of SAUAl15 was given. At 120°C, 8 % weight loss was observed. On the other hand, there was nearly 15 % weight loss at 500°C. The 8% weight loss up to 120°C can be attributed to water loss from the structure of the catalyst. The percent weight loss of the catalyst at 180°C, which was the degradation reaction temperature, is found to be 1.67 %. Hence, it was assumed that the weight

loss of catalyst was negligible. According to TGA analysis result, it can be said that the synthesized catalyst exhibits good thermal stability.

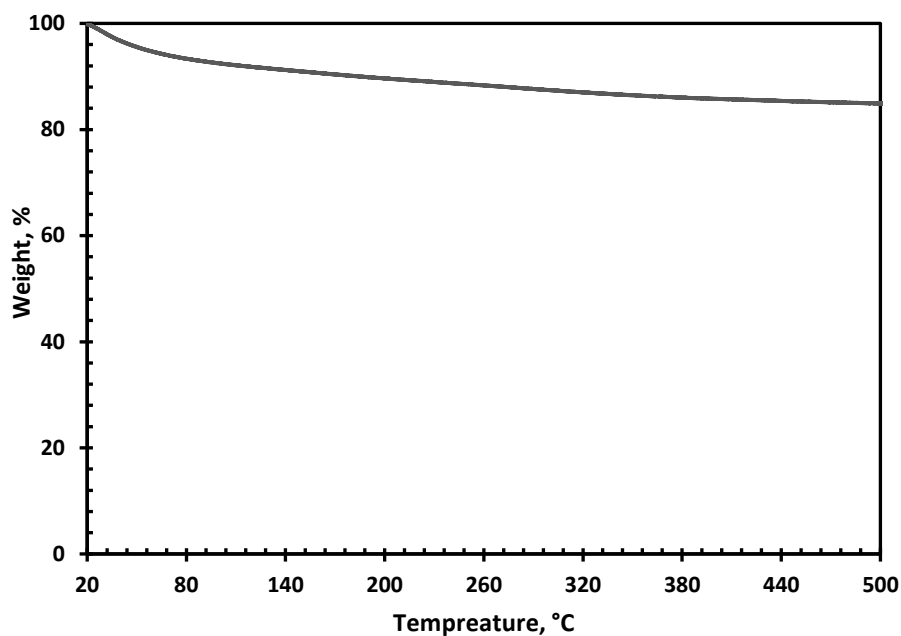


**Figure 3.19.** TGA analysis of SAUA115

### 3.2.2.3 Scanning Electron Microscopy (SEM) Analysis

SEM images of SAUA115 and SAUA125 in different magnifications were shown in Figure 3.20 and Figure 3.21, respectively. According to these images, it was seen that the porous and sponge-like morphological structure of silica aerogel was conserved after loading of aluminum.

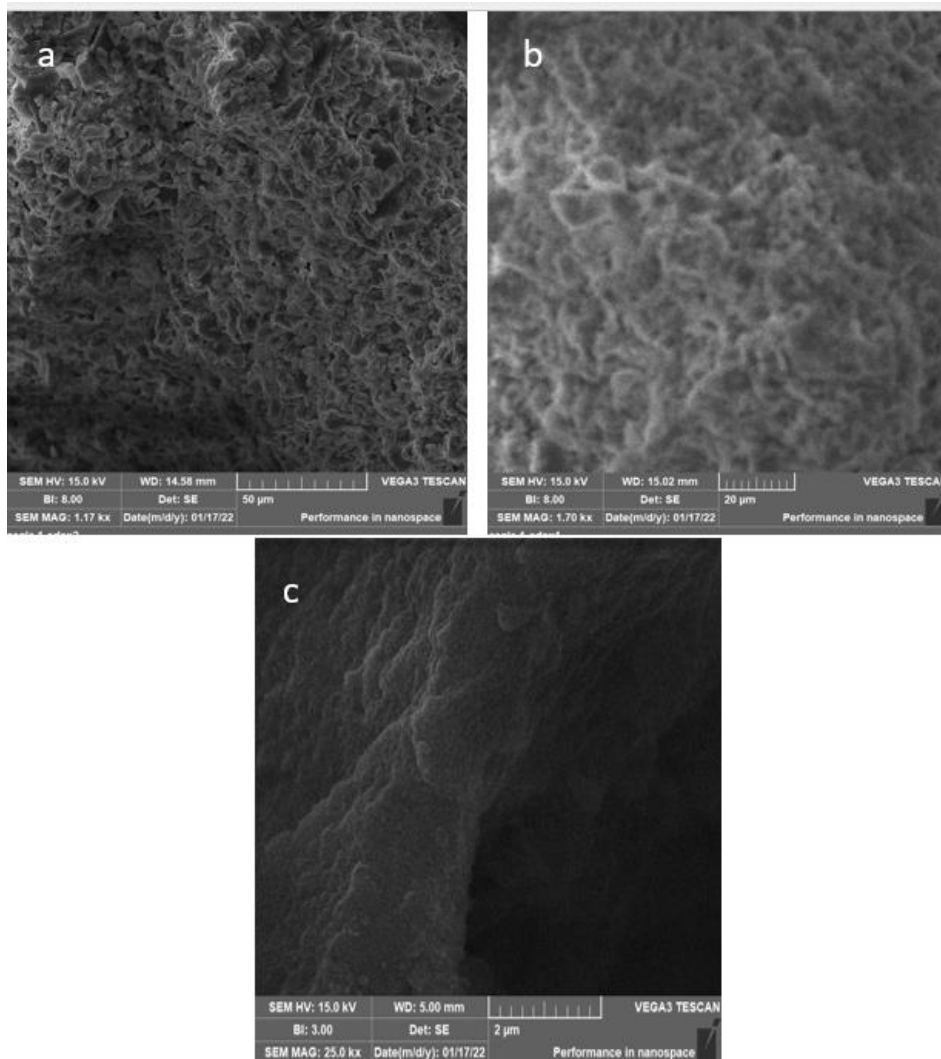


**Figure 3.20.** SEM images of SAUA115 at a) 1170x, b) 1700x, and c) 25000x magnifications

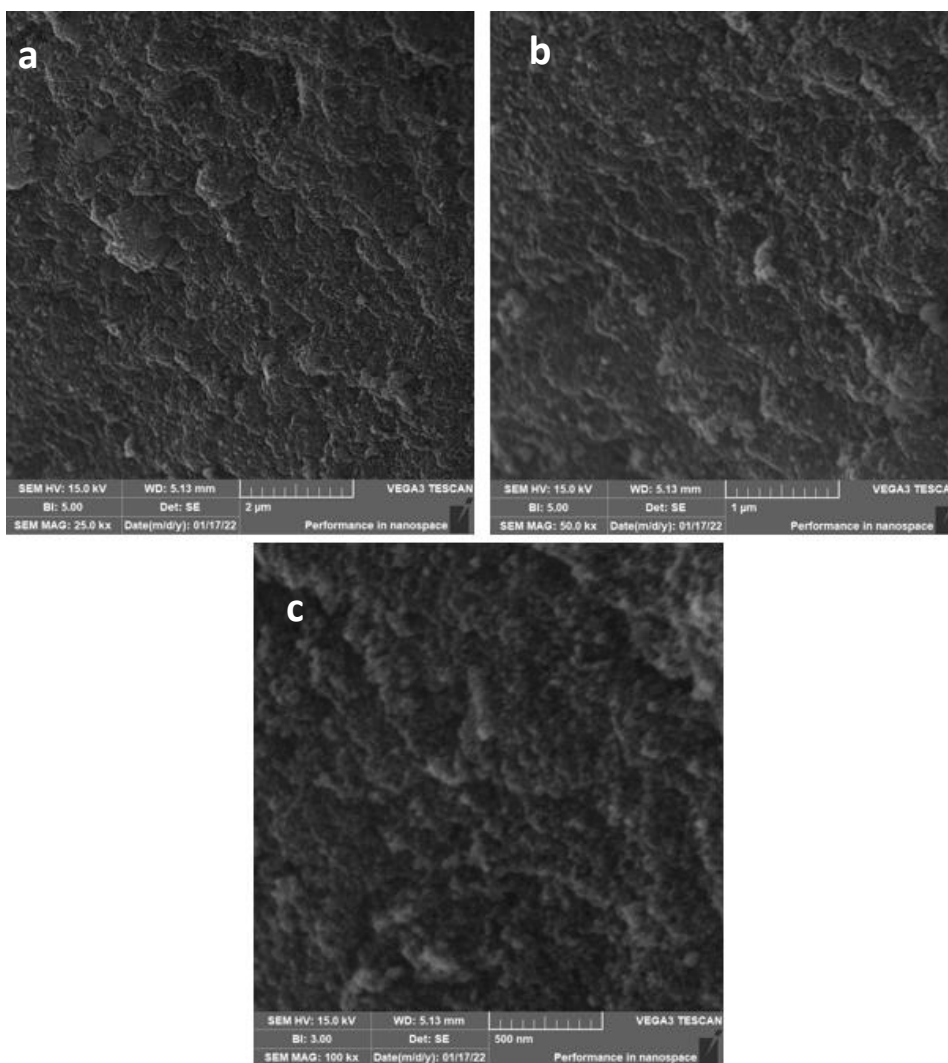


**Figure 3.21.** SEM images of SAUA125 at a) 25000x, b) 50000x, and c) 100000x magnifications

SEM with EDX analyses were carried out for both SAUA115 and SAUA125 catalysts. A typical EDX spectrum of SAUA115 was given in Figure 3.22. In this analysis, silicon, oxygen, carbon, and aluminum elements were detected. Silicon and oxygen were detected due to their presence in the structure of silica aerogel. Aluminum was detected since silica aerogel was loaded with aluminum. Carbon was detected due to the carbon tape which was used for sample preparation in the SEM analysis.

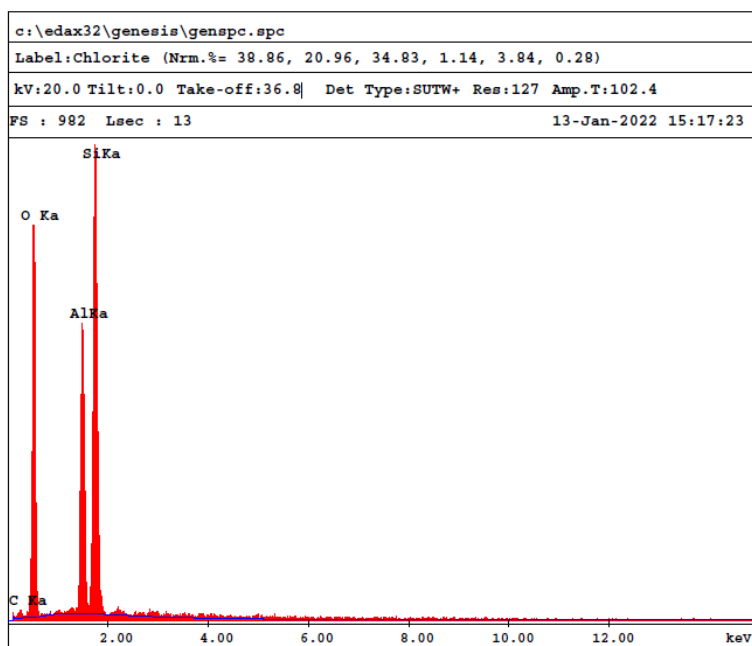


**Figure 3.22.** EDX spectrum of SAUA115

Weight percentages of the detected elements were tabulated in Table 3.4. While presenting the data, weight percentage of carbon was excluded and the values were recalculated. According to the obtained EDX result, in that part of the catalyst, there was nearly 16 wt. % of aluminum within the structure which is consistent with the intended loading amount. In different parts of the catalyst, weight percent of aluminum was detected slightly different (see Table 3.5). EDX spectra of the two regions were provided in Appendix C. The average weight percent of aluminum was found as 13.30 %. This result showed us that aluminum may have not been dispersed within the whole structure uniformly.

**Table 3.4.**Weight percentages of elements in SAUA115 detected by EDX

Element	Weight, %
Oxygen	50.08
Silicon	33.68
Aluminum	16.24



**Table 3.5.** Weight percentages of elements in different parts of SAUA115

Elements	Weight %			Average
	Region 1	Region 2	Region 3	
O	50.08	48.49	50.89	49.82
Si	33.68	39.13	37.83	36.88
Al	16.24	12.38	11.28	13.30

Distribution of elements within the mapped area were shown in Figure 3.23. According to mapping results, it was observed that silicon was distributed evenly within the structure. Oxygen was also spread uniformly, but there were some gaps in which oxygen was absent. Aluminum distribution was also observed as uniform, except some tenuous areas. It can be concluded that elements on the structure were uniformly dispersed within the mapped area.

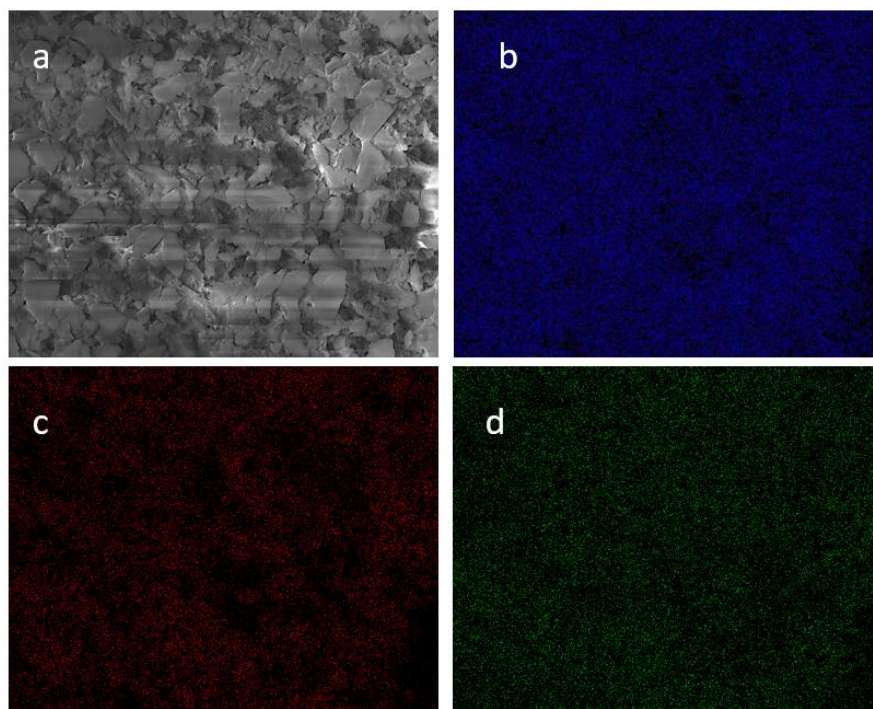


**Figure 3.23.** Mapped area of SAUA115 a): distribution of b) silicon, c) oxygen and d) aluminum

EDX spectrum of SAUA125 was shown in Figure 3.24. EDX spectrum of SAUA125. According to this analysis, oxygen, silicon, and aluminum elements were detected. The weight percentages of this elements were tabulated in Table 3.6.

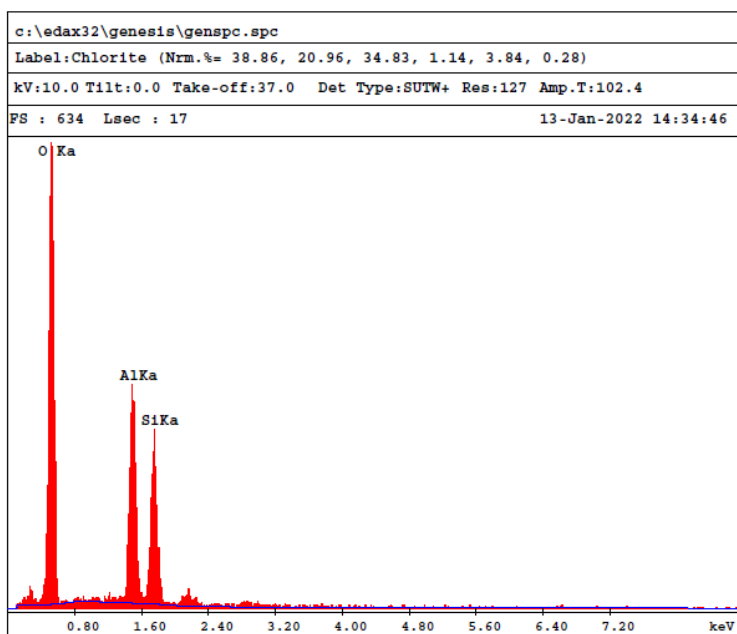


**Figure 3.24.** EDX spectrum of SAUA125

**Table 3.6.** Weight percentages of elements in SAUA125 detected by EDX

Element	Weight, %
Oxygen	50.39
Silicon	24.60
Aluminum	25.01

In this EDX analysis result, it was found that aluminum has 25.01 wt. %, which is in a good agreement with the intended value of loading. Different regions of the catalyst were mapped and the average weight percent of aluminum was found as 24.34 % (see Table 3.7), which is consistent with the actual aluminum loading amount. Hence, it can be concluded that aluminum was loaded at the desired amount. EDX spectra of the other two regions were given in Appendix C.

**Table 3.7.** Weight percentage of elements in different parts of SAUAl25

Elements	Weight %			Average
	Region 1	Region 2	Region 3	
O	50.39	49.33	54.19	51.30
Si	24.6	23.33	25.14	24.36
Al	25.01	27.34	20.68	24.34

Distribution of elements within the mapped area of SAUAl25 were shown in Figure 3.25.

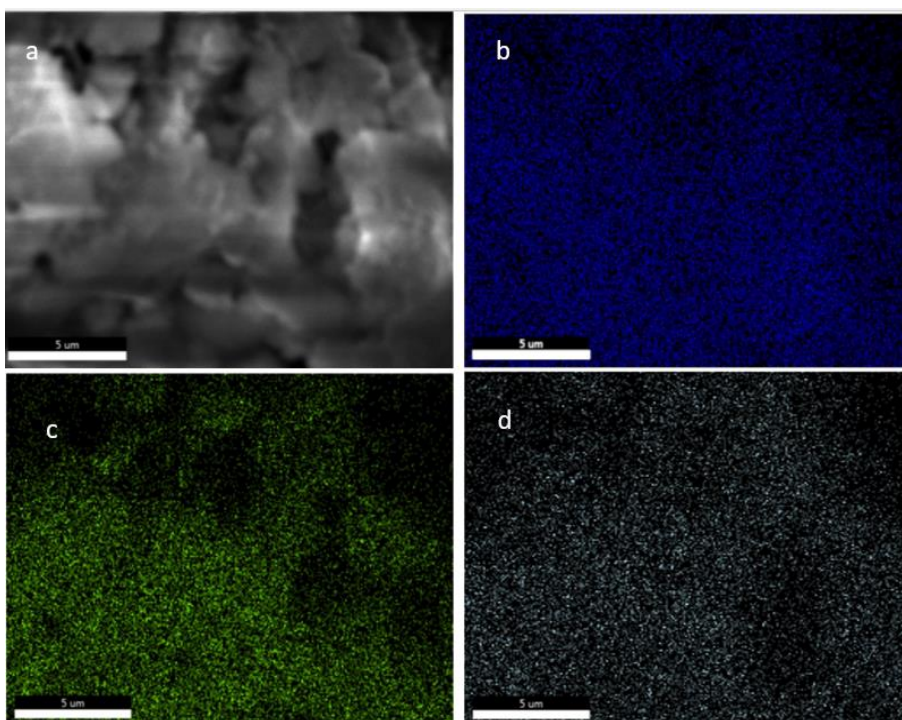


**Figure 3.25.** Mapped area of SAUAl25 a): distribution of b) silicon, c) oxygen, and d) aluminum

Silicon was distributed uniformly within the structure. In terms of oxygen, although some oxygen free parts were seen within the structure, it was because of the gaps in

the mapped region (see Figure 3.25 a). Except these parts, oxygen distribution seems even. Aluminum was also be observed to be dispersed uniformly within the structure.

#### 3.2.2.4 Diffuse Reflectance Infrared Fourier Transform Spectroscopy (DRIFTS) Analysis

DRIFTS analyses were performed to observe acid sites of the synthesized catalysts. DRIFTS spectra of pyridine adsorbed and fresh catalysts were obtained and the difference between these spectra gave information about the existence of Lewis or Brønsted acid sites. In Figure 3.26, DRIFTS spectra of SAUAl15 and SAUAl25 were shown.

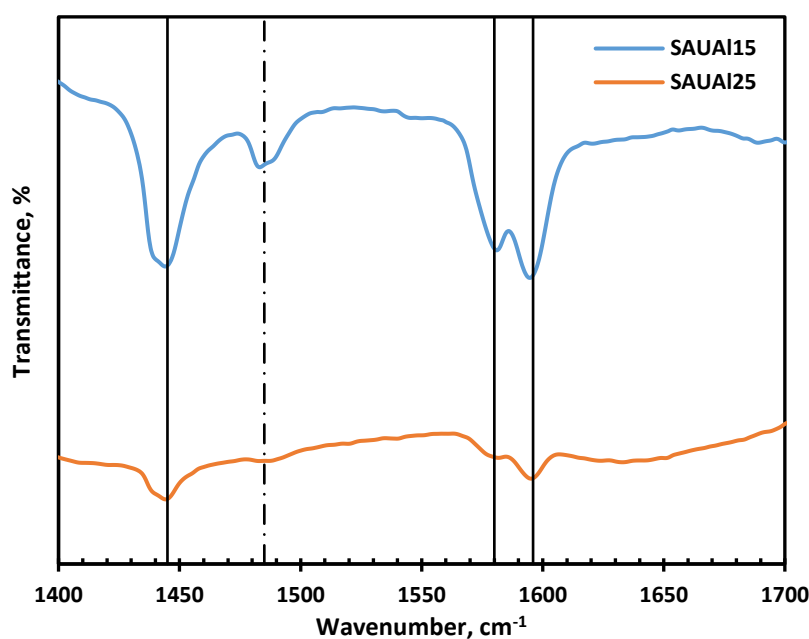


**Figure 3.26.** DRIFTS spectra of the synthesized catalysts

Both of the catalysts exhibited peaks at 1596, 1580, and 1445 cm<sup>-1</sup>, which represent Lewis acid sites (straight line) (Aydemir, 2013). In addition, peak at 1485 cm<sup>-1</sup> which corresponded to the combination of Lewis and Brønsted acid sites (dashed line) was also observed in both catalysts. From the Figure 3.26, it was clear that SAUAl25 had

lower peak intensities at all specified wavenumbers even though it was loaded with more aluminum.

The ratio of Lewis acid sites to the combination of Lewis and Bronsted acid site was shown as  $L/(L+B)$ . This ratio was calculated by dividing the intensities of Lewis acid sites to the intensity of Lewis and Bronsted acid site.  $L/(L+B)$  ratio of SAUA115 was found as 2.49, and that of SAUA125 was 1.86. Hence, SAUA115 had more acidic property.

### **3.3 PLA Degradation Reaction Results**

Degradation reactions were carried out in batch and semi-batch systems. In order to test the activity of the synthesized catalysts, thermogravimetric analyzer was used.

The degradation reaction was intended to be carried out at a higher temperature than the melting temperature of PLA (~160°C). In the literature, the important weight loss of DES was reported to occur at between 200-475°C (Tran et al., 2018). Therefore, it was necessary to work at a temperature below 200°C. The PLA degradation rate is faster between 300 and 360°C (Sivri et al., 2019), so higher temperatures are preferred. However, the degradation of DES at high temperatures led to the reaction temperature to be chosen at lower temperatures. As a result, 180°C, which is above the melting temperature of PLA and below the decomposition temperature of DES, was decided as the reaction temperature.

Reaction time and amount of PLA were decided according to the preliminary experiments. In those experiments, PLA amount was 0.5 g and 2 hours of reaction was carried out. However, in that experiment PLA pellets didn't melt and dissolve in DES. Then, the reaction time was set to 4 hours, but this time the resulting products were not in a detectable amount. Hence, the amount of PLA was increased to 3 g, and in order to melt the PLA pellets, reaction time was set as 8 hours.

Reactions in batch and semi-batch systems were performed at 180°C, for 8 hours.

### 3.3.1 Performance of Aluminum Loaded Silica Aerogel Supports Using Thermogravimetric Analyzer

The performance of aluminum loaded silica aerogel catalysts which contain 15 % and 25 % aluminum, by weight, on the PLA degradation was evaluated using thermogravimetric analyzer. In Figure 3.27, the TGA curves of PLA with/without catalyst are shown. PLA to catalyst weight ratio was kept constant as 2.

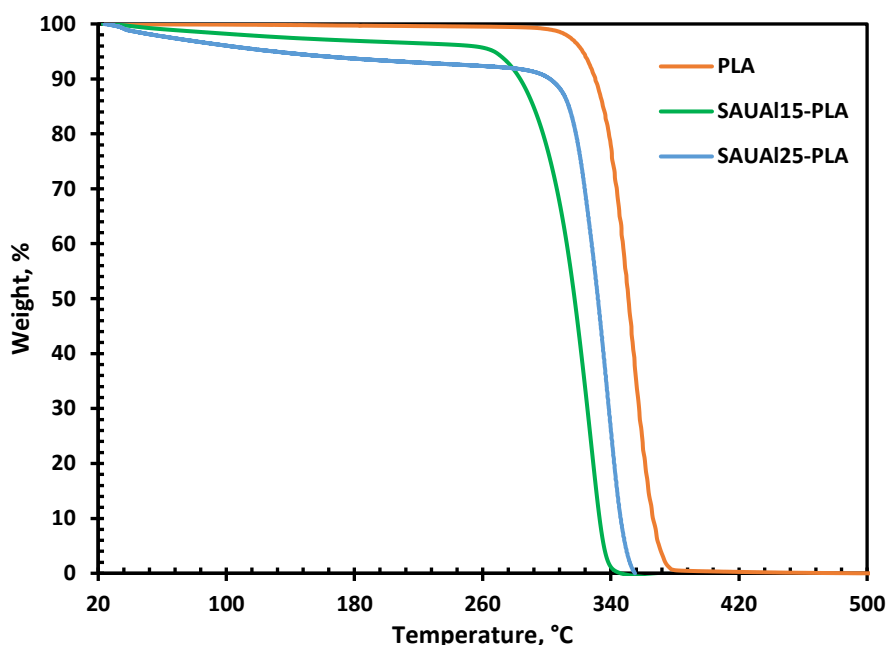


**Figure 3.27.** TGA behavior of PLA in presence of aluminum loaded silica aerogels compared with neat PLA

Unlike PLA, aluminum loaded silica aerogel catalysts are hydrophilic and the weight loss until 180°C can be attributed to removal of moisture content. From Figure 3.27, it can be declared that aluminum loaded silica aerogel catalysts shifted the TGA curve of PLA to the left hand side which is an indication of the decreasing degradation temperature. Neat PLA started to degrade at 315°C, with the presence of 15 % aluminum and 25 % aluminum loaded silica aerogel catalysts, degradation started at 266°C and 303°C, respectively. In Table 3.8, various weight loss amounts, and their corresponding temperature values were summarized.

**Table 3.8.** Temperature values corresponds to 10, 50, and 90% weight loss

	Temperature, °C		
	10 % Weight Loss	50 % Weight Loss	90 % Weight Loss
<b>PLA</b>	330	350	366
<b>SAUA115</b>	284	317	333
<b>SAUA125</b>	303	332	346

As seen in Table 3.8 and Figure 3.27, although weight percentage of aluminum is lower in SAUA115, it decreased the degradation temperature and shifted the TGA curve to the left more than SAUA125. This may be caused by the drastic decrease in surface area, and pore volume of SAUA125 ( Table 3.3). Worsening in its physical properties and having less Lewis acid sites in its structure can cause underperforming of SAUA125.

Kinetic parameters of degradation reaction of PLA, the apparent activation energies, were calculated by using TGA data and power law model. The procedure described in Coats and Redfern (1964) was applied to find kinetic parameters. Detailed calculations were given in Appendix D.

In Table 3.9, the apparent activation energies of PLA degradation reactions with and without catalyst are summarized. The apparent activation energy of PLA degradation reaction was found to be 262 kJ/mol, which is consistent with the literature data (Sivri et al., 2019; Auras, 2022). SAUA115 decreased the apparent activation energy of PLA degradation reaction to 193 kJ/mol, whereas SAUA125 decreased to 238 kJ/mol. SAUA115 performed more efficiently than SAUA125 in terms of decreasing the apparent activation energy of PLA degradation reaction. As explained, decrease in pore volume and surface area of SAUA125 may cause it to perform worse than SAUA115. Also, SAUA125 had less acid sites than SAUA115 i.e., intensities of acid sites at the specified wavelengths were lower in SAUA125 (see Figure 3.26). Thus,

SAUA125 performed worse in terms of decreasing the apparent activation energy of thermal degradation reaction of PLA. On the whole, SAUA125 decreased the apparent activation energy as well, but it was expected that it should have lowered the activation energy more than SAUA115. Due to this result, for the catalytic PLA degradation reactions in DES medium, SAUA115 catalyst was used.

**Table 3.9.** Apparent activation energy values of PLA degradation reaction and its values in the presence of catalyst

Sample	Activation Energy (kJ/mol)
PLA	262
PLA-SAUA115	193
PLA-SAUA125	238

In a previous study carried out by our research group, catalytic effect of neat silica aerogel on thermal degradation of PLA was investigated (Sivri et al., 2019). According to this study, in the presence of silica aerogel, the degradation temperature of PLA increased. Hence, it can be said that neat silica aerogel increased the thermal stability of PLA.

### 3.3.2 Zinc Chloride-Ethylene Glycol DES Medium in Batch System

Due to the solidification problems in zinc chloride-urea DES, zinc chloride-ethylene glycol DES was selected to be used as reaction medium for PLA degradation reaction due to the reasons explained in sections 3.1.1.3.

Degradation reaction of PLA in DES medium was performed at 180°C for 8 hours. When the system reached to 180°C, PLA dissolved in DES and a homogenous clear solution was obtained. As the reaction proceeded, the colour of the solution changed due to the formation of products. At the end of the reaction, the reaction mixture was in liquid form. After cooled to room temperature, it retained its liquid state. To



extract the products from the reaction mixture, an appropriate solvent was required to dissolve the products which should not miscible with DES. For this purpose, water, hexane, toluene, chloroform, and acetone were tried and they didn't meet the requirements. Ethyl acetate; however, was immiscible with DES, i.e., it created a heterogenous solution upon mixing with DES. Two-phased mixture was obtained, and to verify this insolubility, FTIR technique was used. Spectrums of pure DES and the bottom phase of DES-ethyl acetate mixture (which was thought to be DES) were compared. In Figure 3.28, FTIR spectra of DES and bottom phase of the heterogeneous mixture are shown.

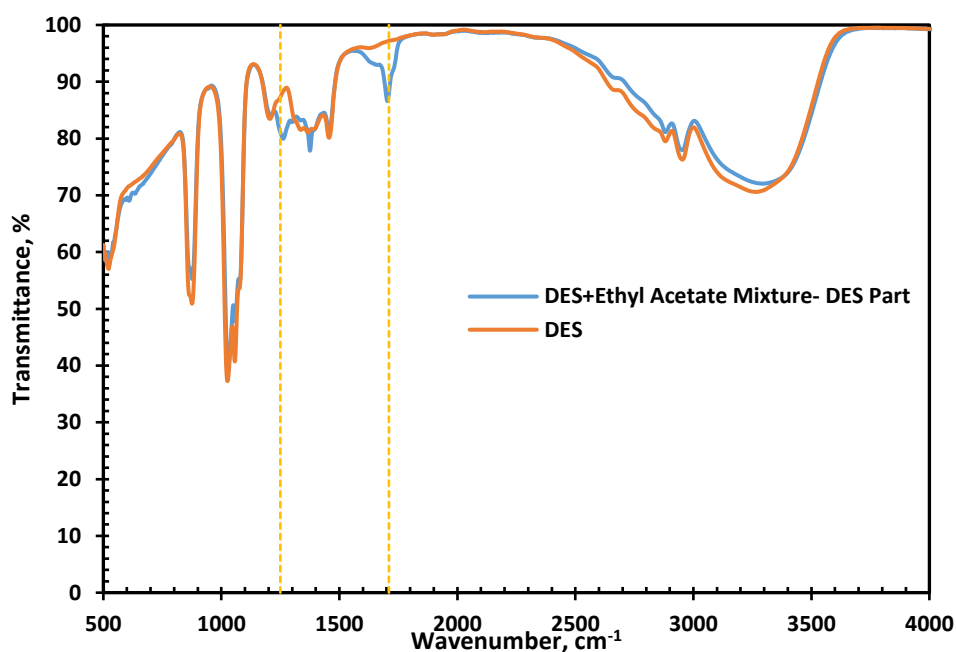


**Figure 3.28.** Comparison of FTIR spectra of DES and the bottom phase of DES+ethyl acetate mixture

All the peaks in both spectra overlapped with each other, except two peaks. At  $1720$  and  $1250\text{ cm}^{-1}$ , there are new peaks in the spectrum of bottom phase of the mixture. Pure ethyl acetate has peaks at both wavenumbers. Hence, it can be said that some ethyl acetate is slightly miscible with DES.

In Figure 3.29, spectra of ethyl acetate and the top phase of the mixture were compared. It can be seen that all the peaks in two spectra overlap with each other. As a result, it can be concluded that DES is insoluble or has negligible solubility in ethyl acetate.

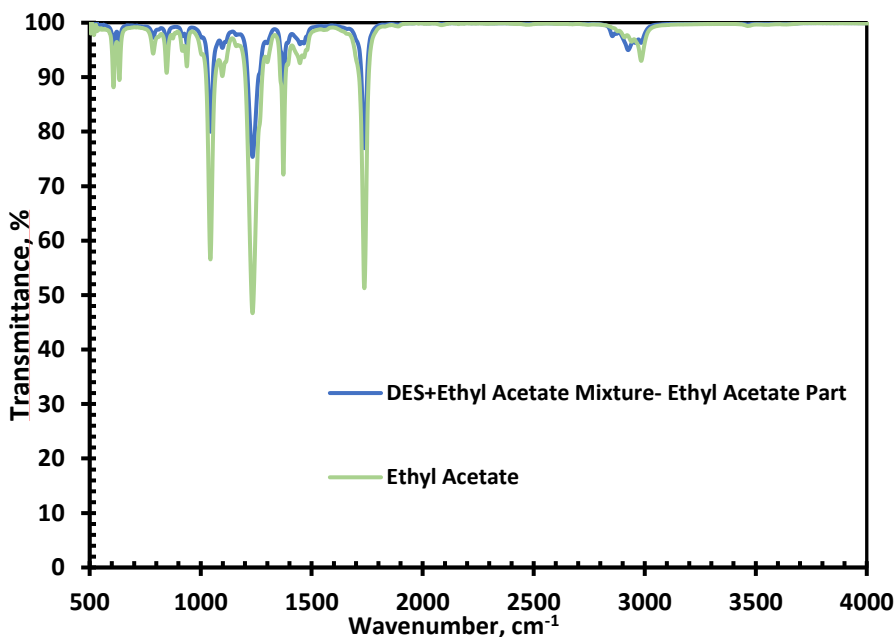


**Figure 3.29.** Comparison of FTIR spectra of ethyl acetate and the top phase of DES+ethyl acetate mixture

Solubility of possible products i.e., lactic acid and lactate in ethyl acetate was searched in literature. It was found that both of them are soluble in ethyl acetate (Glotova, 2016). Hence, as the extraction solvent, ethyl acetate was selected.

Degradation reaction of PLA in DES medium was done at 180°C, for 8 hours. At the end of reaction, products were extracted with ethyl acetate. The distribution of the reaction products extracted by ethyl acetate was determined with GC-MS analysis. Compounds which have peak area more than 2 % are listed in Table 3.10. The original GC-MS report was given in Appendix A (see Figure A. 3).

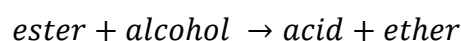
**Table 3.10.** Products obtained from the PLA degradation reaction in ethylene glycol-zinc chloride DES medium

<b>Product Name</b>	<b>Name in GC-MS Report</b>	<b>Peak Area (%)</b>
Diethylene glycol	Ethanol, 2,2'-oxybis-	12.82
Triethylene glycol	Ethanol, 2,2'-[1,2-ethanediylbis(oxy)]bis-	12.61
Dioxane	1,4 Dioxane	10.91
Acetic acid hydrazino ethyl ester	Acetic acid hydrazino ethyl ester	7.78
3-methyl-2-hexanone	3-methylhexan-2-one-	7.14
Tetraethylene glycol, monoacetate	2-[2-[2-(2-Hydroxyethoxy)ethoxy]ethoxy]ethyl acetate	6.09
Ethyl lactate	Propanoic acid, 2-hydroxy-, ethyl ester	5.45
Diethylene glycol monoacetate	Diethylene glycol monoacetate	4.88
Propanoic acid, 2-(methoxymethoxy)	Propanoic acid, 2-(methoxymethoxy)	4.76
Triethylene glycol monoethyl ether	Ethanol, 2-[2-(2-ethoxyethoxy)ethoxy]	4.61
Triethylene glycol monoethyl ether, acetate	2-[2-(2-Ethoxyethoxy)ethoxy]ethyl acetate	3.54

Summation of peak areas equals to 80.6%, and the other 19.4% part consists of chemicals having peak area lower than 2%. According to this result, dioxane (10.91%), diethylene glycol (12.82%) and triethylene glycol (12.61%) have the

highest peak area values. Dioxane was formed due to degradation of DES, which was explained in Section 3.1.2.4. From literature survey, it was found that ethylene glycol may be the source for dioxane production (Kobayashi et al., 2013; Popoola, 1991). Popoola (1991) investigated the formation of by-products during the esterification reaction between dimethyl terephthalate and ethylene glycol. In this study, it was stated that ethylene glycol and ester interactions lead to formation of diethylene glycol, and the resulting diethylene glycol became the precursor of dioxane i.e., it triggers the dioxane production. They concluded that the dioxane formation could be explained by intramolecular elimination reaction caused by half esterified diethylene glycol after cyclization and proton transfer from diethylene glycol to acetate anion of the excess ester.

The DES used in this study contained ethylene glycol while PLA has also ester linkages. Diethylene glycol was also detected in the GC-MS analysis. Thus, the production of dioxane and diethylene glycol can be attributed to the mechanism which is proposed by Popoola (1991).



The interaction between ester linkages and ethylene glycol may lead to the formation of dioxane (classified as ether) and acidic products. Ethyl lactate was considered as the product of PLA and ethylene glycol interaction. In a PLA degradation study, which was carried out in ethanol medium, it was observed that one of the products was ethyl lactate (Nim et al., 2020). Lamberti et al. (2020), studied the ethyl lactate formation from alcoholysis of PLA. Therefore, the formation of ethyl lactate may also be attributed to the interaction of ethylene glycol with PLA. Formation of diethylene glycol and triethylene glycol can be attributed to the degradation of DES. Holding DES at 180°C for 8 hours caused degradation of DES. In literature, diethylene glycol and triethylene glycol were the products which were formed from reactions of ethylene glycol with different compounds (Hovenkamp et al., 1970; Godjoian et al., 1996). Formation of diethylene glycol was explained above, the reason is the interaction between ester linkages and alcohol group. Triethylene glycol

formation can be attributed to the presence of acetal since it was reported that a reaction between ethylene glycol and acetal resulted in triethylene glycol (Godjoian et al., 1996). In GC-MS results acetal was reported; however, it has 0.58 % peak area. Hence, it wasn't included into Table 3.10.

### **3.3.3 Zinc Chloride-Ethylene Glycol DES Medium in Semi-Batch System**

PLA degradation reaction was carried out at 180°C for 8 hours in semi-batch reactor as well.

By subtracting the weights of contents of reactor and the first trap contents from the summation of initial amounts of PLA and DES, amount of gas product was calculated. By using the data obtained from DES degradation reaction in the semi-batch reactor, amounts of gas, liquid and solid products resulted from PLA degradation were calculated. Conversion of PLA was also found from the initial weight of PLA and the amount of PLA left in reactor. Detailed calculations were provided in Appendix B. Conversion of PLA was calculated as 97.31 %. Yields of gas and liquid products, and solid part resulted from PLA were found to be 56.83 %, 40.56 %, and 2.61 %, respectively.

To see the PLA degradation products, GC-MS analysis was performed on the liquid products obtained from PLA degradation reaction in the semi-batch system. According to the analysis result, mainly 1,3-dioxolane, 2,2-dimethyl, 2-pentanol acetate, 3(2H)-Furanone, dihydro-2-methyl, dioxane, and ethyl lactate were obtained. In Table 3.11, peak area values of these products were given. The original GC-MS analysis report was revealed in Appendix A (see Figure A. 4)

**Table 3.11.** PLA degradation products in the semi-batch system

Product Name	Peak Area (%)
1,3-Dioxolane, 2,2-dimethyl	44.7
2-pentanol acetate	14.84
3(2H)-Furanone, dihydro-2-methyl	12.97
Dioxane	10.9
Ethyl lactate	10.64

The sum of the peak areas is equal to 95.05 %, the other 5.95 % part consists of compounds having lower than 2 % peak area. Formation of 1,3-Dioxolane, 2,2-dimethyl was attributed to ethylene glycol in DES experiment. When the chemical structures of PLA, 2-pentanol acetate, and 3(2H)-Furanone, dihydro-2-methyl considered (see Figure 3.30), it can be said that 2-pentanol acetate and 3(2H)-Furanone, dihydro-2-methyl were the degradation products of PLA.

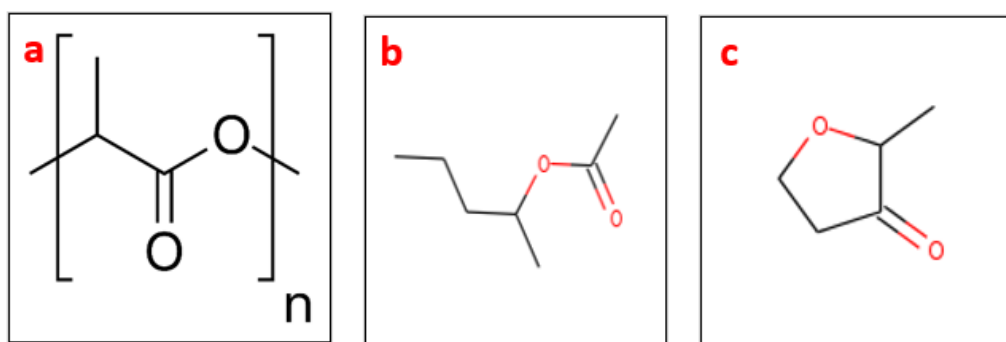


**Figure 3.30.** Chemical structures of a) PLA, b) 2-pentanol acetate, c) 3(2H)-Furanone, dihydro-2-methyl (Lenga, 1988)

In three compounds, there are carbonyl group and oxygen. 2-pentanol acetate has similar chain with the repeating unit of PLA, it has an additional  $\text{C}_2\text{H}_5$  group. 3(2H)-Furanone, dihydro-2-methyl has a ring structure, this ring structure may be formed

from PLA. Ethyl lactate formation was attributed to the interaction of PLA with ethylene glycol in the previous section (Section 3.3.2).

Among the main products common chemicals of PLA degradation formed in batch and semi-batch systems are dioxane and ethyl lactate. Peak area of dioxane was 10.91% in the batch system, and likewise, in the semi-batch system it had 10.90% peak area. Formation of dioxane was attributed to DES degradation in Section 3.1.2.4. It can be said that peak area of dioxane was unaffected by the system change. Ethyl lactate has 5.45% peak area in batch system, whereas it had 10.64% peak area in the semi-batch system. From this result, it can be concluded that in terms of ethyl lactate formation semi-batch system offered better outcome.

Analyses of gas products were performed for PLA degradation in DES medium in the semi-batch system using GC. As in DES reaction in the semi-batch system, hydrogen, carbon dioxide, carbon monoxide, and an unidentified component were detected.

Hydrogen production amounts in DES experiment and PLA degradation reaction in DES medium were shown in Figure 3.31.

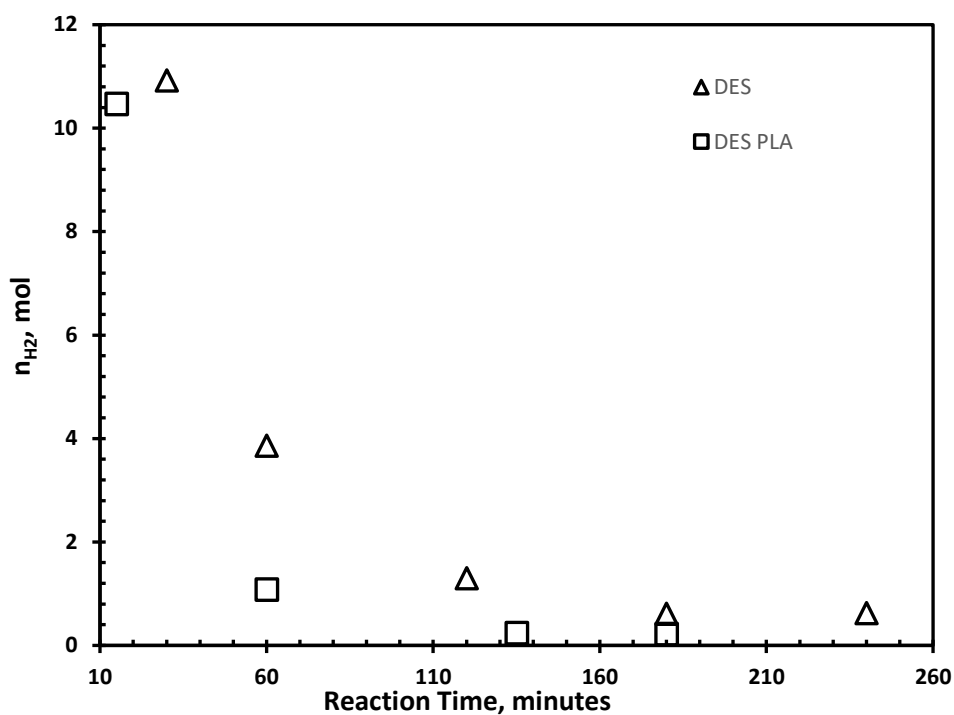


**Figure 3.31.** Change of hydrogen production amounts with time in DES and DES+PLA experiments performed in the semi-batch system

A similar decreasing trend in hydrogen amount was also observed in PLA degradation reaction. The decrease in hydrogen amount may be related to reaction of hydrogen with other substances and forming new compounds. Hydrogen production from degradation of PLA was reported by Tseng et al. (2019).

In Figure 3.32, production amounts of carbon dioxide in DES and DES+PLA experiment were revealed.



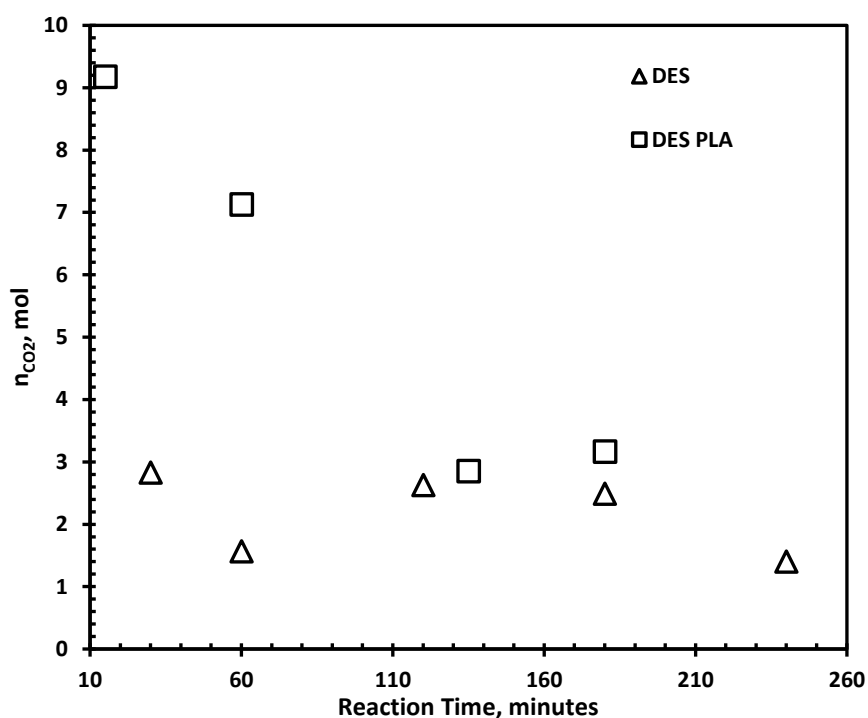


**Figure 3.32.** Change of carbon dioxide production amounts with time in DES and DES+PLA experiments performed in the semi-batch system

Amount of carbon dioxide formed in DES experiment was lower than that of produced in PLA degradation experiment. Nearly 3 moles of carbon dioxide were produced by ethylene glycol degradation, the remaining amount was resulted from PLA degradation. Also, decreasing trend of carbon dioxide production in PLA degradation experiment shows that amount of carbon dioxide coming from PLA is more than that of ethylene glycol because as the PLA depleted, the released carbon dioxide decreased as well. On the other hand, in DES experiment carbon dioxide amount was more or less stayed the same. In literature, there were studies which reported the carbon dioxide formation due to degradation of PLA (Kopinke et al., 1996; Zou et al., 2009).

Peak areas of carbon monoxide and nitrogen were given in Figure 3.33.

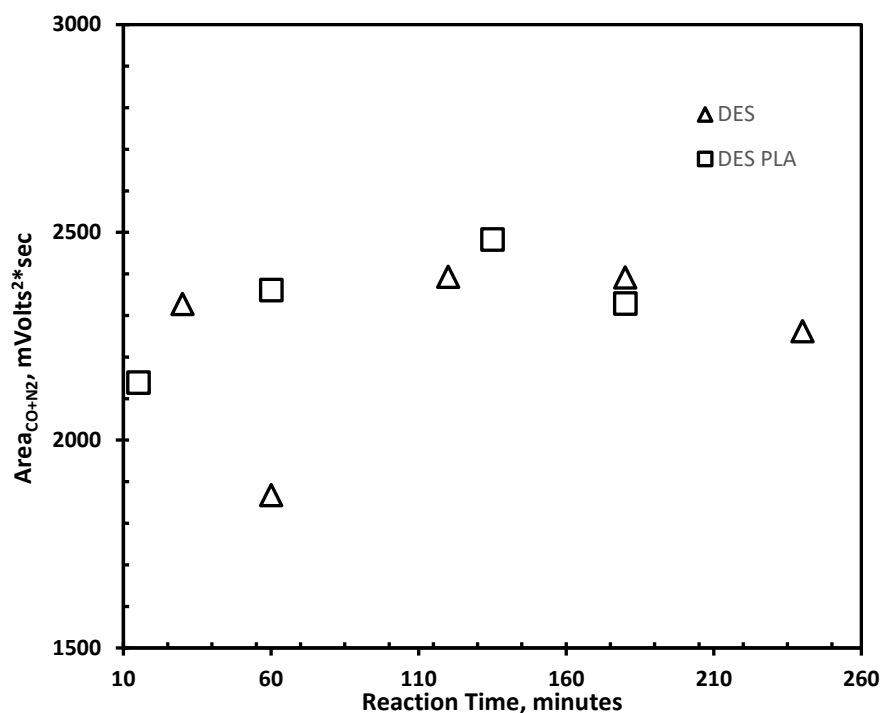


**Figure 3.33.** Peak area values of carbon monoxide and nitrogen in DES and DES+PLA experiments

From the figure it can be seen that there were some differences at the beginning of the reactions; however, as the reactions proceeded the peak areas were nearly remained constant. Hence, it may be concluded that mainly nitrogen was detected and the produced carbon monoxide could have reacted with other components and new products were formed. Carbon monoxide formation was expected because in literature there were studies in which carbon monoxide production was observed in ethylene glycol decomposition (Kim et al., 2007; Saliccioli et al., 2011) and also PLA degradation (Kopinke et al., 1996; Zou et al., 2009).

The peak areas of the unidentified component at retention time of 33 seconds were given in Figure 3.34.

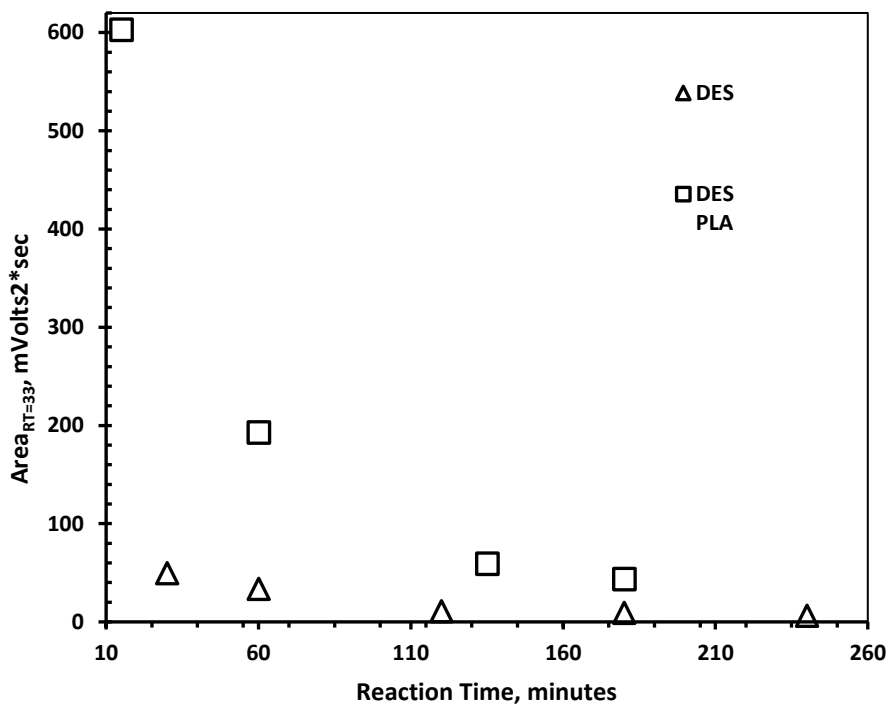


**Figure 3.34.** Peak area values of the unidentified peak with time in DES and DES+PLA experiments

For two of the experiments, similar trend in peak areas was observed. Peak areas were smaller in DES experiment at all reaction times, presence of PLA caused rise in peak areas.

### 3.4 Catalytic Degradation of PLA in DES Medium

#### 3.4.1 Catalytic Degradation in Batch System

SAUA115 catalyst was used as catalyst in degradation reaction of PLA in zinc chloride-ethylene glycol DES medium. This reaction was carried out at 180°C for 8 hours. PLA:catalyst weight ratio was 2, and DES/PLA weight ratio was 2.7. After the reaction, ethyl acetate extraction was performed in the same manner with non-catalytic reaction. GC-MS analysis was performed to see product distribution in ethyl

acetate rich phase. In Appendix A (Figure A. 5), detailed GC-MS report was given. In Table 3.12, products which have peak area higher than 2 % were revealed.

**Table 3.12.** Products obtained from the catalytic PLA degradation reaction in zinc chloride-ethylene glycol DES medium in the batch system

<b>Product Name</b>	<b>Product Name in GCMS Report</b>	<b>Peak Area (%)</b>
Dioxane	1,4 Dioxane	18.14
Triethylene glycol	Ethanol, 2,2'-[1,2-ethanediylbis(oxy)]bis-	13.14
Ethyl lactate	Propanoic acid, 2-hydroxy-, ethyl ester	11.21
Acetaldehyde, diethyl acetal	Ethane, 1,1-diethoxy-	7.48
3-methyl-2-hexanone	3-methyl-hexan-2-one	6.75
Diethylene glycol	Ethanol, 2,2,'-oxybis-	4.97
Decane	Decane	3.29
Acetic acid, hydrazino-ethyl ester	Acetic acid, hydrazino-ethyl ester	3.27
2-decanol	2-decanol	3.27

The summation of peak areas equal to 71.5 %, the remaining part consists of chemicals having peak area less than 2 %. GC-MS analysis revealed that the main products are dioxane, triethylene glycol, and ethyl lactate.

Peak area of ethyl lactate which is formed by the PLA catalytic degradation is higher than that of formed via non-catalytic degradation reaction of PLA. Acetaldehyde, diethyl acetal was the new product formed with the presence of catalyst. Dioxane, triethylene glycol and diethylene glycol were considered to be formed from ethylene

glycol. In Table 3.13, the common products and their peak area changes are summarized.

**Table 3.13.** Comparison of peak areas of products obtained from the catalytic and non-catalytic PLA degradation reaction in zinc chloride-ethylene glycol DES medium

<b>Product Name</b>	<b>Peak Area in DES+PLA (%)</b>	<b>Peak Area in DES+PLA+Catalyst (%)</b>
Dioxane	10.91	18.14
3-methylhexan-2-one	7.14	6.75
Diethylene glycol	12.82	2.65
Ethyl lactate	5.45	11.21
Triethylene glycol	12.61	13.14
Acetic acid hydrazino ethyl ester	7.78	3.27

Peak areas of dioxane and triethylene glycol, which were the products of DES degradation, were also increased with the addition of catalyst. These results showed that SAUA115 catalyst possibly changed the mechanism of PLA degradation reaction in DES medium. The usage of catalyst increased the peak area of ethyl lactate which is a degradation product of PLA. As a result, it can be stated that SAUA115 is an effective catalyst for PLA degradation reaction in DES medium.

Interaction of DES with aluminum loaded silica aerogel (SAUA115) at 180°C for 8 hours was also investigated. 8.2 g of DES and 1.5 g of SAUA115 were reacted at the specified reaction conditions. Ethyl acetate extraction was carried out, and GC-MS analysis was performed to see product distribution of ethyl acetate-rich phase. In

Table 3.14, products having peak area greater than 2 % were shown. Original GC-MS report was provided in Appendix A (see Figure A. 6)

**Table 3.14.** Products formed when DES and catalyst were reacted at 180°C for 8 hours

<b>Product Name</b>	<b>Peak Area (%)</b>
Butyl ethyl ether	17.74
Acetic acid propyl ester	14.97
Dioxane	10.26
Decane	7.87
Undecane	6.14

It was observed that DES and catalyst interacted with each other. Carbonyl group is absent in structure of butyl ethyl ether when its chemical structure is compared with that of acetic acid propyl ester. Except for carbonyl group and a -CH<sub>2</sub> group, butyl ethyl ether had a similar structure with acetic acid propyl ester. Formation of dioxane, decane and undecane was attributed to the existence of ethylene glycol and explained in previous sections.

### 3.4.2 Catalytic Reaction in Semi-Batch System

Catalytic degradation reaction of PLA was carried out in the semi-batch system. PLA: Catalyst weight ratio was 2 and, DES: PLA weight ratio was 2.7. Reaction was carried out at 180°C for 8 hours under nitrogen atmosphere.

While calculating the contents of reactor after reaction, catalyst amount was subtracted from the weight of reactor contents. The main reason was the thermal stability of SAUA115. Hence, it was assumed that all of the catalyst remained in the reactor. Calculations of PLA conversion and gas, liquid and solid product yields are given in Appendix B. The conversion of PLA was found to be 97 %. Yields of the

gas and liquid products and the solid part in reactor resulted from PLA degradation were calculated as 59.50 %, 37.41 %, and 3.09 %, respectively. Conversion of PLA and yields of gas and liquid products and solid part from PLA were similar with that of non-catalytic PLA degradation reaction in the semi-batch system.

Catalytic degradation reaction of PLA was performed in the semi-batch system. GC-MS analysis of liquid product showed that the main products are 1,3-Dioxolane, 2,2-dimethyl, 3(2H)-Furanone, dihydro-2-methyl, dioxane, and diethylene glycol, 1,3-Dioxolane, 2,2,4,5-tetramethyl. In Table 3.15, peak areas of these products were given. The original GC-MS report was shown in Appendix A (see Figure A. 7).

**Table 3.15.** PLA catalytic degradation products resulted in the semi-batch system

<b>Product</b>	<b>Peak Area (%)</b>
1,3-Dioxolane, 2,2-dimethyl	36.86
3(2H)-Furanone, dihydro-2-methyl	16.52
Dioxane	14.67
Diethylene glycol	13.10
1,3-Dioxolane, 2,2,4,5-tetramethyl	12.50

The sum of peak areas is equal to 93.65 %, the other 6.35 % part consists of compounds having lower than 2 % peak area. From DES experiment in the semi-batch system, it was anticipated that 1,3-Dioxolane, 2,2-dimethyl and dioxane were produced due to ethylene glycol. The new product 1,3-Dioxolane, 2,2,4,5-tetramethyl has a similar structure with 1,3-Dioxolane, 2,2-dimethyl, the only difference is additional two methyl groups. Therefore, 1,3-Dioxolane, 2,2,4,5-tetramethyl might have also be formed from ethylene glycol. 3(2H)-Furanone, dihydro-2-methyl was produced also in non-catalytic degradation of PLA. It was anticipated that 3(2H)-Furanone, dihydro-2-methyl was a degradation product of PLA. Diethylene glycol formation was unexpected due to its boiling point which is

246°C (Nist Chemistry WebBook). Reaction was carried out at 180°C, hence diethylene glycol was expected to stay in reactor. However, being exposed to heat for 8 hours may have caused evaporation of diethylene glycol from the reactor.

Dioxane and diethylene glycol are the common products mainly formed in batch and semi-batch systems. In the batch system, dioxane had 18.14% peak area. On the other hand, the peak area of dioxane was 14.67% in the semi-batch system. A slight decrease in the peak area of dioxane was observed in semi-batch system. In terms of diethylene glycol, it had 4.97 % peak area in batch system; however, its peak area increased to 14.67% in the semi-batch system. An important change in product distribution of PLA catalytic degradation reaction performed in two different systems was about ethyl lactate. In batch system, it had 11.21% peak area; however, it was not detected in the semi-batch system. Due to its wide usage areas such as, pharmaceutical, food, paints etc and being classified as green solvent, ethyl lactate formation was important (Lamberti et al., 2020). It was detected in the semi-batch system non-catalytic PLA degradation, but presence of catalyst changed the mechanism of reaction and ethyl lactate was not formed.

When the GC-MS results of batch and semi-batch systems were compared, it can be said that in the semi-batch system due to the separation of non-condensable products from the reactor, reaction mechanism may changed.

Analyses of gas products were performed for PLA catalytic degradation in DES medium experiment using GC. Similar with other experiments, hydrogen, carbon dioxide, carbon monoxide, and an unidentified component were detected.

Hydrogen production amounts in three experiments were shown in Figure 3.35.



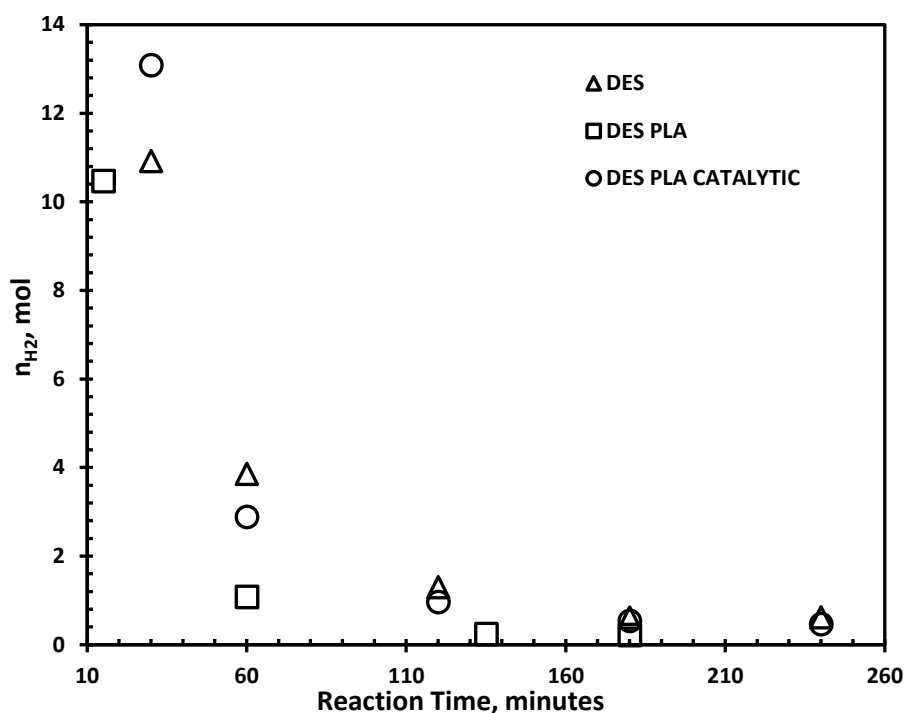


**Figure 3.35.** Change of hydrogen production amounts with time in experiments performed in semi-batch system

In all experiments, there was a decrease in hydrogen production as the reaction proceeded. The decrease in hydrogen amount may be related to reaction of hydrogen with other substances and forming new compounds. Hydrogen production in DES experiment shows that ethylene glycol degradation caused hydrogen formation. Presence of catalyst increased the amount of produced hydrogen when compared to the non-catalytic experiment. Similar to the PLA degradation reaction in DES in the batch system, decrease in the amount of hydrogen may have been due to its reaction with newly formed substances in the reaction medium.

In Figure 3.36, production amounts of carbon dioxide in three experiments were shown.

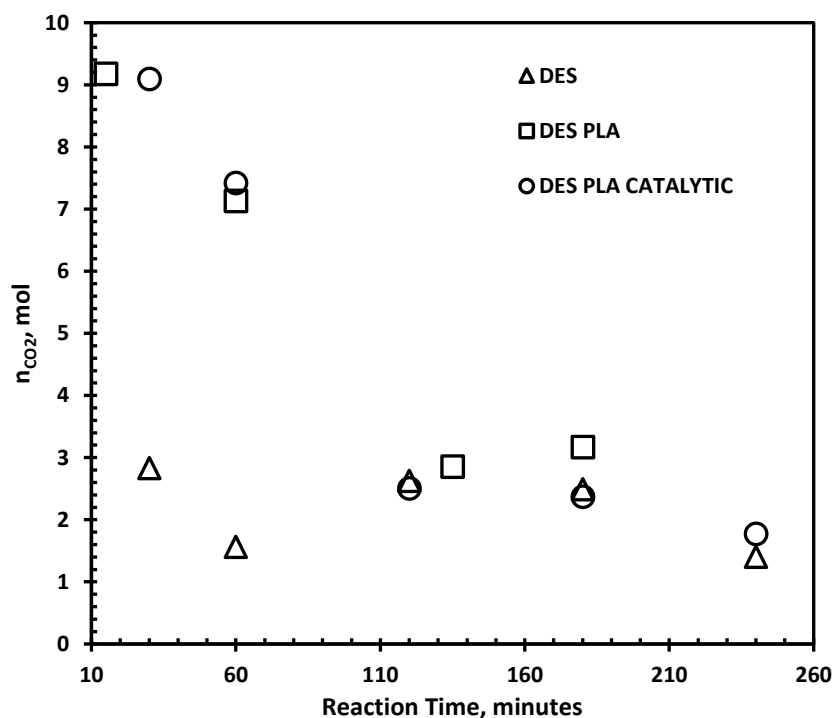


**Figure 3.36.** Change of carbon dioxide production amounts with time in experiments performed in semi-batch system

It was observed that carbon dioxide was formed in all experiments. Amount of carbon dioxide formed in DES experiment was lower than that of produced in PLA degradation experiments. When the catalytic and non-catalytic degradation reactions of PLA were compared in terms of carbon dioxide formation, it can be said that the presence of catalyst did not affect the carbon dioxide formation.

Peak areas of carbon monoxide and nitrogen were presented in Figure 3.37.

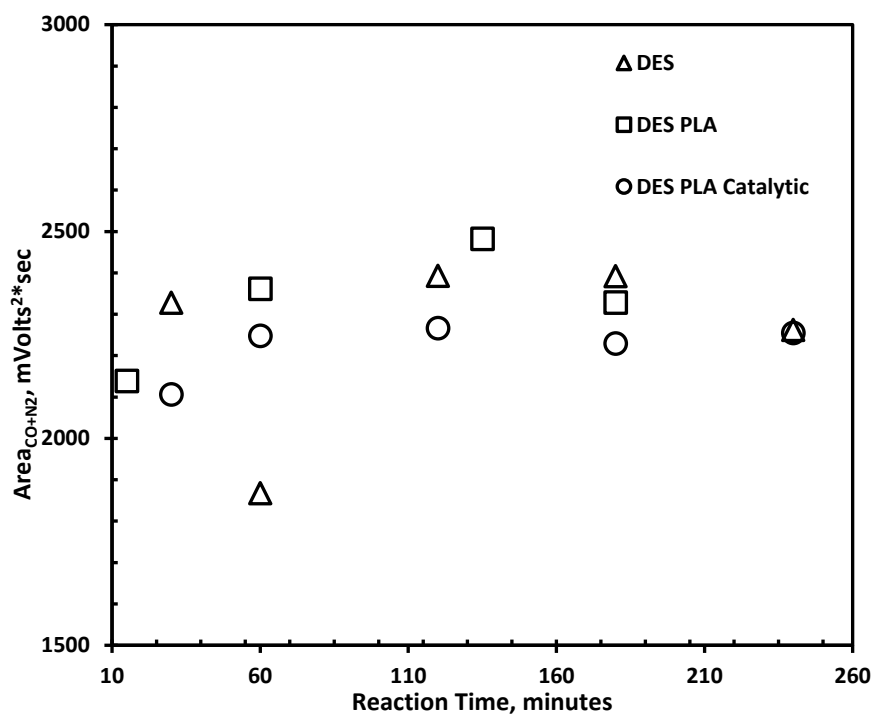


**Figure 3.37.** Peak area values of carbon monoxide and nitrogen with time in all experiments

When the peak areas of catalytic experiment were observed, its peak areas did not also change considerably. This situation may also be an evidence for the presence of mainly nitrogen rather than carbon monoxide.

The peak areas of unidentified substance were given in Figure 3.38.

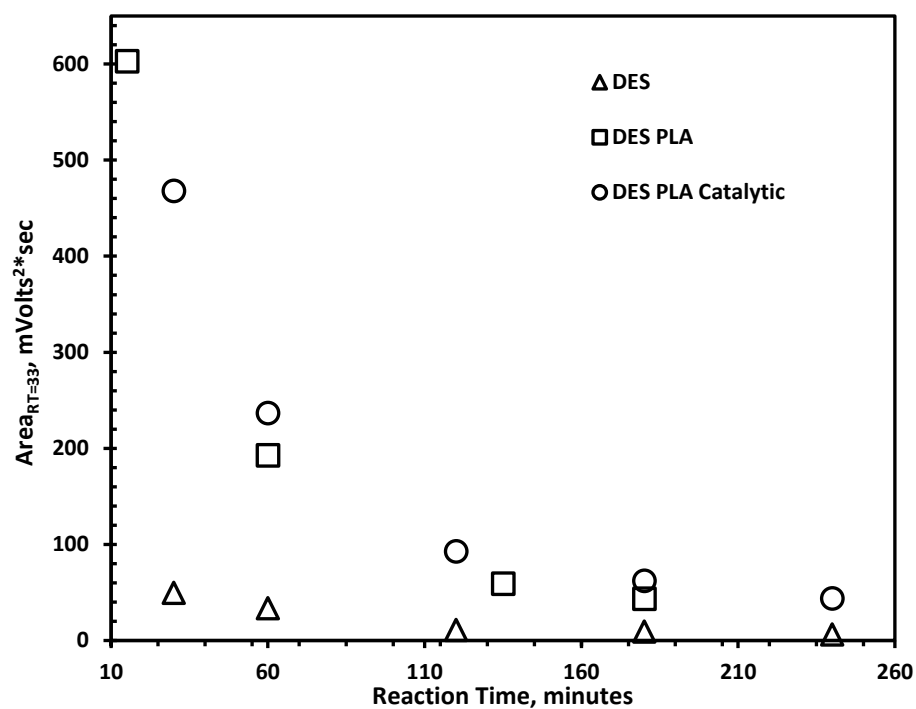


**Figure 3.38.** Peak area values of the unidentified component

For all experiments, similar trend in peak areas was observed. Peak areas were smaller in DES experiment at all reaction times, presence of PLA caused rise in the peak areas. The effect of catalyst was observed at the early stages of the reactions; however, as the reactions proceeded, the peak areas of the catalytic and non-catalytic reactions approach each other.

## CHAPTER 4

### CONCLUSIONS

The purpose of this study was to develop an environmentally benign degradation technique for the PLA waste problem. Deep eutectic solvents were utilized as reaction media for the degradation reaction of PLA. Degradation reactions were carried out in two different systems with batch and semi-batch reactors. The effect of aluminum loaded silica aerogel catalyst on the PLA degradation was also investigated.

Firstly, zinc chloride-ethylene glycol DES was used as reaction medium. This DES gave promising results in terms of stability, i.e. it remains as liquid for more than seven months at room temperature. However, when zinc chloride-ethylene glycol DES was kept at the PLA degradation reaction conditions, i.e., 180°C, 8 hours in batch system followed by ethyl acetate extraction, main degradation products resulted from ethylene glycol were identified as dioxane, decane and undecane. Nonetheless, ethyl lactate, 3-methyl-2-hexanone, and acetic acid hydrazino ethyl ester products were formed due to degradation of PLA in zinc chloride-ethylene glycol DES medium in addition to dioxane which was a DES degradation product. Among the PLA-originated products, ethyl lactate is the most widely used chemical and it is also classified as a green solvent.

DES degradation and PLA degradation reaction in DES medium were also studied in the semi-batch reactor. In the DES degradation study, the main products were: 1,3-dioxolane, 2,2-dimethyl and dioxane. In the PLA degradation reaction, the main products were: 2-pentanol acetate, 3(2H)-Furanone dihydro-2-methyl, and ethyl lactate in addition to 1,3-dioxolane, 2,2-dimethyl and dioxane which were DES degradation products.

For DES degradation reaction, conversion of DES was found as 35.4%. In PLA degradation reaction, conversion of PLA was 97.3%. Yields of gas and liquid products, and solid part in the reactor resulting from PLA were 56.8%, 40.6%, and 2.6%, respectively.

Catalyst usage is important in polymer degradation reactions. Aluminum loaded silica aerogel catalyst was synthesized and used in the PLA degradation in the DES medium. Aluminum was loaded on silica aerogel at two different weight percentages, which were 15 % and 25 %. By thermogravimetric analysis, it was found that SAUA15 decreased the apparent activation energy of PLA thermal degradation reaction more than SAUA125. SAUA15 decreased the apparent activation energy by 26 %, whereas SAUA125 decreased by 9 %. SAUA15 had a surface area of 482 m<sup>2</sup>/g and a pore diameter of 2.61 nm. It had a mesoporous structure.

The presence of catalyst contributed to an increase in the amount of ethyl lactate in the batch system which was considered to be the degradation product of PLA. With the catalyst usage, 1,3-dioxolane, 2,2,4,5-tetramethyl was newly formed, and amounts of dioxane and 3(2H)-furanone dihydro-2-methyl increased. In PLA catalytic degradation reaction, conversion of PLA was 97%. Yields of gas and liquid products and solid part resulting from PLA catalytic degradation were calculated as 59.5%, 37.4%, and 3.1%, respectively.

In semi-batch experiments, hydrogen and carbon dioxide were mainly detected as gaseous products.

Aluminum loaded silica aerogel catalysts showed a promising activity in the degradation reaction of PLA.

Zinc chloride-ethylene glycol DES degraded at the specified reaction conditions and some products were formed due to this degradation. The interaction of PLA with DES also caused formation of various value-added products.

In terms of separation of non-condensable products from the reactor and analyzing gas products, semi-batch system can be evaluated as more advantageous compared to the batch system.





## CHAPTER 5

### RECOMMENDATIONS

To be used in degradation reaction of PLA, thermally more stable DES's can be searched and used. Due to reported TGA data of some choline chloride based DES's, they can be utilized as reaction medium in the degradation reaction of PLA. Additionally, less volatile organic solvents degrading at relatively high temperatures can be used as reaction medium.

In order to see the effect of catalyst more clearly, the amount of catalyst can be increased in reactions or different catalysts can be utilized to increase the selectivity of ethyl lactate.

In order to be able to do quantitative analysis for liquid products formed in both systems, the chemicals having high peak area in GC-MS analyses should be bought. Then, the products could be analyzed via GC or HPLC according to suitability of chemicals.

In semi-batch system, the solid residue left in reactor after the reaction was not analyzed in this study. With an appropriate analysis technique, this residue can be identified. For instance, Gel Permeation Chromatography (GPC) analysis can be performed to see whether lower molecular weight PLA is present or not.

Degradation of DES at different temperatures can also be studied due to the observation of DES degradation in this study. The interaction between DES and catalyst in the semi-batch reactor can also be investigated since an interaction was observed in the batch system.



## REFERENCES

- Abbott, A. P., Barron, J. C., Ryder, K. S., and Wilson, D. (2007). Eutectic-based ionic liquids with metal-containing anions and cations. *Chemistry - A European Journal*, 13(22), 6495–6501. <https://doi.org/10.1002/chem.200601738>
- Abbott, A. P., Capper, G., Davies, D. L., Rasheed, R. K., and Tambyrajah, V. (2003). Novel solvent properties of choline chloride/urea mixtures. *Chemical Communications*, 1, 70–71. <https://doi.org/10.1039/b210714g>
- Al-Oweini, R., and El-Rassy, H. (2009). Synthesis and characterization by FTIR spectroscopy of silica aerogels prepared using several Si(OR)<sub>4</sub> and R''Si(OR')<sub>3</sub> precursors. *Journal of Molecular Structure*, 919(1–3), 140–145. <https://doi.org/10.1016/j.molstruc.2008.08.025>
- Amiri, T. Y., and Moghaddas, J. (2015). Cogeled copperesilica aerogel as a catalyst in hydrogen production from methanol steam reforming. *International Journal of Hydrogen Energy*, 40(3), 1472–1480. <https://doi.org/10.1016/j.ijhydene.2014.11.104>
- Arrieta, M. P., Parres, F., López, J., and Jiménez, A. (2013). Development of a novel pyrolysis-gas chromatography/mass spectrometry method for the analysis of poly(lactic acid) thermal degradation products. *Journal of Analytical and Applied Pyrolysis*, 101, 150–155. <https://doi.org/10.1016/j.jaap.2013.01.017>
- Auras, R., Harte, B., and Selke, S. (2004). An overview of polylactides as packaging materials. *Macromolecular Bioscience*, 4(9), 835–864. <https://doi.org/10.1002/mabi.200400043>
- Aydemir, B. and Sezgi, N. A. (2013). Alumina and tungstophosphoric acid loaded mesoporous catalysts for the polyethylene degradation reaction. *Industrial and Engineering Chemistry Research*, 52(44), 15366–15371. <https://doi.org/10.1021/ie400634m>
- Bacher, A. (2002). Infrared Spectroscopy. Retrieved from <https://www.chem.ucla.edu/~bacher/spectroscopy/IR1.html>
- Badia, J. D., Santonja-Blasco, L., Martínez-Felipe, A., and Ribes-Greus, A. (2012). A methodology to assess the energetic valorization of bio-based polymers from the packaging industry: Pyrolysis of reprocessed polylactide. *Bioresource Technology*, 111, 468–475. <https://doi.org/10.1016/j.biortech.2012.02.013>
- Bahl, S., Dolma, J., Singh, J. J., and Sehgal, S. (2020). Biodegradation of plastics: A state of the art review. *Materials Today: Proceedings*, 39, 31–34. <https://doi.org/10.1016/j.matpr.2020.06.096>

- Benninga H. (1990) A History of Lactic Acid Making, Kluwer micrographs. Academic Publishing, Boston, London, Dordrecht.
- Carothers W.H., Dorough G.L., and Van Natta F.J. (1932) Journal of the American Chemical Society 54, 761–772.
- Corbion Netherlands. (2016). Annual report 2016 -. Annual Report . Retrieved January 14, 2022, from [http://www.corbion.com/media/580437/corbion-annual-report-2016\\_final.pdf](http://www.corbion.com/media/580437/corbion-annual-report-2016_final.pdf)
- Cristina, A. M., Sara, F., Fausto, G., Vincenzo, P., Rocchina, S., and Claudio, V. (2018). Degradation of Post-consumer PLA: Hydrolysis of Polymeric Matrix and Oligomers Stabilization in Aqueous Phase. Journal of Polymers and the Environment, 26(12), 4396–4404. <https://doi.org/10.1007/s10924-018-1312-6>
- Custelcean, R., Moyer, B. A., Bryantsev, V. S., and Hay, B. P. (2006). Anion coordination in metal-organic frameworks functionalized with urea hydrogen-bonding groups. Crystal Growth and Design, 6(2), 555–563. <https://doi.org/10.1021/cg0505057>
- Değirmenciöğlü, P. (2018). Methanol Steam Reforming Over Silica Aerogel Supported Catalyst for Hydrogen Production. MSc Thesis. METU.
- Di Marino, D., Stöckmann, D., Kriescher, S., Stiefel, S., and Wessling, M. (2016). Electrochemical depolymerisation of lignin in a deep eutectic solvent. Green Chemistry, 18(22), 6021–6028. <https://doi.org/10.1039/c6gc01353h>
- Dunn, B. C., Cole, P., Covington, D., Webster, M. C., Pugmire, R. J., Ernst, R. D., Eyring, E. M., Shah, N., and Huffman, G. P. (2005). Silica aerogel supported catalysts for Fischer-Tropsch synthesis. Applied Catalysis A: General, 278(2), 233–238. <https://doi.org/10.1016/j.apcata.2004.10.002>
- Ebeling, W., Hennrich, N., Klockow, M., Metz, H., Orth, H. D., and Lang, H. (1974). Proteinase K from *Tritirachium album Limber*. European Journal of Biochemistry, 47(1), 91–97.
- Enomoto K., Ajioka M., and Yamaguchi A. (1992). Polyhydroxycarboxylic acid and preparation process thereof. 19. <https://patents.google.com/patent/US5310865A/en>
- European Bioplastics, nova Institute (2019). Retrieved from <https://www.european-bioplastics.org/market/>
- European Bioplastics. (2020). Mechanical Recycling - European Bioplastics. Retrieved from, [https://docs.european-bioplastics.org/publications/bp/EUBP\\_BP\\_Mechanical\\_recycling.pdf](https://docs.european-bioplastics.org/publications/bp/EUBP_BP_Mechanical_recycling.pdf)

- Farah, S., Anderson, D. G., and Langer, R. (2016). Physical and mechanical properties of PLA, and their functions in widespread applications. A comprehensive review. *Advanced Drug Delivery Reviews*, 107, 367–392. <https://doi.org/10.1016/j.addr.2016.06.012>
- Garforth, A. A., Ali, S., Hernández-Martínez, J., and Akah, A. (2004). Feedstock recycling of polymer wastes. *Current Opinion in Solid State and Materials Science*, 8(6), 419–425. <https://doi.org/10.1016/j.cossms.2005.04.003>
- Garlotta, D. (2019). A Literature Review of Poly ( Lactic Acid ) A Literature Review of Poly ( Lactic Acid ). *Journal of Polymers and the Environment*, 9(2), 63–84.
- Ghareh Bagh, F. S., Shahbaz, K., Mjalli, F. S., Hashim, M. A., and Alnashef, I. M. (2015). Zinc (II) chloride-based deep eutectic solvents for application as electrolytes: Preparation and characterization. *Journal of Molecular Liquids*, 204, 76–83. <https://doi.org/10.1016/j.molliq.2015.01.025>
- Gianino, C. (2006). Measurement of surface tension by the dripping from a needle. *Physics Education*, 41(5), 440–444. <https://doi.org/10.1088/0031-9120/41/5/010>
- Glotova, V. (2016). Lactide and lactic acid oligomer solubility in certain solvents. *Petroleum and Coal*, 58(5): 573-579.
- Godjoian G., Wang V.R., Ayala A.M., Martinez R.V., Martinez-Bernhard R., and Gutierrez C.G. (1996). Substituted Triethylene Glycols from Dibutylstannylene Acetals. *Tetrahedron Letters*, Vol. 37, No. 4, pp. 433-436, 1996
- Gözde, E. (2019). Investigation of Deep Eutectic Solvents as a Reaction Medium for Metal Chloride Based Chemical Heat Pumps. MSc Thesis. METU.
- Grand View Research. (2014). Retrieved from <http://energyandgold.com/2016/03/10/an-enormous-investment-opportunity-in-a-rapidly-growing-space/>
- Grand View Research. (2021). Polylactic Acid Market Size, Share & Trends Analysis Report by End-use by Region, and Segment Forecasts, 2021-2028. Report ID: GVR-2-68038-669-1
- Gurav, J. L., Jung, I. K., Park, H. H., Kang, E. S., and Nadargi, D. Y. (2010). Silica aerogel: Synthesis and applications. *Journal of Nanomaterials* Volume 2010, Article ID 409310. <https://doi.org/10.1155/2010/409310>
- Habib, A. (2019). Production of Valuable Chemicals from Plastic Wastes Containing Polyethylene and Polypropylene. MSc Thesis. METU

- Hammond, O. S., Bowron, D. T., and Edler, K. J. (2016). Liquid structure of the choline chloride-urea deep eutectic solvent (reline) from neutron diffraction and atomistic modelling. *Green Chemistry*, 18(9), 2736–2744. <https://doi.org/10.1039/c5gc02914g>
- Hansen, B. B., Spittle, S., Chen, B., Poe, D., Zhang, Y., Klein, J. M., Horton, A., Adhikari, L., Zelovich, T., Doherty, B. W., Gurkan, B., Maginn, E. J., Ragauskas, A., Dadmun, M., Zawodzinski, T. A., Baker, G. A., Tuckerman, M. E., Savinell, R. F., and Sangoro, J. R. (2021). Deep Eutectic Solvents: A Review of Fundamentals and Applications. *Chemical Reviews*, 121(3), 1232–1285. <https://doi.org/10.1021/acs.chemrev.0c00385>
- Harkins, W. D., and Cheng Y.C. (1921). The Orientation of Molecules in Surfaces. VI. Cohesion, Adhesion, Tensile Strength, Tensile Energy, Negative Surface Energy, Interfacial Tension, and Molecular Attraction. *J. Am. Chem. Soc.*, 43, 1, 35–53, <https://doi.org/10.1021/ja01434a006>
- Hirao, K., Nakatsuchi, Y., and Ohara, H. (2010). Alcoholysis of Poly(l-lactic acid) under microwave irradiation. *Polymer Degradation and Stability*, 95(6), 925–928. <https://doi.org/10.1016/j.polymdegradstab.2010.03.027>
- Hoshino, A., and Isono, Y. (2002). Degradation of aliphatic polyester films by commercially available lipases with special reference to rapid and complete degradation of poly(L-lactide) film by lipase PL derived from *Alcaligenes sp.* *Biodegradation*, 13(2), 141–147. <https://doi.org/10.1023/A:1020450326301>
- Hovenkamp S.G., and Munting J.P. (1970). Formation of diethylene glycol as a side reaction during production of polyethylene terephthalate. *Journal of Polymer Science Part A-1: Polymer Chemistry*. Vol. 8, 679682.
- International Energy Agency (2020). Production of key thermoplastics, 1980-2050 – charts – Data & Statistics. IEA. Retrieved from <https://www.iea.org/data-and-statistics/charts/production-of-key-thermoplastics-1980-2050>
- Jarerat, A., and Tokiwa, Y. (2001). Degradation of Poly(L-lactide) by a Fungus. *Macromolecular Bioscience*, 1(4), 136–140. [https://doi.org/10.1002/1616-5195\(20010601\)1:4<136::AID-MABI136>3.0.CO;2-3](https://doi.org/10.1002/1616-5195(20010601)1:4<136::AID-MABI136>3.0.CO;2-3)
- Jones F., Tran H., Lindberg D., Zhao L., and Hupa M. (2013). Thermal Stability of Zinc Compounds. *Energy&Fuels*. Special Issue: Impacts of Fuel Quality on Power Production and the Environment. <https://doi.org/10.1021/ef400505u> |
- Kale, G., Auras, R., and Singh, S. P. (2007). Comparison of the degradability of poly(lactide) packages in composting and ambient exposure conditions. *Packaging Technology and Science*, 20(1), 49–70. <https://doi.org/10.1002/pts.742>
- Kale, G., Auras, R., Singh, S. P., and Narayan, R. (2007). Biodegradability of polylactide bottles in real and simulated composting conditions. *Polymer*

Testing, 26(8), 1049–1061.  
<https://doi.org/10.1016/j.polymertesting.2007.07.006>

- Karamanlioglu, M., and Robson, G. D. (2013). The influence of biotic and abiotic factors on the rate of degradation of poly(lactic) acid (PLA) coupons buried in compost and soil. *Polymer Degradation and Stability*, 98(10), 2063–2071. <https://doi.org/10.1016/j.polymdegradstab.2013.07.004>
- Karamanlioglu, M., Preziosi, R., and Robson, G. D. (2017). Abiotic and biotic environmental degradation of the bioplastic polymer poly(lactic acid): A review. *Polymer Degradation and Stability*, 137, 122–130. <https://doi.org/10.1016/j.polymdegradstab.2017.01.009>
- Kim K.N., and Hoffmann H.R. (2007). Heterogeneous photocatalytic degradation of ethylene glycol and propylene glycol. *Korean J. Chem. Eng.*, 25(1), 89-94 (2008).
- Kistler, S. S., “Coherent Expanded Aerogels and Jellies.” *Nature*, 127, 741, 1931.
- Kobayashi, H., and Fukuoka A. (2013). Current Catalytic Processes for Biomass Conversion. *New and Future Developments in Catalysis* (pp.29-52). <https://doi.org/10.1016/B978-0-444-53878-9.00002-3>
- Kolstad, J. J., Vink, E. T. H., De Wilde, B., and Debeer, L. (2012). Assessment of anaerobic degradation of Ingeo™ polylactides under accelerated landfill conditions. *Polymer Degradation and Stability*, 97(7), 1131–1141. <https://doi.org/10.1016/j.polymdegradstab.2012.04.003>
- Kopinke F.D., Remmler M., Mackenzie K., Möder M., and Wachsen O. (1996). Thermal decomposition of biodegradable polyesters - Poly(lactic acid). *Polymer Degradation and Stability*. 53. 329-342.
- Lamberti, F. M., Román-Ramírez, L. A., Mckeown, P., Jones, M. D., and Wood, J. (2020). Kinetics of alkyl lactate formation from the alcoholysis of poly(lactic acid). *Processes* 2020. 8, 738. <https://doi.org/10.3390/PR8060738>
- Lenga R.E. (1988). *The Sigma-Aldrich library of chemical safety data*. Milwaukee, Wis., USA : Sigma-Aldrich Corp.
- Lian, H., Hong, S., Carranza, A., Mota-Morales, J. D., and Pojman, J. A. (2015). Processing of lignin in urea-zinc chloride deep-eutectic solvent and its use as a filler in a phenol-formaldehyde resin. *RSC Advances*, 5(36), 28778–28785. <https://doi.org/10.1039/c4ra16734a>
- Liu, D., Yan, X., Zhuo, S., Si, M., Liu, M., Wang, S., Ren, L., Chai, L., and Shi, Y. (2018). *Pandora* sp. B-6 assists the deep eutectic solvent pretreatment of rice straw via promoting lignin depolymerization. *Bioresource Technology*, 257, 62–68. <https://doi.org/10.1016/j.biortech.2018.02.029>

- Lopes S.M., Jardini, A. L., and Filho, R. M. (2012). Poly (lactic acid) production for tissue engineering applications. *Procedia Engineering*, 42, 1402–1413. <https://doi.org/10.1016/j.proeng.2012.07.534>
- Lowell, S. (2005). Characterization of porous solids and powders: surface area, pore size, and density. *Choice Reviews Online*, 42(09), 42-5288-42–5288. <https://doi.org/10.5860/choice.42-5288>
- Malfait, W. J., Zhao, S., Verel, R., Iswar, S., Rentsch, D., Fener, R., Zhang, Y., Milow, B., and Koebel, M. M. (2015). Surface Chemistry of Hydrophobic Silica Aerogels. *Chemistry of Materials*, 27(19), 6737–6745. <https://doi.org/10.1021/acs.chemmater.5b02801>
- Masaki, K., Kamini, N. R., Ikeda, H., and Iefuji, H. (2005). Cutinase-like enzyme from the yeast *Cryptococcus* sp. strain S-2 hydrolyzes polylactic acid and other biodegradable plastics. *Applied and Environmental Microbiology*, 71(11), 7548–7550. <https://doi.org/10.1128/AEM.71.11.7548-7550.2005>
- Mjalli, F. S. (2016). Mass connectivity index-based density prediction of deep eutectic solvents. *Fluid Phase Equilibria*, 409, 312–317. <https://doi.org/10.1016/j.fluid.2015.09.053>
- Mjalli, F. S., and Ahmed, O. U. (2015). Characteristics and intermolecular interaction of eutectic binary mixtures : Reline and Glyceline. 32(4), 1–7. <https://doi.org/10.1007/s11814-015-0134-7>
- Mota-Morales, J. D., Gutiérrez, M. C., Sanchez, I. C., Luna-Bárcenas, G., and Del Monte, F. (2011). Frontal polymerizations carried out in deep-eutectic mixtures providing both the monomers and the polymerization medium. *Chemical Communications*, 47(18), 5328–5330. <https://doi.org/10.1039/c1cc10391a>
- Mudliar, S., Giri, B., Padoley, K., Satpute, D., Dixit, R., Bhatt, P., Pandey, R., Juwarkar, A., and Vaidya, A. (2010). Bioreactors for treatment of VOCs and odours - A review. *Journal of Environmental Management*, 91(5), 1039–1054. <https://doi.org/10.1016/j.jenvman.2010.01.006>
- Muley, P. D., Mobley, J. K., Tong, X., Novak, B., Stevens, J., Moldovan, D., Shi, J., and Boldor, D. (2019). Rapid microwave-assisted biomass delignification and lignin depolymerization in deep eutectic solvents. *Energy Conversion and Management*, 196, 1080–1088. <https://doi.org/10.1016/j.enconman.2019.06.070>
- Nakamiya, K., Hashimoto, S., Ito, H., and Edmonds, J. S. (2005). Degradation of 1,4-Dioxane and Cyclic Ethers by an Isolated Fungus. 71(3), 1254–1258. <https://doi.org/10.1128/AEM.71.3.1254>



- Nampoothiri, K. M., Nair, N. R., and John, R. P. (2010). An overview of the recent developments in polylactide (PLA) research. *Bioresource Technology*, 101(22), 8493–8501. <https://doi.org/10.1016/j.biortech.2010.05.092>
- Nim, B., Opaprakasit, M., Petchsuk, A., and Opaprakasit, P. (2020). Microwave-assisted chemical recycling of polylactide (PLA) by alcoholysis with various diols. *Polymer Degradation and Stability*, 181, 109363. <https://doi.org/10.1016/j.polymdegradstab.2020.109363>
- Nishida, H., Mori, T., Hoshihara, S., Fan, Y., Shirai, Y., and Endo, T. (2003). Effect of tin on poly(L-lactic acid) pyrolysis. *Polymer Degradation and Stability*, 81(3), 515–523. [https://doi.org/10.1016/S0141-3910\(03\)00152-6](https://doi.org/10.1016/S0141-3910(03)00152-6)
- NIST Chemistry WebBook, NIST Standard Reference Database for Phase Change Data of Diethylene Glycol.
- Noda M., and Okuyama H. (1994). Thermal Catalytic Depolymerization of PLA Oligomer into LL-lactide: Effects of Al, Ti, Zn and Zr Compounds as Catalysts. *Chemical Pharmaceutical Bulletin*, 17(11), 1460–1462. <https://doi.org/10.1248/cpb.47.467>
- Obali, Z., Sezgi, N. A., and Dogu, T. (2012). Catalytic degradation of polypropylene over alumina loaded mesoporous catalysts. *Chemical Engineering Journal*, 207–208, 421–425. <https://doi.org/10.1016/j.cej.2012.06.146>
- Piemonte, V., and Gironi, F. (2013). Lactic Acid Production by Hydrolysis of Poly(Lactic Acid) in Aqueous Solutions: An Experimental and Kinetic Study. *Journal of Polymers and the Environment*, 21(1), 275–279. <https://doi.org/10.1007/s10924-012-0468-8>
- Piemonte, V., Sabatini, S., and Gironi, F. (2013). Chemical Recycling of PLA: A Great Opportunity Towards the Sustainable Development *Journal of Polymers and the Environment*, 21(3), 640–647. <https://doi.org/10.1007/s10924-013-0608-9>
- Plotka-Wasyłka, J., de la Guardia, M., Andruch, V., and Vilková, M. (2020). Deep eutectic solvents vs ionic liquids: Similarities and differences. *Microchemical Journal*, 159(July). <https://doi.org/10.1016/j.microc.2020.105539>
- Pollet, P., Davey, E. A., Ureña-Benavides, E. E., Eckert, C. A., and Liotta, C. L. (2014). Solvents for sustainable chemical processes. *Green Chemistry*, 16(3), 1034–1055. <https://doi.org/10.1039/c3gc42302f>
- Popoola A.V. (1991). Mechanism of the reaction involving the formation of dioxane byproduct during the production of poly(ethylene terephthalate). *Journal of Applied Polymer Science*. Vol. 43, 1875-1877. <https://doi.org/10.1002/app.1991.070431011>

- Pranamuda, H., Tokiwa, Y., and Tanaka, H. (1997). Polylactide degradation by an *Amycolatopsis* sp. *Applied and Environmental Microbiology*, 63(4), 1637–1640. <https://doi.org/10.1128/aem.63.4.1637-1640.1997>
- Premanathan, M., Karthikeyan, K., Jeyasubramanian, K., and Manivannan, G. (2011). Selective toxicity of ZnO Nanoparticles Toward Gram-positive Bacteria and Cancer Cells by Apoptosis Through Lipid Peroxidation. *Nanomedicine: Nanotechnology, Biology and Medicine*, 7(2), 184–192. <https://doi.org/10.1016/j.nano.2010.10.001>
- Qi X., Ren Y., and Wang X. (2017). New advances in the biodegradation of Poly(lactic) acid. *International Biodeterioration & Biodegradation*, 117 215–223.
- Ragaert, K., Delva, L., and Van Geem, K. (2017). Mechanical and chemical recycling of solid plastic waste. *Waste Management*, 69, 24–58. <https://doi.org/10.1016/j.wasman.2017.07.044>
- Rong, X., and Keif, M. (2007). A study of PLA printability with flexography. *Proceedings of the Technical Association of the Graphic Arts, TAGA*, 605–613.
- Saliccioli, M., and Vlachos, D. G. (2011). Kinetic modeling of PT catalyzed and computation-driven catalyst discovery for ethylene glycol decomposition. *ACS Catalysis*, 1(10), 1246–1256. <https://doi.org/10.1021/cs2003593>
- Sanderson J.R., Lin J.R., Duranleau R.G., Yeakey E.L., Marquis E.T. (1987). Free Radicals in Organic Synthesis. A Novel Synthesis of Glycerol Based on Ethylene Glycol and Formaldehyde. *J. Org. Chem.* 1988, 53, 2859-2861.
- Sangwan, P., and Wu, D. Y. (2008). New insights into polylactide biodegradation from molecular ecological techniques. *Macromolecular Bioscience*, 8(4), 304–315. <https://doi.org/10.1002/mabi.200700317>
- Sert, M., Arslanoğlu, A., and Ballice, L. (2018). Conversion of sunflower stalk-based cellulose to the valuable products using choline chloride based deep eutectic solvents. *Renewable Energy*, 118, 993–1000. <https://doi.org/10.1016/j.renene.2017.10.083>
- Siparsky, G. L., Voorhees, K. J., and Miao, F. (1998). Hydrolysis of polylactic acid (PLA) and polycaprolactone (PCL) in aqueous acetonitrile solutions: Autocatalysis. *Journal of Environmental Polymer Degradation*, 6(1), 31–41. <https://doi.org/10.1023/A:1022826528673>
- Sivri, S., Dilek, C., and Sezgi, N. A. (2019). Synthesis and characterization of aluminum containing silica aerogel catalysts for degradation of PLA. *International Journal of Chemical Reactor Engineering*, 17(5), 1–10. <https://doi.org/10.1515/ijcre-2018-0163>

- Soleimani, A., and Abbasi, M. H. (2008). Silica aerogel; synthesis, properties and characterization. *Journal of Materials Processing Technology*, 199(1), 10–26. <https://doi.org/10.1016/j.jmatprotec.2007.10.060>
- Song, X., Wang, H., Yang, X., Liu, F., Yu, S., and Liu, S. (2014). Hydrolysis of poly(lactic acid) into calcium lactate using ionic liquid [Bmim][OAc] for chemical recycling. *Polymer Degradation and Stability*, 110, 65–70. <https://doi.org/10.1016/j.polymdegradstab.2014.08.020>
- Song, X., Zhang, X., Wang, H., Liu, F., Yu, S., and Liu, S. (2013). Methanolysis of poly(lactic acid) (PLA) catalyzed by ionic liquids. *Polymer Degradation and Stability*, 98(12), 2760–2764. <https://doi.org/10.1016/j.polymdegradstab.2013.10.012>
- Şener, M.İ. (2019). Development of Bifunctional Catalyst for the Single-Step Synthesis of Dimethyl Ether. MSc Thesis. METU.
- Thapliyal, P. C., and Singh, K. (2014). Aerogels as Promising Thermal Insulating Materials: An Overview. *Journal of Materials*, 2014, 1–10. <https://doi.org/10.1155/2014/127049>
- Theophanides, T., and Harvey, P. D. (1987). Structural and spectroscopic properties of metal-urea complexes. *Coordination Chemistry Reviews*, 76(C), 237–264. [https://doi.org/10.1016/0010-8545\(87\)85005-1](https://doi.org/10.1016/0010-8545(87)85005-1)
- Thompson, R. C., Moore, C. J., Saal, F. S. V., and Swan, S. H. (2009). Plastics, the environment and human health: Current consensus and future trends. *Philosophical Transactions of the Royal Society B: Biological Sciences*, 364(1526), 2153–2166. <https://doi.org/10.1098/rstb.2009.0053>
- Tokiwa, Y., and Jarerat, A. (2004). Biodegradation of poly(L-lactide). *Biotechnology Letters*, 26(10), 771–777. <https://doi.org/10.1023/B:BILE.0000025927.31028.e3>
- Tokiwa, Y., and Calabia, B. P. (2006). Biodegradability and biodegradation of poly(lactide). *Applied Microbiology and Biotechnology*, 72(2), 244–251. <https://doi.org/10.1007/s00253-006-0488-1>
- Toxqui-Terán, A., Leyva-Porras, C., Ruíz-Cabrera, M. ángel, Cruz-Alcantar, P., and Saavedra-Leos, M. Z. (2018). Thermal study of polyols for the technological application as plasticizers in food industry. *Polymers*, 10(5), 1–13. <https://doi.org/10.3390/polym10050467>
- Tran, P. H., and Thi Hang, A. H. (2018). Deep eutectic solvent-catalyzed arylation of benzoxazoles with aromatic aldehydes. *RSC Advances*, 8(20), 11127–11133. <https://doi.org/10.1039/c8ra01094c>

- Tsuji, H., and Suzuyoshi, K. (2002). Environmental degradation of biodegradable polyesters 2. Poly( $\epsilon$ -caprolactone), poly[(R)-3-hydroxybutyrate], and poly(L-lactide) films in natural dynamic seawater. *Polymer Degradation and Stability*, 75(2), 357–365. [https://doi.org/10.1016/S0141-3910\(01\)00239-7](https://doi.org/10.1016/S0141-3910(01)00239-7)
- Türkiye İstatistik Kurumu (TÜİK). (2020). Data Portal: Foreign Trade Indices 2020.
- United States Environmental Protection Agency (2020). Assessing Trends in Materials Generation and Management in the United States. Retrieved from [https://www.epa.gov/sites/default/files/2021-01/documents/2018\\_tables\\_and\\_figures\\_dec\\_2020\\_fnl\\_508.pdf](https://www.epa.gov/sites/default/files/2021-01/documents/2018_tables_and_figures_dec_2020_fnl_508.pdf)
- Van Osch, D. J. G. P., Dietz, C. H. J. T., Van Spronsen, J., Kroon, M. C., Gallucci, F., Van Sint Annaland, M., and Tuinier, R. (2019). A Search for Natural Hydrophobic Deep Eutectic Solvents Based on Natural Components. *ACS Sustainable Chemistry and Engineering*, 7(3), 2933–2942. <https://doi.org/10.1021/acssuschemeng.8b03520>
- Yurdakal, S., Garlisi, C., Özcan, L., Bellardita, M., & Palmisano, G. (2019). (photo)catalyst characterization techniques. *Heterogeneous Photocatalysis*, 87–152. <https://doi.org/10.1016/b978-0-444-64015-4.00004-3>
- Wang, Q., Yao, X., Geng, Y., Zhou, Q., Lu, X., and Zhang, S. (2015). Deep eutectic solvents as highly active catalysts for the fast and mild glycolysis of poly(ethylene terephthalate)(PET). *Green Chemistry*, 17(4), 2473–2479. <https://doi.org/10.1039/c4gc02401j>
- Wang, X., Huang, Z., Wei, M., Lu, T., Nong, D., Zhao, J., Gao, X., and Teng, L. (2019). Catalytic effect of nanosized ZnO and TiO<sub>2</sub> on thermal degradation of poly(lactic acid) and isoconversional kinetic analysis. *Thermochimica Acta*, 672, 14–24. <https://doi.org/10.1016/j.tca.2018.12.008>
- Williams, D. F. (1981). Enzymic hydrolysis of polylactic acid. *Engineering in Medicine*, 10(1), 5–7. [https://doi.org/10.1243/EMED\\_JOUR\\_1981\\_010\\_004\\_02](https://doi.org/10.1243/EMED_JOUR_1981_010_004_02)
- Wu, G., Yu, Y., Cheng, X., & Zhang, Y. (2011). Preparation and surface modification mechanism of silica aerogels via ambient pressure drying Preparation and surface modification mechanism of silica aerogels via ambient pressure drying. *Materials Chemistry and Physics*, 129(1–2), 308–314. <https://doi.org/10.1016/j.matchemphys.2011.04.003>
- Yu, P. J., Lee, M. H., Hsu, H. M., Tsai, H. M., and Chen-Yang, Y. W. (2015). Silica aerogel-supported cobalt nanocomposites as efficient catalysts toward hydrogen generation from aqueous ammonia borane. *RSC Advances*, 5(18), 13985–13992. <https://doi.org/10.1039/c4ra14002h>

- Zenkiewicz, M., Richert, J., Rytlewski, P., Moraczewski, K., Stepczyńska, M., and Karasiewicz, T. (2009). Characterisation of multi-extruded poly(lactic acid). *Polymer Testing*, 28(4), 412–418. <https://doi.org/10.1016/j.polymertesting.2009.01.012>
- Zou, H., Yi, C., Wang, L., Liu, H., and Xu, W. (2009). Thermal degradation of poly(lactic acid) measured by thermogravimetry coupled to Fourier transform infrared spectroscopy. *Journal of Thermal Analysis and Calorimetry*, 97(3), 929–935. <https://doi.org/10.1007/s10973-009-0121-5>



## APPENDICES

### A. GC-MS Reports

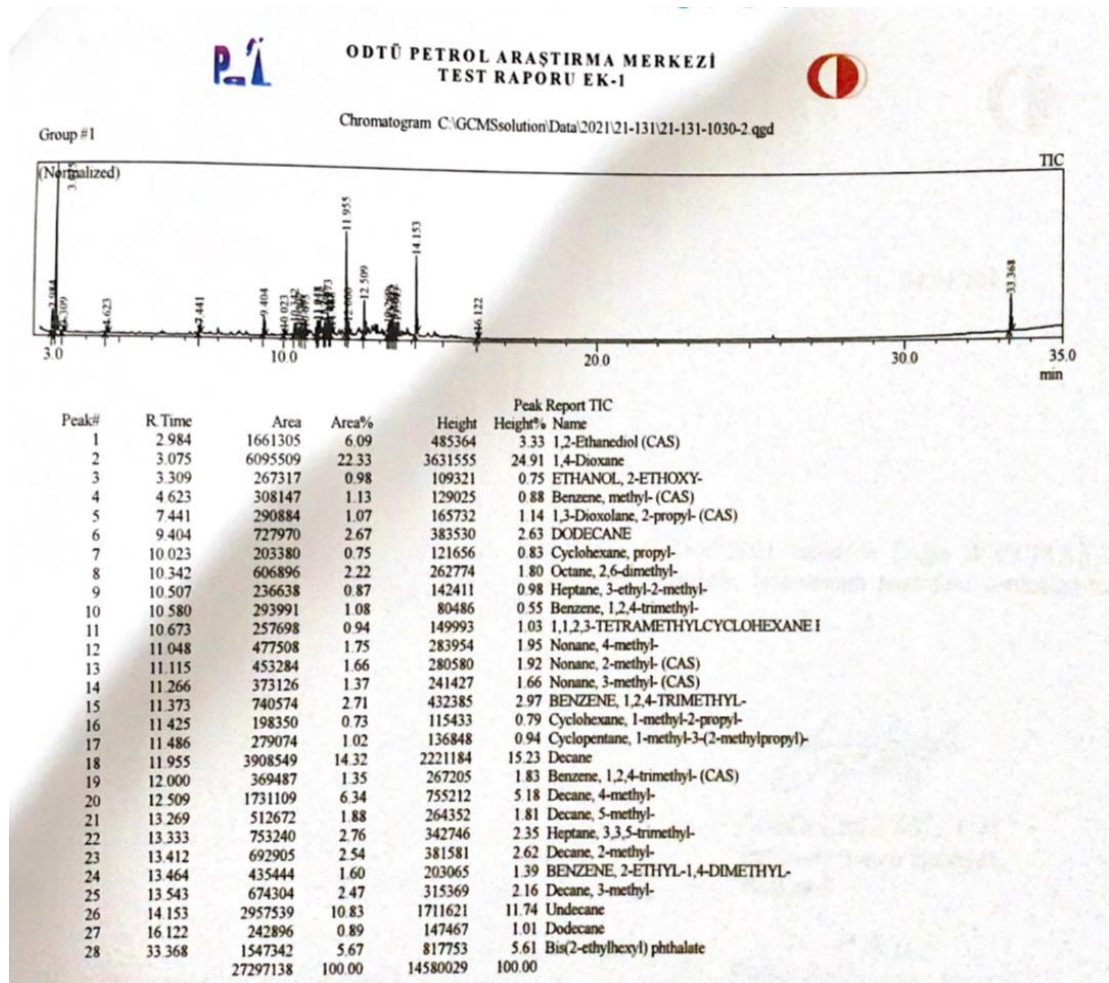
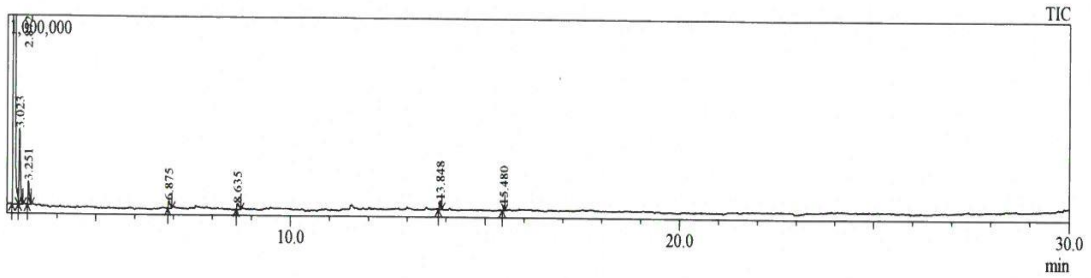


**Figure A. 1.** GC-MS Report of Zinc Chloride-Ethylene Glycol DES Degradation in Batch System



Chromatogram C:\GCMSolution\Data\2022\22-114\22-114-026-1.qgd

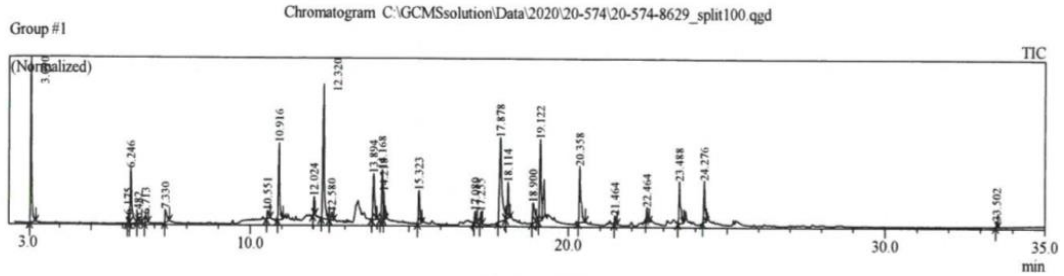
Group #1



Peak#	R.Time	Area	Area%	Height	Height%	Name
1	2.872	39973131	96.07	18690038	96.70	1,3-DIOXOLANE, 2,2-DIMETHYL-
2	3.023	894564	2.15	382533	1.98	1,4-Dioxane
3	3.251	326646	0.79	118424	0.61	ETHANOL, 2-ETHOXY-
4	6.875	153927	0.37	39271	0.20	2-PENTANONE, 4-HYDROXY-4-METHYL-
5	8.635	129344	0.31	29584	0.15	2-Cyclopenten-1-one, 2-methyl- (CAS)
6	13.848	83347	0.20	44856	0.23	Ethanol, 2,2'-[1,2-ethanediylbis(oxy)]bis-, diac
7	15.480	46022	0.11	23857	0.12	Ethanol, 2,2'-oxybis-, dipropoate
		41606981	100.00	19328563	100.00	

**Figure A. 2.** GC-MS Report of Heating only Zinc Chloride-Ethylene Glycol DES in Semi-Batch System



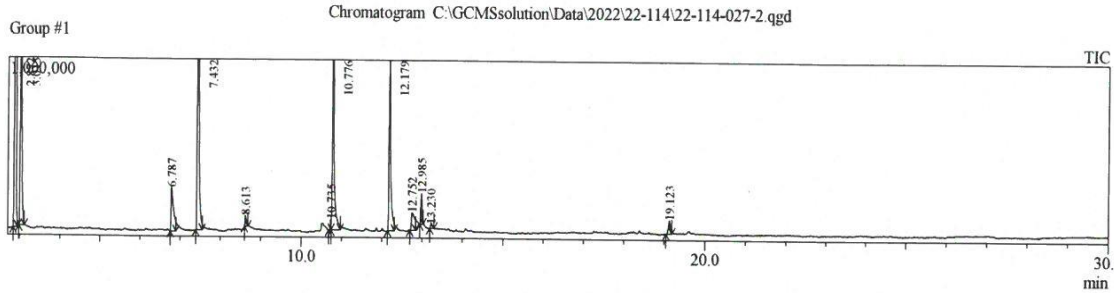


Peak#	R. Time	Area	Area%	Height	Height%	Name
1	3.090	23619067	10.91	10746158	15.59	1,4-Dioxane
2	6.175	1255603	0.58	510477	0.74	Ethane, 1,1-diethoxy- (CAS)
3	6.246	11803047	5.45	3542597	5.14	Propanoic acid, 2-hydroxy-, ethyl ester, (S)-
4	6.482	882723	0.41	244749	0.36	1,3-Dioxolane, 2,4,5-trimethyl-
5	6.713	1642309	0.76	520787	0.76	Ethanol, 2-chloro-, acetate
6	7.330	3534707	1.63	851136	1.23	1,2-Ethanediol, monoacetate
7	10.551	1771989	0.82	517751	0.75	Ethanol, 2-(2-chloroethoxy)-
8	10.916	15452237	7.14	4968495	7.21	3-METHYLHEXAN-2-ONE-6-D3
9	12.024	1869566	0.86	1164244	1.69	Decane (CAS)
10	12.320	27750887	12.82	8682752	12.60	Ethanol, 2,2'-oxybis- (CAS)
11	12.580	1926453	0.89	506635	0.73	Decane, 4-methyl- (CAS)
12	13.894	10564814	4.88	2961755	4.30	DIETHYLENEGLYCOL MONOACETATE
13	14.168	10300794	4.76	3221541	4.67	Propanoic acid, 2-(methoxymethoxy)-
14	14.218	3743100	1.73	1773732	2.57	Undecane
15	15.323	6377502	2.95	2123647	3.08	Ethanol, 2-[2-(2-methoxyethoxy)ethoxy]-, ace
16	17.080	1396852	0.65	742382	1.08	Ethanol, 2,2'-oxybis-, diacetate
17	17.255	1302753	0.60	749896	1.09	Tetraethylene glycol, diacetate
18	17.878	27291510	12.61	5408670	7.85	Ethanol, 2,2'-[1,2-ethanediyl(bis(oxy))]bis- (CA
19	18.114	6250954	2.89	2305857	3.34	Ethanol, 2-[2-(2-chloroethoxy)ethoxy]- (CAS)
20	18.900	6183949	2.86	1306367	1.90	2-[2-(2-(2-Hydroxyethoxy)ethoxy)ethoxy]ethy
21	19.122	16834137	7.78	5269515	7.64	Acetic acid, hydrazino-, ethyl ester
22	20.358	13189382	6.09	3655170	5.30	2-[2-(2-(2-Hydroxyethoxy)ethoxy)ethoxy]ethy
23	21.464	1162536	0.54	555423	0.81	Ethanol, 2,2'-[1,2-ethanediyl(bis(oxy))]bis-, diac
24	22.464	1936148	0.89	822430	1.19	Ethanol, 2-[2-(2-chloroethoxy)ethoxy]- (CAS)
25	23.488	9972845	4.61	2726262	3.95	Ethanol, 2-[2-(2-ethoxyethoxy)ethoxy]- (CAS)
26	24.276	7654836	3.54	2676354	3.88	2-[2-(2-Ethoxyethoxy)ethoxy]ethyl acetate
27	33.502	752487	0.35	380431	0.55	Bis(2-ethylhexyl) phthalate
		216423187	100.00	68935213	100.00	

**Figure A. 3.** GC-MS Report of PLA Degradation Reaction in Zinc Chloride-Ethylene Glycol DES in Batch System



ODTÜ PETROL ARAŞTIRMA MERKEZİ  
TEST RAPORU EK-1



Peak#	R.Time	Area	Area%	Height	Height%	Name
1	2.872	14292576	44.70	7429631	50.73	1,3-DIOXOLANE, 2,2-DIMETHYL-
2	3.015	3485014	10.90	1698093	11.60	1,4-Dioxane
3	6.787	1019747	3.19	248336	1.70	2-PENTANONE, 4-HYDROXY-4-METHYL-
4	7.432	4745185	14.84	1951387	13.32	2-Pentanol, acetate (CAS)
5	8.613	181846	0.57	61678	0.42	2-Cyclopenten-1-one, 2-methyl- (CAS)
6	10.735	81689	0.26	57910	0.40	Bis(2-chloroethyl) ether
7	10.776	4146953	12.97	1733285	11.84	3(2H)-Furanone, dihydro-2-methyl- (CAS)
8	12.179	2859578	8.94	1096752	7.49	Propanoic acid, 2-hydroxy-, ethyl ester (CAS)
9	12.752	542251	1.70	98850	0.67	Propanoic acid, 2-hydroxy-, ethyl ester, (S)-
10	12.985	310848	0.97	172967	1.18	Propanoic acid, 2-chloro-, ethyl ester
11	13.230	73746	0.23	22483	0.15	Diethyl pyrocarbonate
12	19.123	235936	0.74	73647	0.50	Propanoic acid, 2-(methoxymethoxy)-
		31975369	100.00	14645019	100.00	

**Figure A. 4.** GC-MS Report of PLA Degradation Reaction in Zinc Chloride-Ethylene Glycol DES in Semi-Batch System

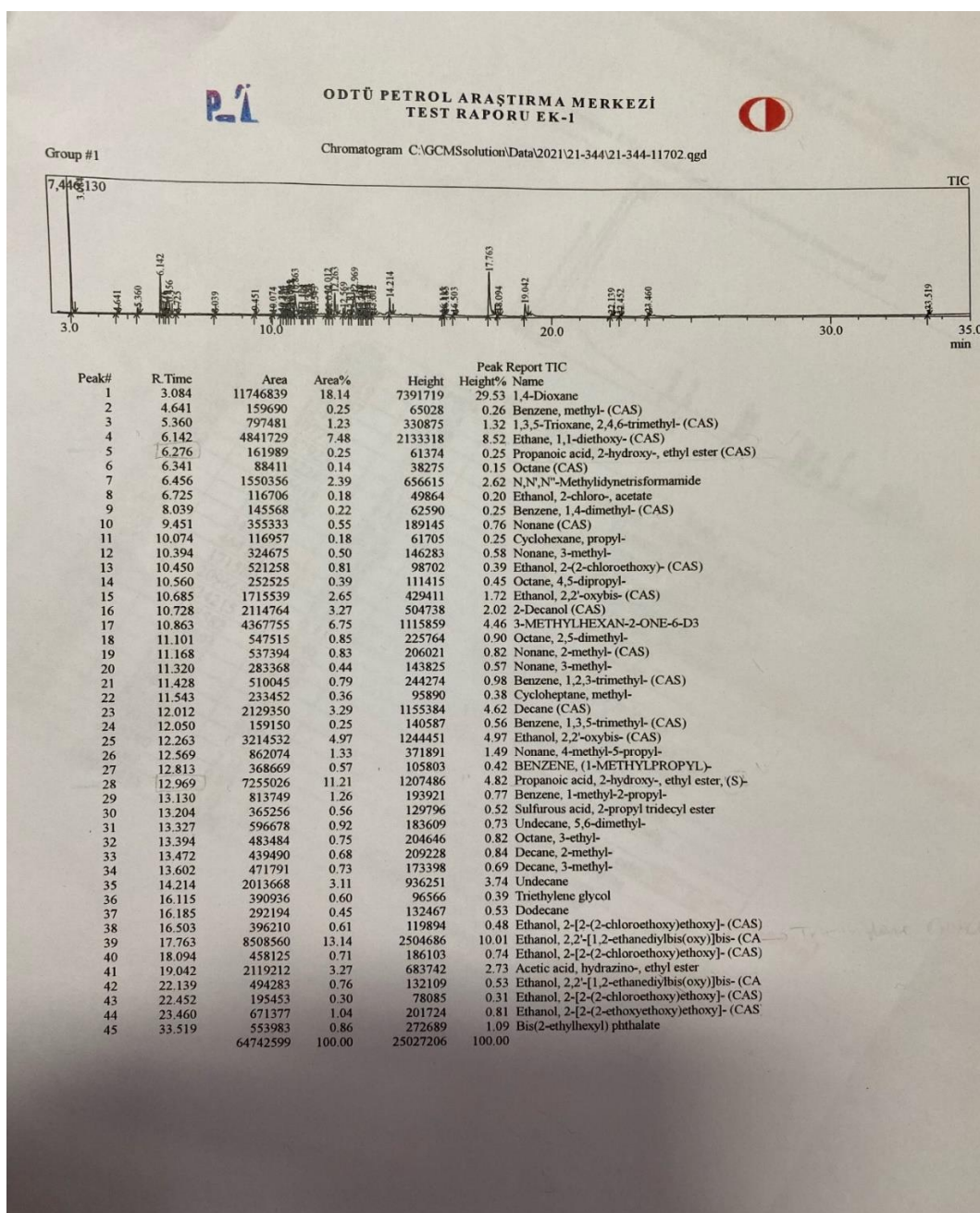
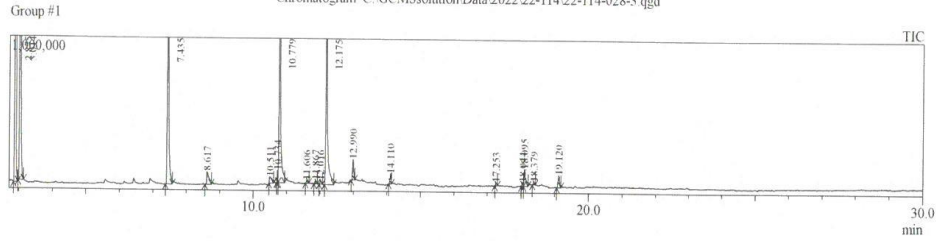


**Figure A. 5.** GC-MS Report of PLA Catalytic Degradation Reaction in Zinc Chloride-Ethylene Glycol DES in Batch System





Chromatogram C:\GCMSSolution\Data\2022\22-114\22-114-028-3.qgd



Peak#	R.Time	Area	Area%	Height	Height%	Name
1	2.875	12882737	36.86	7013821	42.92	1,3-DIOXOLANE, 2,2-DIMETHYL-
2	3.014	5126848	14.67	2555273	15.64	1,4-Dioxane
3	7.435	4367171	12.50	1769136	10.83	1,3-Dioxolane, 2,2,4,5-tetramethyl-, trans-
4	8.617	415629	1.19	86777	0.53	2-Cyclopenten-1-one, 2-methyl- (CAS)
5	10.511	227329	0.65	41846	0.26	Ethanol, 2-(2-chloroethoxy)- (CAS)
6	10.734	122243	0.35	81520	0.50	Bis(2-chloroethyl) ether
7	10.779	5773382	16.52	2507279	15.34	3(2H)-Furanone, dihydro-2-methyl- (CAS)
8	11.606	50245	0.14	18230	0.11	12-Crown-4
9	11.867	52445	0.15	24027	0.15	Ethanone, 1-(1-cyclohexen-1-yl)- (CAS)
10	12.016	59225	0.17	23791	0.15	2,4-Dimethylfuran
11	12.175	4578390	13.10	1759926	10.77	Ethanol, 2,2-oxybis- (CAS)
12	12.990	301276	0.86	137270	0.84	Propanoic acid, 2-chloro-, ethyl ester
13	14.110	153355	0.44	65000	0.40	CIS 5,6 DIHYDROXY DIHYDRO THYMIN
14	17.253	53742	0.15	22996	0.14	Ethane-1,1-diol dipropanoate
15	18.044	69366	0.20	25201	0.15	Ethanol, 1-[2-(2-chloroethoxy)ethoxy]-
16	18.095	425679	1.21	111056	0.68	Propanoic acid, 2-(methoxymethoxy)-
17	18.379	37312	0.11	17406	0.11	1,1-Bis(2-chloroethoxy)-ethane
18	19.120	252607	0.72	80801	0.49	Propanoic acid, 2-(methoxymethoxy)-
		34946981	100.00	16341356	100.00	

**Figure A. 7.** GC-MS Report of PLA Catalytic Degradation Reaction in Zinc Chloride-Ethylene Glycol DES in Semi-Batch System

## B. Mass Balances for Degradation Reactions in Semi-Batch System

In all experiments DES was prepared with 6.0 g ZnCl<sub>2</sub> and 8.2 g ethylene glycol. In the experiments of PLA decomposition, PLA/ DES and PLA/catalyst weight ratio were kept constant at 0.37 and 2.0, respectively. Calculations of DES conversion, PLA conversion, and the gas and liquid products' yields are given below:

### B.1. Mass Balances for Degradation Reaction of DES

The weight percent of ZnCl<sub>2</sub> in synthesized DES is calculated using Eqn. (B.1.1).

$$wt\%_{ZnCl_2} = \frac{m_{ZnCl_2,prep}}{m_{ZnCl_2,prep} + m_{EG,prep}} \times 100 \quad (B.1.1)$$

The desired amount of DES used in the degradation reaction is represented with  $m_{DES,0}$ . Mass of zinc chloride is calculated as in Eqn. (B.1.2).

$$m_{ZnCl_2} = m_{DES,0} \times wt\%_{ZnCl_2} \quad (B.1.2)$$

Initial total mass in the reactor  $m_{T,i}$  equals to;

$$m_{T,i} = m_{DES,0} \quad (B.1.3)$$

The mass of the gas products obtained from DES degradation reaction and the conversion of DES are calculated from Eqn. (B.1.4) and Eqn. (B.1.5), respectively.

$$m_{gas} = m_{T,i} - m_{liq} - m_{left\ in\ reactor} \quad (B.1.4)$$

$$X_{DES} = \frac{m_{gas} + m_{liq}}{m_{DES,0}} \times 100 \quad (B.1.5)$$

Weight percentages of gas and liquid products are found as follows;

$$wt\%_{gas\ product\ from\ DES} = \frac{m_{gas}}{m_{DES,0}} \times 100 \quad (B.1.6)$$

$$wt\%_{liq\ product\ from\ DES} = \frac{m_{liq}}{m_{DES,0}} \times 100 \quad (B.1.7)$$

Weight percent of solid products except zinc chloride was calculated from Eqn. (B.1.8)

$$wt\%_{solid\ product\ from\ DES} = \frac{m_{left\ in\ reactor} - m_{ZnCl_2}}{m_{DES,o}} \times 100 \quad (B.1.8)$$

## B.2. Mass Balances for Degradation Reaction of PLA in DES

Initial total mass is given by Eqn. (B.1.9).

$$m_{T,i} = m_{DES,o} + m_{PLA,o} \quad (B.1.9)$$

Mass of gas products are calculated by using Eqn. (10).

$$m_{gas} = m_{T,i} - m_{liq} - m_{left\ in\ reactor} \quad (B.1.10)$$

To calculate the amount of gas and liquid products which are produced due to PLA degradation, Eqn. (B.1.11) and Eqn. (B.1.12) are used.

$$m_{gas\ product\ from\ PLA} = m_{gas} - \left( m_{DES,o} \times \frac{wt\%_{gas\ product\ from\ DES}}{100} \right) \quad (B.1.11)$$

$$m_{liq\ product\ from\ PLA} = m_{liq} - \left( m_{DES,o} \times \frac{wt\%_{liq\ product\ from\ DES}}{100} \right) \quad (B.1.12)$$

Mass of solid products resulted by PLA, except zinc chloride, is calculated from Eqn (B.1.13).

$$m_{solid\ in\ reactor\ from\ PLA} = m_{left\ in\ reactor} - \left( m_{DES,o} \times \frac{wt\%_{solid\ in\ reactor\ from\ DES}}{100} \right) - m_{ZnCl_2} \quad (B.1.13)$$

The yields of the gas, liquid and solid products obtained from the PLA degradation reaction is:

$$Y_{gas} = \frac{m_{gas\ product\ from\ PLA}}{m_{PLA,o}} \quad (B.1.14)$$

$$Y_{liq} = \frac{m_{liq\ product\ from\ PLA}}{m_{PLA,o}} \times 100 \quad (B.1.15)$$

$$Y_{solid\ in\ reactor} = \frac{m_{solid\ in\ reactor\ from\ PLA}}{m_{PLA,o}} \times 100 \quad (B.1.16)$$

Conversion of PLA is calculated from Eqn. (B.1.17).

$$X_{PLA} = \frac{m_{PLA,o} - m_{solid\ in\ reactor\ from\ PLA}}{m_{PLA,o}} \times 100 \quad (B.1.17)$$

### B.3. Mass Balances for Catalytic Degradation Reaction of PLA in DES

In these calculations, it was assumed that catalyst remained in the reactor without being decomposed due to its high thermal stability (Results and Discussion, Section 3.2.2.4, Figure 3.19).

Calculation steps were same as those of the non-catalytic PLA degradation reaction. The only differences were that the amount of catalyst was subtracted from  $wt\%_{solid\ in\ reactor\ from\ DES}$ ,  $m_{T,i}$ , and  $m_{solid\ in\ reactor\ from\ PLA}$

$$m_{T,i} = m_{DES,o} + m_{PLA,o} + m_{catalyst,o} \quad (B.1.18)$$

$$\frac{wt\%_{solid\ in\ reactor\ from\ DES} = m_{left\ in\ reactor} - m_{ZnCl_2} - m_{catalyst,o}}{m_{DES,o}} \times 100 \quad (B.1.19)$$

$$m_{left\ in\ reactor} - \left( m_{DES,o} \times \frac{m_{solid\ in\ reactor\ from\ PLA} = wt\%_{solid\ in\ reactor\ from\ DES}}{100} \right) - m_{ZnCl_2} - m_{catalyst} \quad (B.1.20)$$



**Table B. 3.1.** The weight measurements before and after the reactions

Mass of the materials (g)	EXPERIMENT		
	DES	DES+PLA	DES+PLA+CATALYST
$m_{DES,o}$	8.23	8.20	8.22
$m_{PLA,o}$	0	2.99	3.03
$m_{Catalyst,o}$	0	0	1.49
$m_{Liq}$	2.44	3.64	3.57
$m_{left\ in\ reactor}$	4.20	4.28	5.78

### C. EDX Spectra of Different Mapped Areas of Catalysts

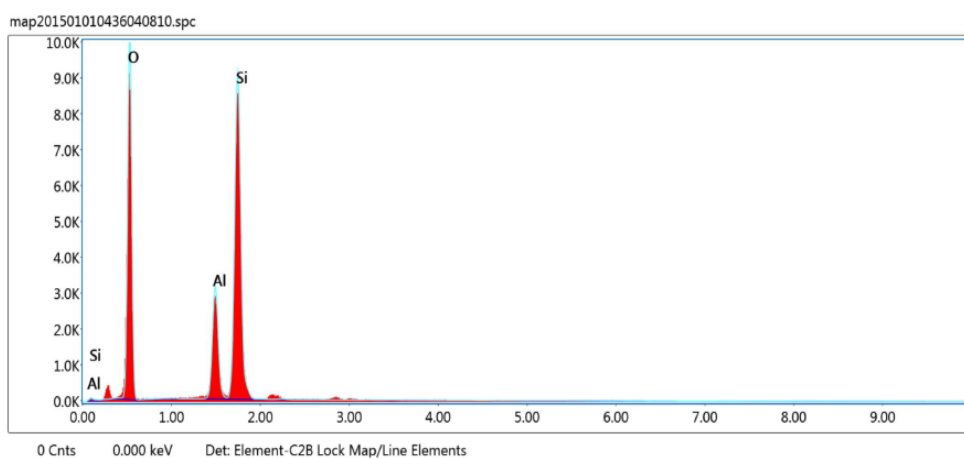
EDAX APEX

EDAX  
AMETEK  
MATERIAL ANALYSIS DIVISION

Page 3

kV: 15    Mag: 2268    Takeoff: 35    Live Time(s): 292.8    Amp Time(μs): 3.84    Resolution:(eV) 127.9

#### Sum Spectrum



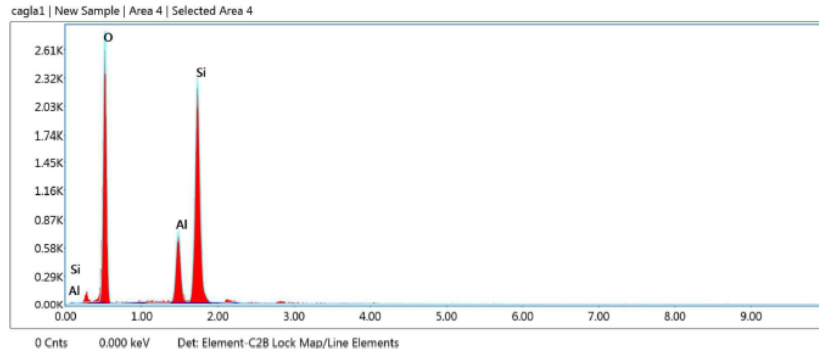
#### Smart Quant Results

Element	Weight %	Atomic %	Error %
O K	48.49	62.07	7.03
Al K	12.38	9.40	3.85
Si K	39.13	28.53	3.57

Figure C. 1. EDX Spectrum of Region 2 in SAUA115

Selected Area 4

kV: 15      Mag: 1559      Takeoff: 35      Live Time(s): 50      Amp Time(μs): 3.84      Resolution(eV) 127.9



**Smart Quant Results**

Element	Weight %	Atomic %	Error %
O K	50.89	64.31	7.36
Al K	11.28	8.45	4.82
Si K	37.83	27.24	3.98

**Figure C. 2.** EDX Spectrum of Region 3 in SAUA115

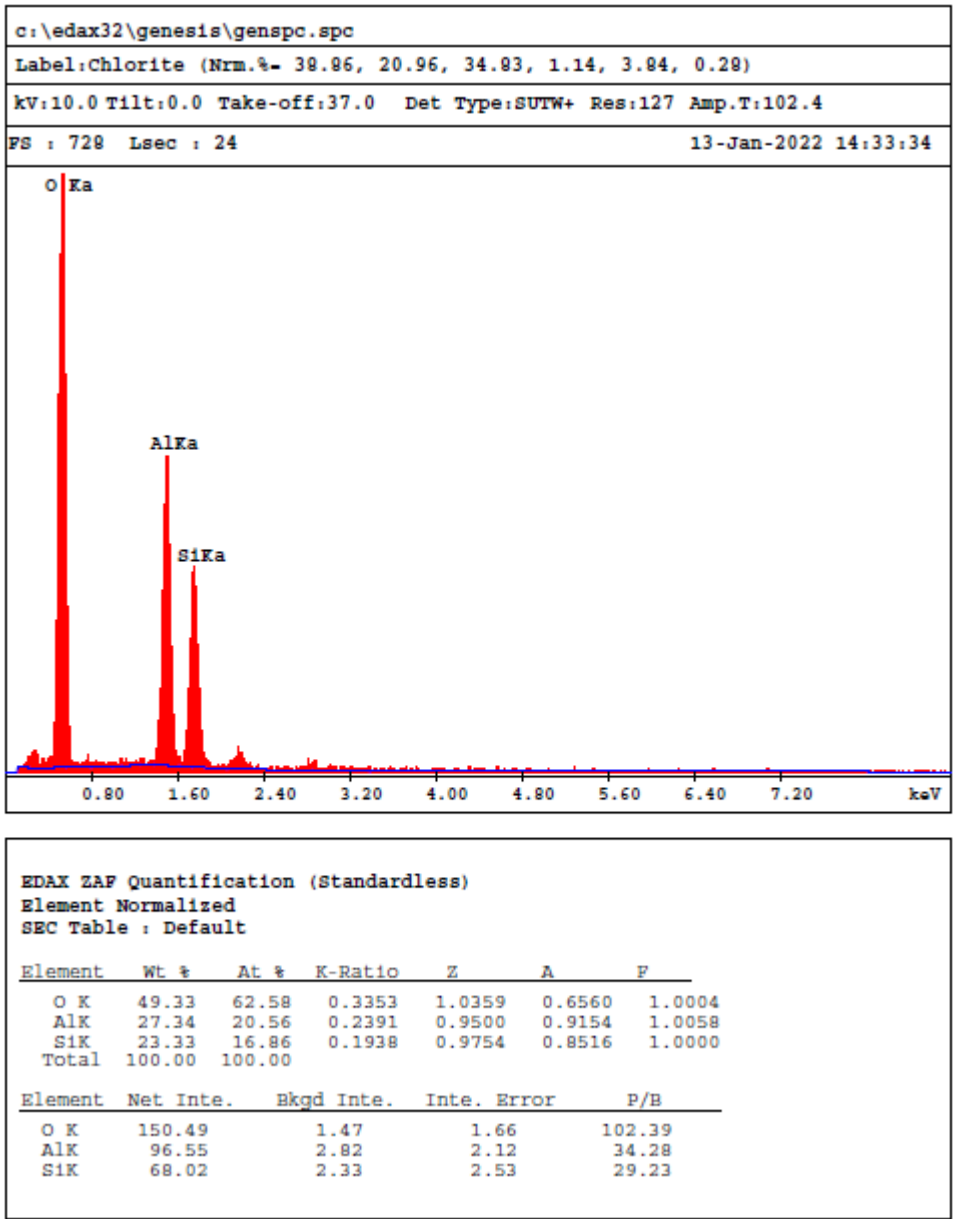
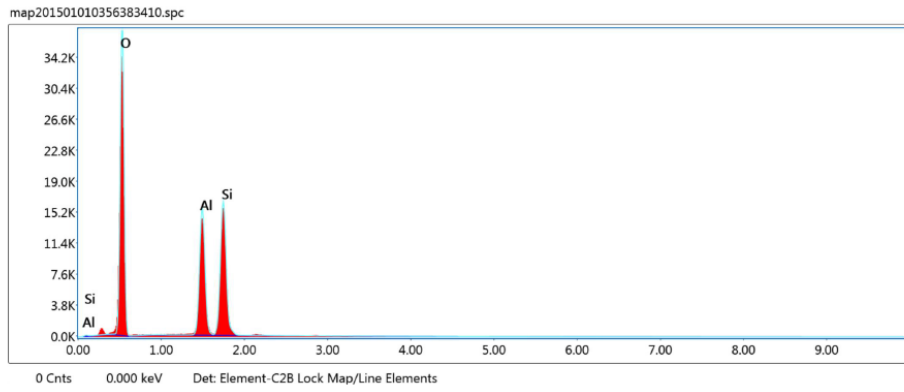


Figure C. 3. EDX Spectrum of Region 2 in SAUA125

kV: 15    Mag: 13330    Takeoff: 35    Live Time(s): 481.9    Amp Time(μs): 3.84    Resolution:(eV) 127.9

Sum Spectrum



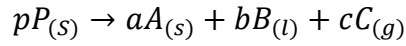
Smart Quant Results

Element	Weight %	Atomic %	Error %
O K	54.19	67.09	6.33
Al K	20.68	15.18	3.51
Si K	25.14	17.73	4.09

Figure C. 4. EDX Spectrum of Region 3 in SAUA125

#### D. Calculation of Activation Energy of PLA Thermal Degradation Reaction with Presence of Catalysts Using Thermogravimetric Analyzer

The procedure to find the kinetic parameters with TGA data for the catalytic and non-catalytic degradation of PLA follows the method presented by Habib (2019). The reaction taking place in degradation of PLA is described as follows.



The rate of disappearance of polymer is expressed in Eqn. (D.1).

$$\frac{d\alpha}{dt} = k_{avg} \times (1-\alpha)^n \quad (D.1)$$

where

$$k_{avg} = A \times e^{\frac{-E_a}{R \times T}} \quad (D.2)$$

Eqn. (D.1) becomes Eqn. (D.3).

$$\frac{d\alpha}{dt} = A \times e^{\frac{-E_a}{R \times T}} \times (1-\alpha)^n \quad (D.3)$$

where,

$A$ : Pre-exponential factor of the reaction

$E_a$ : Activation energy of the reaction

$n$ : Overall reaction order

$\alpha$ : Fraction of PLA degraded at a time  $t$ , and it is calculated with Eqn.(D.2)

$$\alpha = \frac{W_0 - W_t}{W_0 - W_\infty} \quad (D.4)$$

$W_0$ : Initial sample weight,  $W_t$ : sample weight at time  $t$

$W_\infty$ : Sample weight at infinite time

By taking the integral of Eqn. (D.3) and assuming linear heating rate  $q=dT/dt$ , we obtain,

$$\frac{1 - (1-\alpha)^{1-n}}{(1-n) \times T^2} = \frac{A \times R}{q \times E_a} \times \left(1 - \frac{2 \times R \times T}{E_a}\right) \times e^{\frac{-E_a}{R \times T}} \text{ for } n \neq 1 \quad (D.5)$$

In Eqn. (D.5), the  $\frac{2 \times R \times T}{E_a}$  term can be neglected, because it is too small when compared to 1. If natural logarithm of both sides of Eqn. (D.5) is taken, Eqn. (D.6) is obtained,

$$\ln \frac{1 - (1-\alpha)^{1-n}}{(1-n) \times T^2} = \ln \frac{A \times R}{q \times E_a} - \frac{E_a}{R \times T} \text{ for } n \neq 1 \quad (D.6)$$

For first order reactions (n=1), Eqn. (D.6) becomes Eqn. (D.7),

$$\ln \frac{-\ln(1-\alpha)}{T^2} = \ln \frac{A \times R}{q \times E_a} - \frac{E_a}{R \times T} \text{ for } n = 1 \quad (D.7)$$

Slope of  $-\ln \frac{-\ln(1-\alpha)}{T^2}$  versus  $1/T$  plot yields  $E_a/R$  and by multiplying the slope with  $R$ , activation energy of the reaction could be obtained.

In Figure D. 1,  $-\ln \frac{-\ln(1-\alpha)}{T^2}$  versus  $1/T$  plot for SAUA115 was shown. By the help of slope value, activation energy was calculated as 193 kJ/mol.

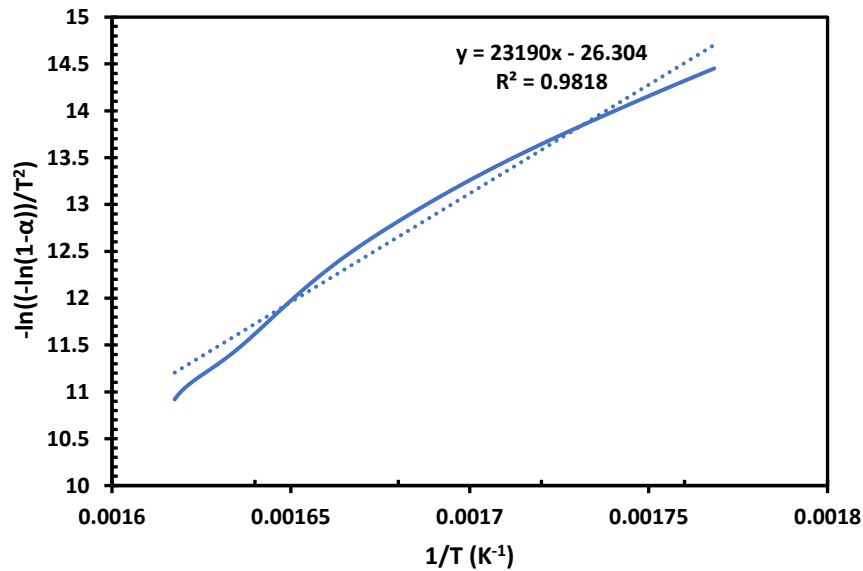


**Figure D. 1.** First order degradation reaction of PLA with SAUA115 catalyst

Sample calculation is described below.

$$\text{Slope} = 23190$$

$$E_a = \text{Slope} \times R$$

$$E_a = 23190 \times 8.314 \times 10^{-3} = 192.8 \cong 193 \text{ kJ/mol}$$

In Figure D. 2,  $-\ln \frac{-\ln(1-\alpha)}{T^2}$  versus  $1/T$  plot for SAUA125 was shown.

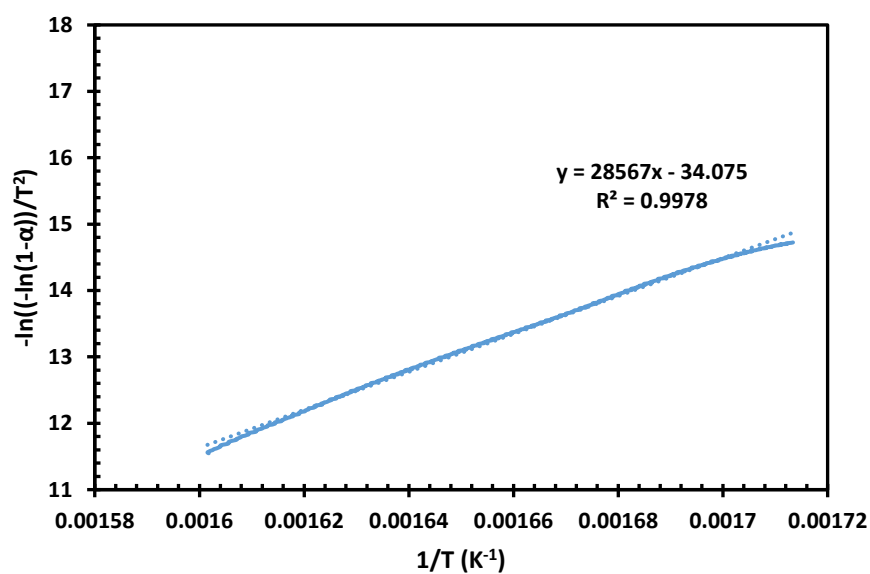


**Figure D. 2.** First order degradation reaction of PLA with SAUA125 catalyst

$$\text{Slope} = 28567$$

$$E_a = \text{Slope} \times R$$

$$E_a = 28567 \times 8.314 \times 10^{-3} = 237.5 \cong 238 \text{ kJ/mol}$$